

Statistics of eigenvalue dispersion indices: quantifying the magnitude of phenotypic integration

Version 2 for *bioRxiv* (2021.08.07)

Junya Watanabe

Department of Earth Sciences, University of Cambridge, Downing Street, Cambridge, CB2

3EQ, United Kingdom

jw2098@cam.ac.uk

<https://orcid.org/0000-0002-9810-5286>

1 **Abstract**

2 Quantification of the magnitude of trait covariation plays a pivotal role in the study of
3 phenotypic evolution, for which statistics based on dispersion of eigenvalues of a covariance
4 or correlation matrix—eigenvalue dispersion indices—are commonly used. This study
5 remedies major issues over the use of these statistics, namely, a lack of clear understandings
6 on their statistical justifications and sampling properties. The relative eigenvalue variance of
7 a covariance matrix is known in the statistical literature a test statistic for sphericity, thus is
8 an appropriate measure of eccentricity of variation. The same of a correlation matrix is equal
9 to the average squared correlation, which has a straightforward interpretation as a measure of
10 integration. Expressions for the mean and variance of these statistics are analytically derived
11 under multivariate normality, clarifying the effects of sample size N , number of variables p ,
12 and parameters on sampling bias and error. Simulations confirmed that approximations
13 involved are reasonably accurate with a moderate sample size ($N \geq 16-64$). Importantly,
14 sampling properties of these indices are not adversely affected by a high $p:N$ ratio, promising
15 their utility in high-dimensional phenotypic analyses. They can furthermore be applied to
16 shape variables and phylogenetically structured data with appropriate modifications.

17

18 **Keywords:** covariance matrix; evolutionary constraint; morphometrics; phenotypic
19 integration; quantitative genetics; Wishart distribution.

20

21 **Introduction**

22 Analysis of trait covariation plays a central role in investigations into evolution of
23 quantitative traits. The well-known quantitative genetic theory of correlated traits predicts
24 that evolutionary response in a population under selection is dictated by the additive genetic
25 covariance matrix \mathbf{G} as well as the selection gradient (Lande, 1979; Lande & Arnold, 1983).

26 Short-term evolutionary changes of a population are expected to be concentrated in major
27 axes of the **G** matrix (Schluter, 1996). Arguably, the structure of the **G** matrix can be
28 approximated by that of the phenotypic covariance matrix for certain types of traits
29 (Cheverud, 1988, 1996; Roff, 1995; Dochtermann, 2011; Sodini et al., 2018), so the latter
30 could be analyzed when accurate estimation of the **G** matrix is not feasible. These theories
31 and conjectures spurred extensive theoretical and empirical explorations on character
32 covariation as an evolutionary constraint (e.g., Steppan et al., 2002; Chenoweth et al., 2010;
33 Pitches et al., 2014; Hansen et al., 2019 and references therein). Partly fueled by these
34 developments, the study of phenotypic integration has developed as an active field of
35 research, where various aspects of character covariation are investigated with diverse
36 motivations and scopes (e.g., Olson & Miller, 1958; Cheverud, 1982; Goswami, 2006;
37 Hallgrímsson et al., 2009; Armbruster et al., 2014; Felice et al., 2018). In the latter context,
38 many different levels of organismal variation can be subjects of research, such as static,
39 ontogenetic, and evolutionary levels (Klingenberg, 2014). For example, relationships
40 between within-population integration and evolutionary rate and/or trajectories have attained
41 much attention as potential links between micro- and macroevolutionary phenomena (e.g.,
42 Klingenberg et al., 2012; Renaud & Auffray, 2013; Bolstad et al., 2014; Goswami et al.,
43 2015; Haber, 2015, 2016).

44 An obvious target of investigation in these contexts is quantitative analysis of the
45 magnitude of constraint or integration entailed in covariance structures. In particular, this
46 paper concerns the methodology for quantifying the overall magnitude of covariation within a
47 set of traits. Quantification of relative (in)dependence between multiple sets of traits—the
48 modularity–integration spectrum—is another major way of studying integration which has
49 separate methodological frameworks (e.g., Goswami & Polly, 2010; Adams, 2016; Goswami
50 & Finarelli, 2016; Adams & Collyer, 2019a). Demonstrating the presence of integration with

51 a statistically justified measure can be the scope of an empirical analysis, sometimes as a part
52 of testing combined hypotheses (e.g., Brommer, 2014; Watanabe, 2018). A univariate
53 summary statistic for magnitude of integration can conveniently be used in comparative
54 analyses across developmental stages, populations, or phylogeny (e.g., Marroig et al., 2009;
55 Porto et al., 2009; Haber, 2016). A plethora of statistics have been proposed for such
56 purposes from various standpoints (e.g., Van Valen, 1974, 2005; Cheverud et al., 1983, 1989;
57 Wagner, 1984; Cane, 1993; Hansen & Houle, 2008; Agrawal & Stinchcombe, 2009;
58 Kirkpatrick, 2009; Pavlicev et al., 2009; Armbruster et al., 2009, 2014; Haber, 2011). One of
59 the most popular classes of such statistics is based on the dispersion of eigenvalues of a
60 covariance or correlation matrix. These statistics have the forms

$$V = \frac{1}{p} \sum_{i=1}^p (\lambda_i - \bar{\lambda})^2,$$
$$V_{\text{rel}} = \frac{\sum_{i=1}^p (\lambda_i - \bar{\lambda})^2}{p(p-1) \bar{\lambda}^2},$$

61 where p is the number of variables (traits), λ_i is the i th eigenvalue of the covariance or
62 correlation matrix under analysis, and $\bar{\lambda}$ is the average of the eigenvalues. Here, V is the most
63 naïve form of eigenvalue dispersion, and V_{rel} is a scaled version which ranges between 0 and
64 1. Formal definitions are given below with distinction between population and sample
65 quantities. Some authors use square root or a constant multiple of these forms, but such
66 variants essentially bear identical information when calculated from the same matrix.
67 Alternative terms for this class of statistics include the tightness (for V_{rel} ; Van Valen, 1974;
68 later used for $\sqrt{V_{\text{rel}}}$ by Van Valen, 2005), integration coefficient of variation (for
69 $\sqrt{(p-1)V_{\text{rel}}}$; Shirai & Marroig, 2010), and phenotypic integration index (for V ; Torices &
70 Muñoz-Pajares, 2015). In this paper, V and V_{rel} are called the eigenvalue variance and
71 relative eigenvalue variance, respectively, to take a balance between brevity and

72 descriptiveness. These quantities are not to be confused with the sampling variance
73 associated with eigenvalues in a sample (see below).

74 Since eigenvalues of a covariance or correlation matrix correspond to the variance
75 along the corresponding eigenvectors (principal components), these statistics are supposed to
76 represent eccentricity of variation across directions in a trait space (Fig. 1; Wagner, 1984).
77 Cheverud et al. (1983) and Wagner (1984) were the first to propose using V of a correlation
78 matrix for quantifying magnitude of integration. Pavlicev et al. (2009) devised V_{rel} for a
79 correlation matrix, and explored its relationships to correlation structures in certain
80 biologically relevant conditions. Haber (2011) pointed out similarity between these indices
81 and Van Valen's (1974) tightness index for a covariance matrix, and proposed that these
82 indices can be applied to either covariance or correlation matrices with slightly different
83 interpretations. Eigenvalue dispersion indices are frequently used in empirical analyses of
84 phenotypic integration at various levels of organismal variation, from phenotypic covariance
85 at the population level to evolutionary covariance at the interspecific level (e.g., Ordano et al.,
86 2008; Torices & Mendez, 2014; Haber, 2016; Haber & Dworkin, 2017; Watanabe, 2018;
87 Arlegi et al., 2020). However, use of these indices has been criticized for a lack of clear
88 statistical justifications; it has not been known—or not widely appreciated by biologists—
89 exactly what they are designed to measure, beyond the intuitive allusion to eccentricity
90 mentioned above (Hansen & Houle, 2008; Blows & McGuigan, 2015; Hansen et al., 2019).

91 Another fundamental issue over the eigenvalue dispersion indices is a virtual lack of
92 systematic understanding of their sampling properties. In empirical analyses, eigenvalue
93 dispersion indices are calculated from sample covariance or correlation matrices, but interests
94 will be in making inferences for the underlying populations. For example, interest may be in
95 detecting the presence of constraint in a population, i.e., testing the null hypothesis of
96 sphericity. As detailed below, however, sample eigenvalues are always estimated with error,

97 so that V and V_{rel} calculated from them take a positive value even if the corresponding
98 population values are 0. In other words, empirical eigenvalue dispersion indices are biased
99 estimators of the corresponding population values under the null hypothesis. For statistically
100 justified inferences, it is crucial to capture essential aspects of their sampling distributions,
101 e.g., expectation and variance.

102 The presence of sampling bias in eigenvalue dispersion indices has been well known
103 in the literature (Wagner, 1984; Cheverud et al., 1989; Grabowski & Porto, 2017; see also
104 Marroig et al., 2012; Björklund, 2019). Simulation-based studies have been undertaken to
105 sketch sampling distributions of eigenvalue dispersion indices and related statistics (Haber,
106 2011; Grabowski & Porto, 2017; Machado et al., 2019; Jung et al. 2020). However, these
107 approaches hardly give any systematic insight beyond the specific conditions considered.
108 Analytic results should preferably be sought to comprehend the sampling bias and error. In
109 this regard, it is notable that Wagner (1984) derived the first two moments of eigenvalues of
110 sample covariance and correlation matrices under the null conditions. The variance of sample
111 eigenvalues obtained from these moments has later been used as an estimate of sampling bias
112 in these conditions (e.g., Cheverud et al., 1989). Strictly speaking, however, the variance of a
113 sample eigenvalue is fundamentally different from the expectation of the eigenvalue variance
114 V . These quantities are identical for correlation matrices under the null hypothesis, but this is
115 not the case for covariance matrices where the covariances between sample eigenvalues
116 cannot be ignored (see below). Furthermore, Wagner's (1984) results have a few restrictive
117 conditions: variables to have the means of 0, or equivalently, to be centered at the population
118 mean rather than the sample mean as is done in most empirical analyses (although this was
119 probably appropriate in the strict context of his theoretical model); and the sample size N to
120 be equal to or larger than the number of variables p , so their applicability to $p > N$ conditions
121 has not been demonstrated.

122 In addition to the naïve null condition of no integration, moments under arbitrary
123 conditions are also desired. Such would be useful in testing hypotheses about the magnitude
124 (rather than the mere presence/absence) of integration (Harder, 2009; Fornoni et al., 2009)
125 and comparing the magnitudes between different samples (Cheverud et al., 1989). Also, the
126 assumption of no covariation is intrinsically inappropriate as a null hypothesis for shape
127 variables where raw data are transformed in such a way that individual “variables” are
128 necessarily dependent on one another (e.g., Mitteroecker et al., 2012). For this type of data, a
129 covariance matrix with an appropriate structure needs to be specified as the null model
130 representing the intrinsic covariation.

131 This paper addresses the issues over the eigenvalue dispersion indices mentioned
132 above. It first gives a theoretical overview of these statistics to clarify their statistical
133 justifications, particularly in connection to the sphericity test in multivariate analysis. Then
134 exact and approximate expressions are analytically derived for the expectation and variance
135 of V and V_{rel} of sample covariance and correlation matrices under the null and arbitrary
136 conditions, assuming the multivariate normality of variables. These expressions are derived
137 without any assumption on p or N , except for the variance of V and V_{rel} of a correlation
138 matrix under arbitrary conditions, which is based on large-sample asymptotic theories.
139 Simulations were subsequently conducted to obtain systematic insights into sampling
140 properties and to evaluate the accuracy of the approximate expressions. Extensions into shape
141 variables and phylogenetically structured data are briefly discussed.

142

143 **Theory**

144 **Preliminaries**

145 For the purpose here, the distinction between population and sample quantities is essential.

146 Corresponding Greek and Latin letters are used as symbols for the former and latter,

147 respectively. Let Σ be the $p \times p$ population covariance matrix, whose (i, j) -th element σ_{ij} is
148 the population variance ($i = j$) or covariance ($i \neq j$). It is a symmetric, nonnegative definite
149 matrix with the eigendecomposition

$$150 \quad \Sigma = \mathbf{Y}\mathbf{\Lambda}\mathbf{Y}^T, \quad (1)$$

151 where the superscript T denotes matrix transposition, \mathbf{Y} is an orthogonal matrix of
152 eigenvectors ($\mathbf{Y}\mathbf{Y}^T = \mathbf{Y}^T\mathbf{Y} = \mathbf{I}_p$ where \mathbf{I}_p is the $p \times p$ identity matrix), and $\mathbf{\Lambda}$ is a diagonal
153 matrix whose diagonal elements are the eigenvalues $\lambda_1, \lambda_2, \dots, \lambda_p$ of Σ (population
154 eigenvalues). For convenience, the eigenvalues are arranged in the non-increasing order:
155 $\lambda_1 \geq \lambda_2 \geq \dots \geq \lambda_p \geq 0$. Let $\boldsymbol{\mu}$ be the $p \times 1$ population mean vector.

156 Let \mathbf{X} be an $N \times p$ observation matrix consisting of p -variate observations, which are
157 individually denoted as \mathbf{x}_i ($p \times 1$ vector; transposed in the rows of \mathbf{X}). (No strict notational
158 distinction is made between a random variable and its realization.) At this point, N
159 observations are assumed to be identically and independently distributed (i.i.d.). The sample
160 covariance matrix \mathbf{S} and cross-product matrix \mathbf{A} are defined as

$$161 \quad \mathbf{S} = \frac{1}{n_*} \mathbf{A} = \frac{1}{n_*} (\mathbf{X} - \mathbf{1}_N \bar{\mathbf{x}}^T)^T (\mathbf{X} - \mathbf{1}_N \bar{\mathbf{x}}^T), \quad (2)$$

162 where $\mathbf{1}_N$ is a $N \times 1$ column vector of 1's, $\bar{\mathbf{x}} = \sum_{i=1}^N \mathbf{x}_i / N$ is the sample mean vector, and n_*
163 denotes an appropriate divisor; e.g., $n_* = N - 1$ for the ordinary unbiased estimator, and
164 $n_* = N$ for the maximum likelihood estimator under the normal distribution. The (i, j) -th
165 element of \mathbf{S} , denoted s_{ij} , is the sample variance or covariance. The eigendecomposition of \mathbf{S}
166 is constructed in the same way as above:

$$167 \quad \mathbf{S} = \mathbf{U}\mathbf{L}\mathbf{U}^T, \quad (3)$$

168 where \mathbf{U} is an orthogonal matrix of sample eigenvectors and \mathbf{L} is a diagonal matrix whose
169 elements are the sample eigenvalues l_1, l_2, \dots, l_p .

170 In what follows, the following identity entailed by the orthogonality of \mathbf{U} is frequently
 171 utilized:

$$172 \quad \sum_{i=1}^p s_{ii}^r = \text{tr}(\mathbf{S}^r) = \text{tr}(\mathbf{ULU}^T \mathbf{ULU}^T \dots \mathbf{ULU}^T) = \text{tr}(\mathbf{L}^r) = \sum_{i=1}^p l_i^r, \quad r = 1, 2, \dots, \quad (4)$$

173 where $\text{tr}(\cdot)$ denotes the matrix trace operator, i.e., summation of the diagonal elements; the
 174 parentheses are omitted for visual clarity when little ambiguity exists. The sum of variances
 175 $\text{tr} \mathbf{S} = \text{tr} \mathbf{L}$ is called total variance. Note that equation 4 holds even when $N - 1 < p$, in
 176 which case $l_i = 0$ for some i . In other words, when $N - 1 < p$, the sample total variance is in
 177 a way concentrated in a subspace with fewer dimensions than the full space.

178 The population and sample correlation matrices \mathbf{P} and \mathbf{R} , whose (i, j) -th elements are
 179 the population and sample correlation coefficients ρ_{ij} and r_{ij} , respectively, are obtained by
 180 standardizing $\mathbf{\Sigma}$ and \mathbf{S} :

$$181 \quad \mathbf{P} = \text{diag}(\sigma_{ii}^{-1/2}) \mathbf{\Sigma} \text{diag}(\sigma_{ii}^{-1/2}),$$

$$182 \quad \mathbf{R} = \text{diag}(s_{ii}^{-1/2}) \mathbf{S} \text{diag}(s_{ii}^{-1/2}), \quad (5)$$

183 where $\text{diag}(\cdot)$ stands for the $p \times p$ diagonal matrix with the designated i th elements. Their
 184 eigendecomposition is defined as for covariance matrices, and the eigenvalues are denoted
 185 with the same symbols. For any i , $\rho_{ii} = r_{ii} = 1$, and hence, for correlation matrices

$$186 \quad \text{tr} \mathbf{P} = \text{tr} \mathbf{\Lambda} = \text{tr} \mathbf{R} = \text{tr} \mathbf{L} = p. \quad (6)$$

187 In what follows, the notations $E(\cdot)$, $\text{Var}(\cdot)$, and $\text{Cov}(\cdot, \cdot)$ are used for the expectation (mean),
 188 variance, and covariance of random variables, respectively.

189

190 **Eigenvalue dispersion**

191 The eigenvalue variance V is defined as:

$$192 \quad V(\mathbf{\Sigma}) = \frac{1}{p} \sum_{i=1}^p (\lambda_i - \bar{\lambda})^2,$$

$$193 \quad V(\mathbf{S}) = \frac{1}{p} \sum_{i=1}^p (l_i - \bar{l})^2, \quad (7)$$

194 where $\bar{\lambda}$ and \bar{l} are the averages of the population and sample eigenvalues, respectively
 195 ($\bar{\lambda} = \sum_{i=1}^p \lambda_i/p = \text{tr } \mathbf{\Lambda} /p$, $\bar{l} = \sum_{i=1}^p l_i/p = \text{tr } \mathbf{L} /p$). Note that $V(\mathbf{\Sigma})$ is a quantity pertaining to
 196 the population, whereas $V(\mathbf{S})$ is a sample statistic. The definition here follows the convention
 197 in the literature that p , rather than $p - 1$, is used as the divisor (e.g., Cheverud et al., 1983;
 198 Pavlicev et al., 2009; Haber, 2011). The latter might be more suitable for $V(\mathbf{S})$ because the
 199 sum of squares is taken around the average sample eigenvalue which is a random variable.
 200 After all, however, the choice of $p - 1$ is not so useful because $V(\mathbf{S})$ cannot be an unbiased
 201 estimator of $V(\mathbf{\Sigma})$ even with that choice (below).

202 Note that the average and sum of squares are taken across all p eigenvalues, even if
 203 some eigenvalues are zero due to the condition $N - 1 < p$. This is reasonable given that
 204 sums of moments across all p sample eigenvalues are comparable in magnitude to those of
 205 population eigenvalues (see below). One could alternatively use eigenvalue standard
 206 deviation \sqrt{V} (Pavlicev et al., 2009; Haber, 2011), but this study concentrates on V rather
 207 than \sqrt{V} , because the former is much more tractable for the purposes of characterizing
 208 distributions.

209 It is obvious that $V(\mathbf{\Sigma})$ takes a single minimum of 0 at $(\lambda_1, \lambda_2, \dots, \lambda_p) = (\bar{\lambda}, \bar{\lambda}, \dots, \bar{\lambda})$.
 210 On the other hand, for a fixed $\bar{\lambda}$, it takes a single maximum of $(p - 1)\bar{\lambda}^2$ at $(p\bar{\lambda}, 0, \dots, 0)$ (e.g.,
 211 Van Valen, 1974; Machado et al., 2019). Hence, not only is $V(\mathbf{\Sigma})$ scale-variant, but also its
 212 range depends on $p - 1$. Therefore, it is often useful to standardize V by division with this
 213 maximum to obtain the relative eigenvalue variance V_{rel} :

$$214 \quad V_{\text{rel}}(\mathbf{\Sigma}) = \frac{\sum_{i=1}^p (\lambda_i - \bar{\lambda})^2}{p(p-1)\bar{\lambda}^2},$$

$$215 \quad V_{\text{rel}}(\mathbf{S}) = \frac{\sum_{i=1}^p (l_i - \bar{l})^2}{p(p-1)\bar{l}^2}. \quad (8)$$

216 Because of the standardization, V_{rel} ranges between 0 and 1. This is a heuristic introduction
 217 of V_{rel} from V , but it will be seen below that $V_{\text{rel}}(\mathbf{S})$ has a clearer theoretical justification.

218 These indices are similarly defined for correlation matrices. By noting $\bar{\lambda} = \bar{l} = 1$ (eq.
219 6), these are

$$220 \quad V(\mathbf{P}) = \frac{1}{p} \sum_{i=1}^p (\lambda_i - 1)^2,$$

$$221 \quad V(\mathbf{R}) = \frac{1}{p} \sum_{i=1}^p (l_i - 1)^2.$$

$$222 \quad V_{\text{rel}}(\mathbf{P}) = \frac{\sum_{i=1}^p (\lambda_i - 1)^2}{p(p-1)},$$

$$223 \quad V_{\text{rel}}(\mathbf{R}) = \frac{\sum_{i=1}^p (l_i - 1)^2}{p(p-1)}. \quad (9)$$

224 In the following discussions, we will concentrate on V_{rel} for correlation matrices, because
225 $V(\mathbf{R})$ and $V_{\text{rel}}(\mathbf{R})$ are proportional to each other by the factor $p - 1$, and hence their
226 distributions are identical up to this scaling. This is in contrast to those of covariance matrices,
227 where \bar{l} in the denominator in $V_{\text{rel}}(\mathbf{S})$ is a random variable and affects sampling properties.

228 Importantly, a single value of V_{rel} in general corresponds to multiple combinations of
229 eigenvalues even if the average eigenvalue is fixed, except when $p = 2$ or under the extreme
230 conditions $V_{\text{rel}} = 0$ and $V_{\text{rel}} = 1$ (Fig. 1). As such, it is not always straightforward to discern
231 how intermediate values of V_{rel} are translated into actual covariance structures when $p > 2$.
232 Nevertheless, it is possible to show that $V_{\text{rel}} > 0.5$ cannot happen when multiple leading
233 eigenvalues are of the same magnitude (Appendix A); in other words, such a large value
234 indicates dominance of the first principal component.

235 As would be obvious from the definition, V and V_{rel} of covariance matrices only
236 describe the (relative) magnitudes of eigenvalues—proportions of the axes of variation—and
237 do not reflect any information of eigenvectors—directions of the axes. A large eigenvalue of
238 a covariance matrix can represent, e.g., strong covariation between equally varying traits or
239 large variation of a single trait uncorrelated with others; either of these cases describes
240 eccentricity of variation in the multivariate space. By contrast, a large eigenvalue of a
241 correlation matrix can only happen in the presence of correlation. Therefore, a large

242 eigenvalue dispersion in a correlation matrix constrains conformation of eigenvectors to a
243 certain extent. The correlations can nevertheless be realized in various ways depending on
244 eigenvectors, whose conformation does influence the sampling distribution of $V_{\text{rel}}(\mathbf{R})$ (see
245 below).

246 For covariance matrices, $V_{\text{rel}}(\mathbf{S})$ has a natural relation to the test of sphericity, i.e., test
247 of the null hypothesis that $\mathbf{\Sigma} = \sigma^2 \mathbf{I}_p$ for an arbitrary positive constant σ^2 . Simple
248 transformations from equation 8 lead to

$$V_{\text{rel}}(\mathbf{S}) = \frac{1}{p-1} \left(p \frac{\sum l_i^2}{(\sum l_i)^2} - 1 \right). \quad (10)$$

250 By noting $\sum l_i^2 / (\sum l_i)^2 = \text{tr}(\mathbf{S}^2) / (\text{tr} \mathbf{S})^2 = \text{tr}(\mathbf{A}^2) / (\text{tr} \mathbf{A})^2$ (see eqs. 2 and 4), $V_{\text{rel}}(\mathbf{S})$ in the
251 form of equation 10 is exactly John's (1972) T statistic for the test of sphericity (see also
252 Ledoit & Wolf, 2002). Beyond the intuition that it measures eccentricity of variation along
253 principal components, this statistic (and its linear functions) can be justified as the most
254 powerful test statistic in the proximity of the null hypothesis under multivariate normality,
255 among the class of such statistics that are invariant against translation by a constant vector,
256 uniform scaling, and orthogonal rotation (John, 1971, 1972; Sugiura, 1972; Nagao, 1973). On
257 the other hand, $V(\mathbf{S})$ does not seem to have as much theoretical justification, but rather has a
258 practical advantage in the tractability of its moments and ease of correcting sampling bias
259 (see below).

260 For a correlation matrix, V_{rel} is a measure of association between variables. Following
261 similar transformations, it is straightforward to see

$$\begin{aligned} V_{\text{rel}}(\mathbf{R}) &= \frac{\text{tr}(\mathbf{R}^2) - p}{p(p-1)} \\ &= \frac{2}{p(p-1)} \sum_{i < j}^p r_{ij}^2, \end{aligned}$$

262 (11)

263 because $r_{ii}^2 = 1$ for all i . This relationship has been known in the statistical literature (e.g.,
264 Gleason & Staelin, 1975; Durand & Le Roux, 2017), and empirically confirmed by Haber
265 (2011). This statistic is used as a measure of overall association between variables (e.g.,
266 Schott, 2005; Durand & Le Roux, 2017), with the corresponding null hypothesis being
267 $\mathbf{P} = \mathbf{I}_p$.

268

269 **Sampling properties of eigenvalues**

270 The distribution of eigenvalues of \mathbf{S} , or equivalently those of \mathbf{A} (which are n_* times those of
271 \mathbf{S}), has been extensively investigated in the literature of multivariate analysis (see, e.g.,
272 Jolliffe, 2002; Anderson, 2003). Unfortunately, however, most of such results are of limited
273 value for the present purposes. On the one hand, forms of the exact joint distribution of the
274 eigenvalues of \mathbf{A} are known under certain assumptions on the population eigenvalues (e.g.,
275 Muirhead, 1982: pp. 107, 388), but they do not allow for much intuitive interpretation (let
276 alone direct evaluation of moments), apart from the following points: 1) sample eigenvalues
277 are *not* stochastically independent from one another; and 2) the distribution of sample
278 eigenvalues are only dependent on the population eigenvalues, but not on the population
279 eigenvectors. On the other hand, a substantial body of results is available for large-sample
280 asymptotic distributions of sample eigenvalues (assuming $n \rightarrow \infty$, p being constant; e.g.,
281 Anderson, 1963, 2003), but their accuracy under finite n conditions is questionable. For
282 example, a well-known asymptotic result states that $l_i \sim N(\lambda_i, 2\lambda_i^2/n)$ and $\text{Cov}(l_i, l_j) \approx 0$ for
283 $i \neq j$, assuming $\lambda_i \neq \lambda_j$ and $n_* = n$ (Girshick, 1939; Anderson, 1963; Srivastava & Khatri,
284 1979). However, these expressions ignore terms of order higher than $O(n^{-1})$ —that is, all
285 terms with >1 powers of n in the denominator—whose magnitude can be substantial for finite
286 n . Indeed, with further evaluation of higher-order terms, it becomes evident that sample

287 eigenvalues are biased estimators of the population equivalents, where large eigenvalues are
288 prone to overestimation and small ones are prone to underestimation, and that $\text{Cov}(l_i, l_j) =$
289 $2\lambda_i\lambda_j/[(\lambda_i - \lambda_j)n]^2 + O(n^{-3})$ for $i \neq j$, again assuming $\lambda_i \neq \lambda_j$ (Lawley, 1956; Srivastava
290 & Khatri, 1979). In general, the covariance between sample eigenvalues is nonzero.

291 Sampling properties of eigenvalues have also been investigated under high-
292 dimensional asymptotic conditions (assuming $n \rightarrow \infty$, $p \rightarrow \infty$, and p/n typically held finite
293 and constant; e.g., Johnstone, 2007; Johnstone & Paul, 2018). Attempts have been made to
294 apply some of these results to \mathbf{G} matrices (Blows & McGuigan, 2015; Sztepanacz & Blows,
295 2017), although these remain highly heuristic in nature and rely more heavily on simulations
296 than analytic results. The theories primarily concern limiting distributions of largest sample
297 eigenvalues or the entire bulk of sample eigenvalues, and do not seem directly applicable to
298 the present analysis, which requires accurate expressions of certain higher-order moments of
299 sum of eigenvalues (see below).

300 Much less is known about eigenvalues of a sample correlation matrix \mathbf{R} (Jolliffe,
301 2002), whose distribution seems intractable except under certain special conditions
302 (Anderson, 1963). Large-sample asymptotic results indicate that the limiting distribution
303 ($n \rightarrow \infty$) of an eigenvalue of \mathbf{R} is centered around the corresponding population eigenvalue
304 but its variance depends on population eigenvectors (Anderson, 1963; Konishi, 1979), unlike
305 that of a covariance matrix where the distribution does not depend on population eigenvectors
306 (above).

307 It is often of practical interest to detect the presence of eccentricity or integration, i.e.,
308 to test the null hypothesis of sphericity $\mathbf{\Sigma} = \sigma^2\mathbf{I}_p$ or no correlation $\mathbf{P} = \mathbf{I}_p$. These hypotheses
309 are equivalent to $V(\mathbf{\Sigma}) = V_{\text{rel}}(\mathbf{\Sigma}) = 0$ and $V_{\text{rel}}(\mathbf{P}) = 0$, respectively. Even under these
310 conditions, nonzero sampling variance in sample eigenvalues renders $V(\mathbf{S}) > 0$, $V_{\text{rel}}(\mathbf{S}) > 0$,
311 and $V_{\text{rel}}(\mathbf{R}) > 0$ with probability 1, because these statistics are calculated from sum of

312 squares. The primary aim here is to derive explicit expressions for this sampling bias
 313 (expectation), as well as sampling variance.

314 It should be remembered that the expectation of the eigenvalue variance $E[V(\mathbf{S})]$ is
 315 fundamentally different from the variance of eigenvalues $\text{Var}(l_i)$. This point will be clarified
 316 by the following transformation:

$$\begin{aligned} E[V(\mathbf{S})] &= \frac{1}{p} E \left(\sum_{i=1}^p l_i^2 \right) - \frac{1}{p^2} E \left[\left(\sum_{i=1}^p l_i \right)^2 \right] \\ &= \frac{p-1}{p^2} \sum_{i=1}^p E(l_i^2) - \frac{1}{p^2} \sum_{i \neq j} [E(l_i)E(l_j) + \text{Cov}(l_i, l_j)]. \end{aligned}$$

317 (12)

318 Under the null hypothesis, the moments are equal across all i , and the above simplifies into

$$319 \quad \frac{p-1}{p} [\text{Var}(l_i) - \text{Cov}(l_i, l_j)], \quad i \neq j. \quad (13)$$

320 If $\text{Cov}(l_i, l_j)$ were zero, the expectation would coincide with $(p-1)\text{Var}(l_i)/p$, which can be
 321 evaluated from, e.g., Wagner's (1984) results. As already mentioned, however, this
 322 covariance is nonzero in general and hence cannot be ignored for covariance matrices. This is
 323 unlike the case for correlation matrices, where $E[V(\mathbf{R})] = \text{Var}(l_i)$ holds under the null
 324 hypothesis, because \bar{l} is a constant and equals $E(l_i) = 1$.

325 In the following discussions on moments of eigenvalue dispersion indices,
 326 observations are assumed to be i.i.d. multivariate normal variables. If the $N \times p$ matrix \mathbf{X}
 327 consists of N i.i.d. p -variate normal variables $\mathbf{x}_i \sim N_p(\boldsymbol{\mu}, \boldsymbol{\Sigma})$, then the distribution of the
 328 sample-mean-centered cross-product matrix \mathbf{A} (eq. 2) is said to be the (central) Wishart
 329 distribution $W_p(\boldsymbol{\Sigma}, n)$, where $n = N - 1$ is the degree of freedom. It is well known that this is
 330 identical to the distribution of $\mathbf{Z}^T \mathbf{Z}$, where the $n \times p$ matrix \mathbf{Z} consists of n i.i.d. p -variate
 331 normal variables $\mathbf{z}_i \sim N_p(\mathbf{0}_p, \boldsymbol{\Sigma})$ with $\mathbf{0}_p$ being the $p \times 1$ column vector of 0's (e.g., Anderson,

2003). Therefore, for analyzing statistics associated with sample covariance or correlation matrices, we can conveniently consider

$$\mathbf{S} = \frac{1}{n_*} \mathbf{Z}^T \mathbf{Z}. \quad (14)$$

without loss of generality, by bearing in mind the distinction between the degree of freedom n and sample size N . From elementary moments of the normal distribution, we have

$$\begin{aligned} E(s_{ij}) &= \frac{1}{n_*} \sum_{k=1}^n E(z_{ki} z_{kj}) = \frac{n}{n_*} \sigma_{ij}, \\ E(s_{ij} s_{km}) &= \frac{n^2}{n_*^2} \left[\sigma_{ij} \sigma_{km} + \frac{1}{n} (\sigma_{ik} \sigma_{jm} + \sigma_{im} \sigma_{jk}) \right], \end{aligned} \quad (15)$$

where z_{ij} , s_{ij} , σ_{ij} and the like are the (i, j) -th elements of \mathbf{Z} , \mathbf{S} , and $\mathbf{\Sigma}$, respectively.

340

341 Moments under null hypotheses

342 Covariance matrix

343 Before proceeding to arbitrary conditions, let us consider the null hypothesis of sphericity:

344 $\mathbf{\Sigma} = \sigma^2 \mathbf{I}_p$. For the expectation of $V(\mathbf{S})$, we need $\text{Var}(l_i)$ and $\text{Cov}(l_i, l_j)$, or equivalently

345 $E(\sum_{i=1}^p l_i^2)$ and $E[(\sum_{i=1}^p l_i)^2]$ (see eqs. 12 and 13); we will proceed with the latter here. By

346 use of equations 4 and 15, we have

$$\begin{aligned} E\left(\sum_{i=1}^p l_i^2\right) &= E\left(\sum_{i,j=1}^p s_{ij}^2\right) \\ &= E\left(\sum_{i=1}^p s_{ii}^2 + \sum_{i \neq j}^p s_{ij}^2\right) \\ &= [pE(s_{ii}^2) + p(p-1)E(s_{ij}^2)] \\ &= \frac{pn}{n_*^2} (p+n+1)\sigma^4, \end{aligned}$$

347 (16)

348 and similarly

$$\begin{aligned}
 E \left[\left(\sum_{i=1}^p l_i \right)^2 \right] &= E \left[\left(\sum_{i=1}^p s_{ii} \right)^2 \right] \\
 &= E \left[\sum_{i=1}^p s_{ii}^2 + \sum_{i \neq j} s_{ii} s_{jj} \right] \\
 &= [pE(s_{ii}^2) + p(p-1)E(s_{ii} s_{jj})] \\
 &= \frac{pn}{n_*^2} (pn + 2)\sigma^4.
 \end{aligned}$$

349 (17)

350 Then, inserting these results into equation 12,

$$E[V(\mathbf{S})] = \frac{n}{pn_*^2} (p-1)(p+2)\sigma^4.$$

351 (18)

352 Alternatively, it could be seen that $\text{Var}(l_i) = n(p+1)\sigma^2/n_*^2$ and $\text{Cov}(l_i, l_j) = -n\sigma^4/n_*^2$

353 for $i \neq j$ (see also Girshick, 1939), with which equation 13 yields the identical result.

354 The variance of $V(\mathbf{S})$ is, by equation 12,

$$\text{Var}[V(\mathbf{S})] = \frac{1}{p^2} \text{Var} \left[\sum_{i=1}^p l_i^2 \right] + \frac{1}{p^4} \text{Var} \left[\left(\sum_{i=1}^p l_i \right)^2 \right] - 2 \frac{1}{p^3} \text{Cov} \left[\sum_{i=1}^p l_i^2, \left(\sum_{i=1}^p l_i \right)^2 \right].$$

355 (19)

356 The relevant moments can most conveniently be found as a special case of general

357 expressions under arbitrary Σ (see below and Appendix B), although direct derivation using

358 normal moments is possible:

$$\begin{aligned}
 E \left[\left(\sum_{i=1}^p l_i^2 \right)^2 \right] &= \frac{pn}{n_*^4} (p^3n + pn^3 + 2p^2n^2 + 2p^2n + 2pn^2 + 8p^2 + 8n^2 + 21pn \\
 &\quad + 20p + 20n + 20)\sigma^8;
 \end{aligned}$$

359 (20)

360 Inserting these into equation 19 yields

$$361 \quad \text{Var}[V(\mathbf{S})] = \frac{4n}{p^3 n^4} (p-1)(p+2)(2p^2 + pn + 3p - 6)\sigma^8. \quad (21)$$

362 Next, consider the first two moments of $V_{\text{rel}}(\mathbf{S})$ under the null hypothesis (which have
363 previously been derived by John [1972]). Recalling the form of equation 10,

$$364 \quad E[V_{\text{rel}}(\mathbf{S})] = \frac{1}{p-1} \left(p E \left[\frac{\sum l_i^2}{(\sum l_i)^2} \right] - 1 \right),$$

$$365 \quad \text{and} \quad \text{Var}[V_{\text{rel}}(\mathbf{S})] = \left(\frac{p}{p-1} \right)^2 \text{Var} \left[\frac{\sum l_i^2}{(\sum l_i)^2} \right]. \quad (22)$$

366 In general, moments of the ratio $\sum l_i^2 / (\sum l_i)^2$ do not coincide with the ratios of the moments
367 of the numerator and denominator. Specifically under the null hypothesis, however,

$$368 \quad E \left[\frac{\sum l_i^2}{(\sum l_i)^2} \right] = \frac{E[\sum l_i^2]}{E[(\sum l_i)^2]}$$

$$369 \quad \text{and} \quad E \left[\frac{(\sum l_i^2)^2}{(\sum l_i)^4} \right] = \frac{E[(\sum l_i^2)^2]}{E[(\sum l_i)^4]} \quad (23)$$

370 hold because of the stochastic independence between $\sum l_i^2 / (\sum l_i)^2$ and $\sum l_i$ in this special
371 condition (which follows from inspection of the density; John, 1972). Therefore, by use of
372 equations 16, 17, and 20,

$$\begin{aligned} E[V_{\text{rel}}(\mathbf{S})] &= \frac{1}{p-1} \left(p \frac{E[\sum l_i^2]}{E[(\sum l_i)^2]} - 1 \right) \\ &= \frac{p+2}{pn+2}, \end{aligned}$$

$$373 \quad (24)$$

374 and

$$\begin{aligned} \text{Var}[V_{\text{rel}}(\mathbf{S})] &= \left(\frac{p}{p-1} \right)^2 \left(\frac{E[(\sum l_i^2)^2]}{E[(\sum l_i)^4]} - \left\{ \frac{E[\sum l_i^2]}{E[(\sum l_i)^2]} \right\}^2 \right) \\ &= \frac{4(p-1)(p+2)(n-1)(n+2)}{(pn+2)^2(pn+4)(pn+6)}. \end{aligned}$$

375 (25)

376 These results are exact (valid across any p and n) under multivariate normality.

377

378 *Correlation matrix*

379 Consider the null hypothesis $\mathbf{P} = \mathbf{I}_p$ or $\rho_{ij} = 0$ for $i \neq j$. The moments can conveniently be

380 obtained from the form of average squared correlation (eq. 11). It is well known that, under

381 the assumptions of normality and $\rho_{ij} = 0$ (for $i \neq j$), r_{ij}^2 is distributed as

382 Beta($1/2, (n - 1)/2$), where n is the degree of freedom (e.g., Anderson, 2003). Therefore,

383 under the null hypothesis,

$$\begin{aligned}
 384 \quad & E(r_{ij}^2) = \frac{1}{n}, \\
 385 \quad & \text{Var}(r_{ij}^2) = \frac{2(n-1)}{n^2(n+2)}. \tag{26}
 \end{aligned}$$

386 The expectation of $V_{\text{rel}}(\mathbf{R})$ is simply the average:

$$387 \quad E[V_{\text{rel}}(\mathbf{R})] = \frac{1}{n}. \tag{27}$$

388 This expression is identical to $(p - 1)^{-1}\text{Var}(l_i)$ obtainable from Wagner's (1984) results,

389 except for having the degree of freedom n rather than the sample size N in the denominator.

390 This is because Wagner (1984) considered N uncentered observations with mean 0 without

391 explicitly distinguishing n and N . Most practical analyses would concern data centered at the

392 sample mean, thus should use n rather than N .

393 Derivation of the variance is more complicated than it may seem, because, in

394 principle,

$$\text{Var}[V_{\text{rel}}(\mathbf{R})] = \frac{4}{p^2(p-1)^2} \left[\sum_{i < j} \text{Var}(r_{ij}^2) + \sum_{\substack{i < j, k < l, \\ (i,j) < (k,l)}} 2 \text{Cov}(r_{ij}^2, r_{kl}^2) \right],$$

395 (28)

396 where the latter summation is across all non-redundant pairs. However, it is possible to show
 397 $\text{Cov}(r_{ij}^2, r_{kl}^2) = 0$ under the null hypothesis (Appendix C). Therefore, from equations 26 and
 398 28,

$$399 \quad \text{Var}[V_{\text{rel}}(\mathbf{R})] = \frac{4(n-1)}{p(p-1)n^2(n+2)} \quad (29)$$

400 These expressions are exact for any p and n . Schott (2005) proposed a test for independence
 401 between sets of normal variables based on these moments.

402

403 **Moments under arbitrary conditions**

404 *Covariance matrix*

405 This section considers moments of eigenvalue dispersion indices under arbitrary
 406 covariance/correlation structures and multivariate normality. It is straightforward to obtain
 407 the first two moments of $V(\mathbf{S})$ under arbitrary $\mathbf{\Sigma}$, provided that moments of relevant terms in
 408 equation 12 are available. The results are (Appendix B)

$$\begin{aligned} \text{E}[V(\mathbf{S})] &= \frac{n}{p^2 n_*^2} [(p-n)(\text{tr } \mathbf{\Lambda})^2 + (pn+p-2) \text{tr}(\mathbf{\Lambda}^2)] \\ &= \frac{n}{pn_*^2} [(pn+p-2)V(\mathbf{\Sigma}) + (p-1)(p+2)(\text{tr } \mathbf{\Lambda})^2/p^2], \\ \text{Var}[V(\mathbf{S})] &= \frac{4n}{p^4 n_*^4} \{2(p-n)^2 \text{tr}(\mathbf{\Lambda}^2) (\text{tr } \mathbf{\Lambda})^2 + (p^2n+p^2-4p+2n)[\text{tr}(\mathbf{\Lambda}^2)]^2 \\ &\quad + 4(p-n)(pn+p-2) \text{tr}(\mathbf{\Lambda}^3) \text{tr } \mathbf{\Lambda} \\ &\quad + (2p^2n^2 + 5p^2n + 5p^2 - 12pn - 12p + 12) \text{tr}(\mathbf{\Lambda}^4)\}. \end{aligned} \quad (30)$$

410 The second expression for the expectation comes from the fact $V(\mathbf{\Sigma}) = [p \text{tr}(\mathbf{\Lambda}^2) - (\text{tr } \mathbf{\Lambda})^2]/$
 411 p^2 , and clarifies that the expectation is a linear function of $V(\mathbf{\Sigma})$. These results are exact, and
 412 it is easily verified that they reduce to equations 18 and 21 under the null hypothesis. Profiles
 413 of $\text{E}[V(\mathbf{S})]$ across a range of $V(\mathbf{\Sigma})$ are shown in Figure 2 (top row), under single large

414 eigenvalue conditions with varying p and N , and fixed $\text{tr } \Sigma$ (detailed conditions are described
415 under simulation settings below).

416 Moments of $V_{\text{rel}}(\mathbf{S})$ are more difficult to obtain, as moments of the ratio $\sum l_i^2 / (\sum l_i)^2$
417 do not coincide with the ratios of moments under arbitrary Σ . Here we utilize the following
418 approximations based on the delta method (e.g., Stuart & Ord, 1994: chapter 10):

$$419 \quad \mathbb{E}\left(\frac{X}{Y}\right) \approx \frac{\mathbb{E}(X)}{\mathbb{E}(Y)} - \frac{\text{Cov}(X,Y)}{\mathbb{E}(Y)^2} + \frac{\mathbb{E}(X)\text{Var}(Y)}{\mathbb{E}(Y)^3},$$

$$420 \quad \text{and} \quad \text{Var}\left(\frac{X}{Y}\right) \approx \frac{\mathbb{E}(X)^2}{\mathbb{E}(Y)^2} \left[\frac{\text{Var}(X)}{\mathbb{E}(X)^2} + \frac{\text{Var}(Y)}{\mathbb{E}(Y)^2} - 2 \frac{\text{Cov}(X,Y)}{\mathbb{E}(X)\mathbb{E}(Y)} \right]. \quad (32)$$

421 The approximate moments are (Appendix B):

$$\begin{aligned} \mathbb{E}\left[\frac{\sum l_i^2}{(\sum l_i)^2}\right] &\approx \frac{(\text{tr } \Lambda)^2 + (n+1)\text{tr}(\Lambda^2)}{n(\text{tr } \Lambda)^2 + 2\text{tr}(\Lambda^2)} - \frac{8(n-1)(n+2)}{n[n(\text{tr } \Lambda)^2 + 2\text{tr}(\Lambda^2)]^3} \\ &\quad \times \{n(\text{tr } \Lambda)^3 \text{tr}(\Lambda^3) - n(\text{tr } \Lambda)^2 [\text{tr}(\Lambda^2)]^2 - [\text{tr}(\Lambda^2)]^3 - 2\text{tr } \Lambda \text{tr}(\Lambda^2) \text{tr}(\Lambda^3) \\ &\quad + 3(\text{tr } \Lambda)^2 \text{tr}(\Lambda^4)\}; \\ \text{Var}\left[\frac{\sum l_i^2}{(\sum l_i)^2}\right] &\approx \frac{4(n-1)(n+2)}{n[n(\text{tr } \Lambda)^2 + 2\text{tr}(\Lambda^2)]^4} \\ &\quad \times \{n(\text{tr } \Lambda)^4 [\text{tr}(\Lambda^2)]^2 + 2n(n+1)(\text{tr } \Lambda)^2 [\text{tr}(\Lambda^2)]^3 + 2(n+1)[\text{tr}(\Lambda^2)]^4 \\ &\quad - 4(n-1)(n+2)(\text{tr } \Lambda)^3 \text{tr}(\Lambda^2) \text{tr}(\Lambda^3) + (2n^2 + 3n - 6)(\text{tr } \Lambda)^4 \text{tr}(\Lambda^4) \\ &\quad - 4n(\text{tr } \Lambda)^2 \text{tr}(\Lambda^2) \text{tr}(\Lambda^4) - 4(\text{tr } \Lambda)^4 [\text{tr}(\Lambda^2)]^2\}. \end{aligned} \quad (33)$$

422
423 Inserting these into equation 22 yields the desired moments. The approximate expectation
424 reduces to equation 24 under the null hypothesis, as the higher-order terms cancel out,
425 whereas this is not the case for the approximate variance. Because these expressions are
426 specified by the population eigenvalues alone, they are invariant with respect to orthogonal
427 rotations, as expected from theoretical considerations above. Also, it is easily discerned that
428 these expressions are invariant with respect to uniform scaling of the variables. The accuracy
429 of these approximations will be examined in simulations below.

430 Profiles of the approximation of $E[V_{\text{rel}}(\mathbf{S})]$ across a range of $V_{\text{rel}}(\mathbf{\Sigma})$ are shown in
 431 Figure 2 (middle row) for the same conditions as above. The profiles are nonlinear; $V_{\text{rel}}(\mathbf{S})$
 432 tends to overestimate $V_{\text{rel}}(\mathbf{\Sigma})$ when the latter is small, but tends to slightly underestimate
 433 when the latter is large. The initial decrease of $E[V_{\text{rel}}(\mathbf{S})]$ observed in some profiles appears
 434 to be an artifact of the approximation.

435

436 *Correlation matrix*

437 The expectation of $V_{\text{rel}}(\mathbf{R})$ under arbitrary conditions can be obtained from equation 11 with
 438 r_{ij}^2 replaced by its expectations, which is known to be (e.g., Soper et al., 1917; Ghosh, 1966;
 439 Muirhead, 1982)

$$440 \quad E(r_{ij}^2) = 1 - \frac{(n-1)(1-\rho_{ij}^2)}{n} {}_2F_1\left(1, 1; \frac{n+2}{2}; \rho_{ij}^2\right), \quad i \neq j, \quad (34)$$

441 where

$$442 \quad {}_2F_1(a, b; c; z) = \sum_{k=0}^{\infty} \frac{(a)_k (b)_k}{(c)_k} \frac{z^k}{k!} \quad (35)$$

443 is the hypergeometric function, with $(x)_k = x(x+1) \dots (x+k-1)$ denoting rising factorial
 444 (formally, $(x)_k = \Gamma(x+k) / \Gamma(x)$ with the gamma function $\Gamma(\cdot)$). Taking the average of
 445 equation 34 across all pairs of variables gives the desired expectation, which is non-
 446 asymptotic and exact. It is seen that equation 34 reduces to equation 26 under the null
 447 hypothesis.

448 When $p = 2$, the exact variance of $V_{\text{rel}}(\mathbf{R})$ is equal to that of the single squared
 449 correlation coefficient (Ghosh, 1966):

$$450 \quad \text{Var}(r_{ij}^2) = \frac{(n-1)(n+1)(1-\rho_{ij}^2)}{2n} \left[F - nF' - \frac{2(n-1)(1-\rho_{ij}^2)}{n(n+1)} F^2 \right], \quad (36)$$

451 where $F = {}_2F_1(1, 1; (n+2)/2; \rho_{ij}^2)$ and $F' = (F-1)/2\rho_{ij}^2 = {}_2F_1(1, 2; (n+4)/2; \rho_{ij}^2)/$
 452 $(n+2)$; this last form is preferred to avoid numerical instability when ρ_{ij}^2 is close to 0. This

453 expression reduces to equation 26 under the null hypothesis. When $p > 2$, we cannot ignore
 454 covariances between squared correlation coefficients (see eq. 28). Unfortunately, no exact
 455 expression seems available for this quantity in the literature, so we resort to approximation.
 456 One option is to utilize the following heuristic approximation from Pan & Frank's (2004)
 457 approach (Appendix D):

$$458 \quad \text{Cov}(r_{ij}^2, r_{kl}^2) \approx 4 E(r_{ij}) E(r_{kl}) \text{Cov}(r_{ij}, r_{kl}) + 2[\text{Cov}(r_{ij}, r_{kl})]^2. \quad (37)$$

459 Exact and large-sample asymptotic expressions under multivariate normality are available for
 460 $E(r_{ij})$ and $\text{Cov}(r_{ij}, r_{kl})$, respectively (e.g., Soper et al., 1917; Ghosh, 1966; Olkin & Siotani,
 461 1976):

$$462 \quad E(r_{ij}) = \frac{2}{n} \left[\frac{\Gamma\left(\frac{n+1}{2}\right)}{\Gamma\left(\frac{n}{2}\right)} \right]^2 {}_2F_1\left(\frac{1}{2}, \frac{1}{2}; \frac{n+2}{2}; \rho_{ij}^2\right), \quad (38)$$

463 Inserting equations 36–38 to equation 28 yields an approximation for $\text{Var}[V_{\text{rel}}(\mathbf{R})]$ in
 464 arbitrary conditions. In terms of consistency, $E(r_{ij})$ and $\text{Var}(r_{ij}^2)$ could be replaced by
 465 respective asymptotic expressions (e.g., Ghosh, 1966; Olkin & Siotani, 1976), but this does
 466 not seem to yield improved accuracy or substantial computational gain.

467 In practice, the variance based on equation 28 can be difficult to calculate for large p ,
 468 because there are $\sim p^4/4$ pairs of correlation coefficients to evaluate. For such cases, the
 469 following asymptotic expression based on Konishi's (1979) theory may be more useful
 470 (Appendix E):

$$471 \quad \text{Var}[V_{\text{rel}}(\mathbf{R})] \approx \frac{8}{p^2(p-1)^2n} \sum_{\alpha, \beta=1}^p \lambda_{\alpha}^2 \lambda_{\beta}^2 \left[\delta_{\alpha\beta} - (\lambda_{\alpha} + \lambda_{\beta}) \sum_{i=1}^p v_{i\alpha}^2 v_{i\beta}^2 + \sum_{i,j=1}^p \rho_{ij}^2 v_{i\alpha}^2 v_{j\beta}^2 \right], \quad (39)$$

472 where δ_{ij} is the Kronecker delta (equals 1 for $i = j$ and 0 otherwise) and $v_{i\alpha}$ is the (i, α) -th
 473 element of the population eigenvector matrix \mathbf{Y} . For $p = 2$, the accuracy of this expression

474 can be compared with the exact expression (Fig. 3); visual inspection of the profiles suggest
475 that the accuracy is satisfactory past $N = 32-64$, except around $V_{\text{rel}}(\mathbf{P}) = 0$ where the
476 asymptotic expression diminishes to 0 (as expected from its formula; Appendix E). For $p > 2$,
477 accuracies of these approximate expressions are to be evaluated with simulations below.

478 Importantly, the expectation of $V_{\text{rel}}(\mathbf{R})$ is a function of $\rho^{2'}$ s rather than $\mathbf{\Lambda}$, and cannot

479 be specified by the latter alone in general. For instance, consider $\begin{pmatrix} 1 & 0.9 & 0 \\ 0.9 & 1 & 0 \\ 0 & 0 & 1 \end{pmatrix}$ and

480 $\begin{pmatrix} 1 & 0.9/\sqrt{2} & 0 \\ 0.9/\sqrt{2} & 1 & 0.9/\sqrt{2} \\ 0 & 0.9/\sqrt{2} & 1 \end{pmatrix}$, both of which are valid correlation matrices. These matrices

481 have identical eigenvalues $\mathbf{\Lambda} = \text{diag}(1.9, 1.0, 0.1)$ and hence an identical value of $V_{\text{rel}}(\mathbf{P}) (=$
482 $0.27)$, but $E[V_{\text{rel}}(\mathbf{R})]$ with $n = 10$ are 0.3326 and 0.3156, respectively. Although the
483 difference diminishes as n increases, this example highlights that the distribution of $V_{\text{rel}}(\mathbf{R})$
484 is partly dependent on population eigenvectors.

485 Profiles of $E[V_{\text{rel}}(\mathbf{R})]$ across a range of $V_{\text{rel}}(\mathbf{P})$ are shown in Figure 2 (bottom row),
486 under the same conditions as above. These conditions with single large eigenvalues are
487 special cases in which $E[V_{\text{rel}}(\mathbf{R})]$ can be specified by $V_{\text{rel}}(\mathbf{P})$ regardless of eigenvectors
488 (detailed in Appendix A). Indeed, the profiles of the expectations are invariant across p in
489 these special conditions. In some way similar to $V_{\text{rel}}(\mathbf{S})$, $V_{\text{rel}}(\mathbf{R})$ tends to overestimate and
490 underestimate small and large values of $V_{\text{rel}}(\mathbf{P})$, respectively.

491

492 **Bias correction**

493 Some authors (Cheverud et al., 1989; Torices & Muñoz-Pajares, 2015) have suggested
494 correcting the sampling bias in eigenvalue dispersion indices by means of subtracting
495 Wagner's (1984) null expectation from empirical values. This method could potentially be
496 used for V and V_{rel} with the correct null expectations derived above, to obtain estimators that

497 is unbiased under the null hypothesis. For $V_{\text{rel}}(\mathbf{S})$ and $V_{\text{rel}}(\mathbf{R})$, however, the subtraction
 498 truncates the upper end of the range, potentially compromising interpretability. To avoid this,
 499 it might be desirable to scale these indices in a way analogous to the adjusted coefficient of
 500 determination in regression analysis (e.g., Cramer, 1987):

$$501 \quad \bar{V}_{\text{rel}}(\mathbf{S}) = 1 - \frac{1 - V_{\text{rel}}(\mathbf{S})}{1 - E_{\text{null}}[V_{\text{rel}}(\mathbf{S})]} = \frac{pn+2}{p(n-1)} V_{\text{rel}}(\mathbf{S}) - \frac{p+2}{p(n-1)},$$

$$502 \quad \bar{V}_{\text{rel}}(\mathbf{R}) = 1 - \frac{1 - V_{\text{rel}}(\mathbf{R})}{1 - E_{\text{null}}[V_{\text{rel}}(\mathbf{R})]} = \frac{n}{n-1} V_{\text{rel}}(\mathbf{R}) - \frac{1}{n-1}, \quad (40)$$

503 where $E_{\text{null}}(\cdot)$ denotes expectation under the null conditions (eqs. 24 and 27). This
 504 adjustment inflates the variance by the factor of $1/[1 - E_{\text{null}}(V_{\text{rel}})]^2$. Furthermore, these
 505 adjusted indices are unbiased only under the null hypothesis (Armbruster et al., 2009; and
 506 trivially the case of complete integration), and uniformly underestimate the corresponding
 507 population values otherwise (Fig. S2). As the population value gets away from 0, the adjusted
 508 index is outperformed by the unadjusted one in both precision and bias (Fig. S3). It should
 509 also be borne in mind that the profiles of expectations are nonlinear and dependent on N (Fig.
 510 2). As the adjusted indices will be increasingly conservative for small N , it is questionable
 511 whether they can be used for comparing samples with different N , as originally intended by
 512 Cheverud et al. (1989). For these reasons, use of this adjustment would be restricted to
 513 estimation of the population value near 0 (up to 0.1–0.2, depending on p and N).

514 On the other hand, a global unbiased estimator of $V(\boldsymbol{\Sigma})$ can be derived from above
 515 results:

$$\begin{aligned} \tilde{V}(\mathbf{S}) &= \frac{n_*^2}{n(pn + p - 2)} \left(pV(\mathbf{S}) - \frac{(p-1)(p+2)}{p^2(n-1)(n+2)} [(n+1)(\text{tr} \mathbf{S})^2 - 2 \text{tr}(\mathbf{S}^2)] \right) \\ &= \frac{1}{p^2 n(n-1)(n+2)} [(pn+2)(\text{tr} \mathbf{A})^2 - (p+n+1) \text{tr}(\mathbf{A}^2)]. \end{aligned}$$

516 (41)

517 Its variance can be similarly obtained as

$$\begin{aligned} \text{Var}[\tilde{V}(\mathbf{S})] = & \frac{4}{p^4 n(n-1)(n+2)} \{2(n-1)(n+2) \text{tr}(\mathbf{\Lambda}^2) (\text{tr} \mathbf{\Lambda})^2 \\ & + (p^2 n + 4p + 2n + 2) [\text{tr}(\mathbf{\Lambda}^2)]^2 - 4p(n-1)(n+2) \text{tr}(\mathbf{\Lambda}^3) \text{tr} \mathbf{\Lambda} \\ & + (2p^2 n^2 + 3p^2 n - 6p^2 - 4pn - 4) \text{tr}(\mathbf{\Lambda}^4)\}, \end{aligned} \tag{42}$$

518

519 which reduces to $4(p-1)(p+2)\sigma^8/p^3 n(n-1)(n+2)$ under the null hypothesis.

520 Comparison with equations 21 and 30 suggests that this variance is smaller than that of $V(\mathbf{S})$,

521 especially under the null hypothesis. Therefore, $\tilde{V}(\mathbf{S})$ seems superior in both precision and

522 bias and can be used when estimation of $V(\mathbf{\Sigma})$ is desired. It can be used to compare multiple

523 samples, provided that its sensitivity to overall scaling is not of concern, e.g., comparison

524 between closely related taxa.

525

526 **Simulation**

527 **Methods**

528 Simulations were conducted under various conditions in order to understand sampling

529 properties of the eigenvalue dispersion indices. All simulations were done assuming

530 multivariate normality, with varying population covariance matrix $\mathbf{\Sigma}$, number of variables p

531 ($= 2, 4, 8, 16, 32, 64, 128, 256$, and 1024), and sample size N ($= 4, 8, 16, 32, 64, 128$, and

532 256).

533 For every p , the following population eigenvalue conformations were considered: 1)

534 the null condition, 2) q -large λ conditions, 3) a linearly decreasing λ condition, and 4) a

535 quadratically decreasing λ condition (see Fig. 4 for examples). The null condition is where all

536 population eigenvalues are equal in magnitude ($V_{\text{rel}}(\mathbf{\Sigma}) = 0$), corresponding to the null

537 hypothesis of sphericity (Fig. 4A). The q -large λ conditions are where the first q ($= 1, 2$, and

538 4 , provided $p > q$) population eigenvalues are equally large and the remaining $p - q$ ones are

539 equally small ($\lambda_1 = \dots = \lambda_q > \lambda_{q+1} = \dots = \lambda_p$), with varying $V_{\text{rel}}(\mathbf{\Sigma})$ ($= 0.1, 0.2, 0.4, 0.6,$
540 and 0.8 ; Fig. 4B–G). The necessary condition $\lambda_p \geq 0$ constrains possible combinations of q
541 and $V_{\text{rel}}(\mathbf{\Sigma})$: the possible choices of $V_{\text{rel}}(\mathbf{\Sigma})$ are 0.1 – 0.8 , 0.1 – 0.4 , and 0.1 – 0.2 for $q = 1, 2$, and
542 4 , respectively (Appendix A). These conditions are intended to represent hypothetical
543 situations where only a few components of meaningful signals are present in the population.
544 Individual eigenvalues were calculated for each combination of p , q , and $V_{\text{rel}}(\mathbf{\Sigma})$ as described
545 in Appendix A. The linearly and quadratically decreasing λ conditions are where the
546 population eigenvalues are linearly and quadratically, respectively, decreasing in magnitude
547 (Fig. 4H; Appendix A), in which cases the value of $V_{\text{rel}}(\mathbf{\Sigma})$ is fixed for a given p . These
548 conditions are intended to represent covariance structures with gradually decreasing signals.
549 One might claim that some of these situations, especially q -large λ conditions, are too
550 simplistic and biologically unrealistic, but these simple settings enable us to clarify
551 systematic relationships between parameters and sampling properties. The primary aim here
552 is to explore sampling properties across a wide range of parameters, rather than focusing on
553 biologically “realistic” regions (which would depend on specific organismal systems). It
554 should also be recalled that sampling error alone can yield gradually decreasing patterns of
555 sample eigenvalues typically observed in empirical datasets (see above and below).

556 For sake of simplicity, all population covariance matrices were scaled to ensure
557 $V(\mathbf{\Sigma}) = V_{\text{rel}}(\mathbf{\Sigma})$; that is, $\text{tr } \mathbf{\Sigma} = p(p - 1)^{-1/2}$. This scaling also makes the magnitude of $V(\mathbf{\Sigma})$
558 comparable across varying p . In addition, a population covariance matrix $\mathbf{\Sigma}$ was constructed
559 from a predefined set of eigenvalues such that its diagonal elements are equal: $\sigma_{ii} = \bar{\lambda} =$
560 $(p - 1)^{-1/2}$ for all i , thereby enforcing $\mathbf{\Sigma} = (p - 1)^{-1/2} \mathbf{P}$. This construction allows for
561 examining both covariance and correlation matrices with the same population V_{rel} from a
562 single simulated dataset, saving computational resources. $\mathbf{\Sigma}$ was constructed from $\mathbf{\Lambda}$ by the
563 iterative Givens rotation algorithm of Davies & Higham (2000), which is guaranteed to

564 converge within $p - 1$ iterations. This algorithm was implemented as coded by Waller (2020),
565 but with the following modifications for reproducibility: no random orthogonal rotation was
566 involved at the initial stage, and rotation axes were chosen in a fixed order. It should be noted
567 that the rotations involved—choice of eigenvectors—would in general influence distributions
568 of $V_{\text{rel}}(\mathbf{R})$, except for certain special cases including the 1-large λ condition (Appendix A). It
569 is impractical to exhaustively examine numerous possible conformations of eigenvectors, so
570 only the single conformation generated by this algorithm was used for each combination of
571 parameters.

572 The eigenvalues of a sample covariance matrix were obtained from singular value
573 decomposition of the data matrix, as the singular values squared and then divided by n_* (see,
574 e.g., Jolliffe, 2002). When $p > N - 1$, 0's were appended to this vector so that p sample
575 eigenvalues were present. Data were centered at the sample mean before the decomposition,
576 therefore $n = N - 1$. It was chosen that $n_* = n$. The eigenvalues for a sample correlation
577 matrix were obtained similarly from the sample-mean-centered data scaled with the sample
578 standard deviation for each variable.

579 To summarize, each set of simulations consists of the following steps: 1) define a
580 desired set of eigenvalues $\mathbf{\Lambda}$; 2) construct the population covariance matrix $\mathbf{\Sigma}$ with the
581 rotation algorithm explained above; 3) generate N i.i.d. normal observations from $N_p(\mathbf{0}, \mathbf{\Sigma})$;
582 4) eigenvalues of sample covariance and correlation matrices were obtained from singular
583 value decomposition of the sample-mean-centered data; 5) $V(\mathbf{S})$, $V_{\text{rel}}(\mathbf{S})$, and $V_{\text{rel}}(\mathbf{R})$ were
584 calculated from the eigenvalues; 6) the steps 3–5 were iterated for 5,000 times in total with
585 the same N and $\mathbf{\Sigma}$. The simulations were conducted on the R environment version 3.5.3 (R
586 Core Team, 2019). The function “genhypergeo” of the package “hypergeo” (Hankin, 2015)
587 was used to evaluate the hypergeometric function in the moments of $V_{\text{rel}}(\mathbf{R})$. The time-
588 consuming calculation of $\text{Var}[V_{\text{rel}}(\mathbf{R})]$ from equations 28 and 36–38 was aided by a C++

589 code via the package “Rcpp” (Eddelbuettel & Balamuta, 2018). The codes are provided as
590 Supplementary Material.

591

592 **Results**

593 Examined individually, sample eigenvalues were biased estimators of population eigenvalues,
594 as expected. Selected eigenvalue distributions of sample covariance and correlation matrices
595 are shown in Figures 4 and S1, respectively. Typically, the first few eigenvalues were
596 overestimated, with the rest being underestimated. Note that gradually decreasing scree-like
597 profiles of sample eigenvalues typical of empirical datasets can arise even when most
598 population eigenvalues are identical in magnitude. The sampling biases decreases as N
599 increases. These overall trends were similarly observed for correlation matrices, although the
600 upper tail of the largest eigenvalue tended to be truncated for correlation matrices because of
601 the constraint $\text{tr } \mathbf{R} = p$, effectively cancelling the tendency of overestimation in this
602 eigenvalue (Fig. S1).

603 Sampling distributions of $V(\mathbf{S})$ are shown in Figures 5 and S4–S6, and their summary
604 statistics are shown in Tables 1 and S1. Distributions were unimodal but highly skewed with
605 long upper tails, especially when N or p is small. As expected, sampling dispersion decreases
606 consistently with increasing N , with skewness decreasing at the same time. Interestingly, the
607 shape of distribution does not visibly change with increasing p , at least with moderately large
608 N (≥ 32 , say). In all conditions, $V(\mathbf{S})$ tended to overestimate the population value $V(\mathbf{\Sigma})$.
609 Increasing $V(\mathbf{\Sigma})$ drastically increased sampling dispersion and skewness, whereas increasing
610 q with a fixed $V(\mathbf{\Sigma})$ decreased sampling dispersion without changing the mean as much.
611 Sampling distributions of $V(\mathbf{S})$ under linearly and quadratically decreasing λ conditions look
612 similar to those under q -large λ conditions with similar $V(\mathbf{\Sigma})$ values for the respective p . The
613 expressions of the expectation and variance of $V(\mathbf{S})$ almost always coincided with the

614 sampling mean and variance within a reasonable range of random fluctuations (as expected,
615 since those results are exact).

616 Results for $V_{\text{rel}}(\mathbf{S})$ are summarized in Figures 6 and S6–S8 and Tables 2 and S2.
617 Distributions were unimodal within the range (0, 1), except when $N = 4$ and $p = 2$ where the
618 distribution was essentially uniform. As was the case for $V(\mathbf{S})$, the sampling dispersion of
619 $V_{\text{rel}}(\mathbf{S})$ decreased drastically with increasing N , and to some extent with increasing p , while
620 the shape of distribution does not seem to change remarkably with increasing p past certain N .
621 $V_{\text{rel}}(\mathbf{S})$ tended to overestimate the population value $V_{\text{rel}}(\mathbf{\Sigma})$, except when the latter is rather
622 large (= 0.8) where slight underestimation was observed. With increasing q for a fixed
623 $V_{\text{rel}}(\mathbf{\Sigma})$, the distributions tended to shrink, but the sampling bias remained virtually
624 unchanged or slightly increased. In the null conditions, the exact expressions of the
625 expectation and variance performed perfectly (as expected). The approximate expectation for
626 arbitrary conditions derived above yielded substantially smaller values than the empirical
627 means when N is small; however, the approximation worked satisfactorily with moderate N
628 (≥ 16 – 32), with the deviations from empirical means mostly falling within 2 standard error
629 units. In addition, the approximate expectation worked rather well, even with small N , under
630 either A) the q -large λ conditions with $q = 2$ and $V_{\text{rel}}(\mathbf{\Sigma}) = 0.4$, B) same with $q = 4$, or C)
631 linearly and quadratically decreasing λ conditions with moderately large p (≥ 16). Other
632 conditions held constant, the accuracy of the approximate expectation in absolute scale
633 tended to slightly improve with increasing p , effectively balancing with the decreasing
634 sampling dispersion, so that the relative bias in standard error unit remains almost invariant
635 across varying p . The approximate variance for arbitrary conditions derived above yielded
636 substantially larger values than the empirical variance, except under the q -large λ conditions
637 with $q = 1$ and $V_{\text{rel}}(\mathbf{\Sigma}) = 0.8$ where it yielded smaller values. Nevertheless, with moderately
638 large N (≥ 64), the inaccuracy typically decreased to $<5\%$ in the scale of standard deviation

639 (SD scale hereafter), except under the linearly and quadratically decreasing λ conditions with
640 moderately large p (≥ 16), where it was more accurate.

641 Results for $V_{\text{rel}}(\mathbf{R})$ are summarized in Figures 7, S6, S9, and S10 and Tables 3 and S3.
642 Distributions were unimodal within the range (0, 1), except when $p = 2$ and $N \leq 8$ where an
643 additional peak is usually present near 0. The overall response to varying p and N is largely
644 similar to that of $V_{\text{rel}}(\mathbf{S})$, although the shape of distribution was substantially different for
645 small N . As expected from the theoretical expectations noted above, $V_{\text{rel}}(\mathbf{R})$ tends to
646 overestimate the population value $V_{\text{rel}}(\mathbf{P})$ when the latter is small but tends to underestimate
647 it when $V_{\text{rel}}(\mathbf{P}) = 0.8$. The expressions of expectation for the null and arbitrary conditions
648 and variance for the null condition derived above showed almost perfect match with the
649 empirical means and variances (as expected). The heuristic approximation of the variance of
650 $V_{\text{rel}}(\mathbf{R})$ for arbitrary conditions using equations 28 and 36–38 yielded larger values than the
651 empirical variances in all cases, except when $V_{\text{rel}}(\mathbf{P}) = 0.8$ where slight underestimation was
652 observed. In all cases, the error of this expression decreased to ~0–2% in the SD scale—
653 statistically indistinguishable from random fluctuation with 5000 iterations—for moderately
654 large N (typically ≥ 64 –128, occasionally ≥ 16 –32). The asymptotic variance of $V_{\text{rel}}(\mathbf{R})$ with
655 equation 39 behaved more idiosyncratically. It yielded similar values to the previous
656 expression, overestimating the true values, under A) the q -large λ conditions with $q = 1$ and
657 $V_{\text{rel}}(\mathbf{P}) = 0.1$ –0.6, B) same with $q = 2$ and $V_{\text{rel}}(\mathbf{P}) = 0.1$ –0.2 except when $p = 4$, and C)
658 the quadratically decreasing λ conditions with $p = 4$; whereas it yielded smaller values than
659 the true values under a) the q -large λ conditions with $q = 1$ and $V_{\text{rel}}(\mathbf{P}) = 0.8$, b) same with
660 $q = 2$ and $V_{\text{rel}}(\mathbf{P}) = 0.4$, c) same with $q = 4$, d) same with $q = 2$ and $p = 4$, e) the linearly
661 decreasing λ conditions, and f) the quadratically decreasing λ conditions except when $p = 4$.
662 This expression was more accurate than the previous one in the cases a and b, but more
663 inaccurate in other cases. Under some conditions, relative error can be extremely large (10–

664 300% in SD scale with $N = 256$), especially when the smallest population eigenvalue was
665 small in magnitude (<0.1). A practical advantage of this approximation over the previous one
666 may lie in the computational resource required for large p . With the present R
667 implementation, evaluation of this expression is faster by a factor of thousands than that of
668 the previous one for a correlation matrix with $p = 1024$ (~ 1 versus ~ 1500 CPU seconds on a
669 regular desktop PC), as the amount of computation increases drastically as p grows (the latter
670 took only ~ 5 CPU seconds for $p = 256$).

671

672 **Discussion**

673 Eigenvalue dispersion indices can be calculated for covariance or correlation matrices in
674 similar ways, but implications are rather different. On the one hand, the relative eigenvalue
675 variance of a sample covariance matrix $V_{\text{rel}}(\mathbf{S})$ is a test statistic for sphericity (John, 1972;
676 Sugiura, 1972; Nagao, 1973), and is thus interpreted as a measure of eccentricity of variation,
677 be it due to large variation of a single trait or covariation between traits. Interpretation of the
678 unstandardized eigenvalue variance of a sample covariance matrix $V(\mathbf{S})$ is less
679 straightforward, but it can potentially be useful in comparing eccentricity between samples
680 when the sensitivity to overall scaling is not of concern, primarily for the presence of an
681 unbiased estimator of the corresponding population value with a known variance (eq. 41). On
682 the other hand, the relative eigenvalue variance of a sample correlation matrix $V_{\text{rel}}(\mathbf{R})$ is
683 identical to the average of the squared correlation coefficients across all pairs of traits
684 (Durand & Le Roux, 2017; see above). The average squared correlation is another commonly
685 used index of phenotypic integration (e.g., Cheverud et al., 1983), but its equivalence to
686 $V_{\text{rel}}(\mathbf{R})$ seems to have been overlooked, apart from an empirical confirmation by Haber's
687 (2011) simulations. Obviously, the choice between covariance and correlation should be
688 made according to the scope of individual analyses (Klingenberg, 1996; Hansen & Houle,

689 2008; Pavlicev et al., 2009; Goswami & Polly, 2010; see also Machado et al., 2019 for an
690 interesting discussion). Usual caveats for the choice between covariance and correlation is
691 also pertinent here (Jolliffe, 2002): covariance between traits have clear interpretability only
692 if all traits are in the same unit. This is despite that $V_{\text{rel}}(\mathbf{S})$ is dimensionless and independent
693 of the overall scaling of traits.

694 Perhaps the most remarkable finding of this study is that the distributions of $V_{\text{rel}}(\mathbf{S})$
695 and $V_{\text{rel}}(\mathbf{R})$ do not seem to vary much with the number of variables p itself. The above
696 expressions for the (approximate) mean and variance can be calculated for any p , and
697 simulation results indicate that their accuracy are not compromised by large p (Figs. 5–7 and
698 S4–S10; Tables 1–3 and S1–S3). This finding highlights potential applicability of these
699 measures to high-dimensional phenotypic data. Nevertheless, it should be remembered that,
700 when p exceeds the degree of freedom n , $p - n$ of the sample eigenvalues are 0 and hence
701 the corresponding population eigenvalues are not estimable. In addition, the first sample
702 eigenvector tends to be consistently diverged from the first population eigenvector in high-
703 dimensional settings (Johnstone, 2007; Johnstone & Paul, 2018).

704

705 **Applications and limitations**

706 The present analytic results assume simple independent sampling from a multivariate normal
707 population and the Wishart-ness of the cross-product matrix. For some biological datasets,
708 certain modifications would be required. A simple example is data consisting of multiple
709 groups with potentially heterogeneous means, e.g., intraspecific variation calculated from
710 multiple geographic populations or sexes. If uniform Σ across groups can be assumed, cross-
711 product matrices from the data centered at the respective group's sample mean can be
712 summed across groups to obtain a pooled cross-product matrix, which is, by the additivity of
713 Wishart variables, distributed as $W_p(\Sigma, N - g)$, where N is the total sample size and g is the

714 number of groups. That is, all above expressions can be applied by simply using the degree of
715 freedom $N - g$. A similar correction is required when eigenvalue dispersion indices are
716 applied to partial correlation matrices (Torices & Méndez, 2014; Torices & Muñoz-Pajares,
717 2015). The distribution of sample partial correlation coefficients in p_1 variables
718 conditionalized on p_2 other variables based on N observations is the same as that of ordinary
719 correlation coefficients based on $N - p_2$ observations with the same corresponding
720 parameters (e.g., Anderson, 2003: p. 143), so the appropriate degree of freedom is $n - p_2$.
721 Both of these procedures are essentially to examine the covariance/correlation matrix of
722 residuals after conditionalizing on covariates.

723 Present analytical results may not be applicable to those empirical covariance or
724 correlation matrices that are not based on a Wishart matrix. Primary examples are the
725 empirical \mathbf{G} matrices estimated from variance components in MANOVA designs or obtained
726 as likelihood-based estimators in mixed models (e.g., Lynch & Walsh, 1998; Meyer &
727 Kirkpatrick, 2005). Mean-standardization, a method recommended for analyzing \mathbf{G} matrices
728 (Houle, 1992; Hereford et al., 2004; Hansen & Houle, 2008), can also violate the
729 distributional assumption if sample means are used in the standardization. If eigenvalue
730 dispersion indices are to be used with any of these methods, their sampling properties need to
731 be critically assessed (see also Sztepanacz & Blows, 2017).

732 The assumption of multivariate normality may be intrinsically inappropriate for some
733 types of data, including meristic (count) data, compositional or proportional data, angles, and
734 directional data. Application of eigenvalue dispersion indices (or indeed
735 covariance/correlation itself) to such data types would require special treatments, which are
736 beyond the scope of this study. Needless to say, the appropriateness of multivariate normality
737 should be critically assessed in every empirical dataset when the present analytic results are

738 to be applied, even if the data type is conformable with normality. Robustness of the above
739 results against non-normality may deserve some investigations.

740

741 **Shape variables**

742 The application to traditional morphometric datasets, in which all variables are typically
743 measured in the same unit, is rather straightforward, as covariance/correlation in such
744 variables has full interpretability in the Euclidean trait space. Quite often, component(s) of
745 little interest, e.g., size, are removed by transforming raw data, inducing covariation in
746 resultant variables that needs to be taken into account in hypothesis tests. The most typical
747 transformation is the division by an isometric or allometric size variable (Jolicoeur, 1963;
748 Mosimann, 1970; Mosimann & James, 1979; Darroch & Mosimann, 1985; Klingenberg,
749 1996, 2016), which can conveniently be done by orthogonal projection in the space of log-
750 transformed variables. The projection of objects onto the hyperplane orthogonal to a subspace,
751 say, the column space of \mathbf{H} ($p \times k$ full-column-rank matrix; for the isometric size vector,
752 $\mathbf{H} = p^{-1/2} \mathbf{1}_p$), can be done by right-multiplying the data by the projection matrix (e.g.,
753 Burnaby, 1966):

$$\mathbf{I}_p - \mathbf{H}(\mathbf{H}^T \mathbf{H})^{-1} \mathbf{H}^T.$$

754 Therefore, the covariance matrix in the resultant space can be obtained from that in the
755 original space $\mathbf{\Sigma}$ as

$$[\mathbf{I}_p - \mathbf{H}(\mathbf{H}^T \mathbf{H})^{-1} \mathbf{H}^T] \mathbf{\Sigma} [\mathbf{I}_p - \mathbf{H}(\mathbf{H}^T \mathbf{H})^{-1} \mathbf{H}^T].$$

756 Under the null condition ($\mathbf{\Sigma} = \sigma^2 \mathbf{I}_p$) specifically, this becomes

$$\sigma^2 [\mathbf{I}_p - \mathbf{H}(\mathbf{H}^T \mathbf{H})^{-1} \mathbf{H}^T],$$

757 because the projection matrix is symmetric and idempotent. This transformation renders k
758 eigenvalues to be 0 by construction. When the focus is on covariance rather than correlation,
759 these null eigenvalues can optionally be dropped from calculation of eigenvalue mean and

760 dispersion, so that the resultant dispersion index quantifies eccentricity of variation in the
761 subspace of interest. Theories derived above can be applied with minimal modifications,
762 although the asymptotic variance of $V_{\text{rel}}(\mathbf{R})$ (eq. 39) may not work well due to singularity.
763 These discussions assume that independence between the raw variables can at least
764 hypothetically be conceived, e.g., when measurements are taken from non-overlapping parts
765 of an organism. If measurements are taken from overlapping parts of an organism, then the
766 dependence between variables due to the geometric configuration needs to be taken into
767 consideration on a case-by-case basis (Mitteroecker et al., 2012).

768 Application to landmark-based geometric morphometric data is more complicated,
769 primarily because the shape space of Procrustes-aligned landmark configurations is (typically
770 a restricted region of) the surface of a hyper(hemi)sphere (e.g., Slice, 2001). In practice,
771 however, empirical analyses are usually conducted on a Euclidean tangent space instead of
772 the shape space itself, assuming that the former gives a satisfactory metric approximation of
773 the latter (e.g., Rohlf, 1999; Marcus et al., 2000; Klingenberg, 2020). It will in principle be
774 possible to obtain an approximate population covariance matrix of landmark coordinates in
775 this tangent space from a hypothetical covariance matrix of raw landmark coordinates before
776 alignment, by using the orthogonal projection method mentioned above with such an \mathbf{H}
777 whose columns represent the non-shape components. Such a set of vectors can be obtained
778 either as a basis of the complement of the tangent space (see Rohlf & Bookstein, 2003) or
779 directly from the consensus configuration (Klingenberg, 2020). The stereographic projection
780 might potentially be preferred over the orthogonal projection in projecting aligned empirical
781 configurations in the shape space to the tangent space—not to be confused with the projection
782 from the raw space to the tangent space—for purposes of analysing eccentricity of variation.
783 This is because the stereographic projection tends to approximately preserve multivariate
784 normality of the raw coordinates into the resultant tangent space, provided that the variation

785 in the raw coordinates is sufficiently small and that the mean configuration is taken as the
786 point of tangency (Rohlf, 1999). It should be noted that Procrustes superimposition changes
787 perceived patterns of variation in landmark coordinates, often rather drastically (Rohlf &
788 Slice, 1990; Walker, 2000). Such phenomena are probably to be seen as properties of shape
789 variables, rather than necessarily nuisance artifacts (Klingenberg, 2021). Whether these can
790 be of concern or not would depend on the scope of individual analyses (see also Machado et
791 al., 2019).

792

793 **Phylogenetic data**

794 So far data were assumed to be i.i.d. multivariate normal variables. Important applications in
795 evolutionary biology involve non-i.i.d. observations, most notably phylogenetically
796 structured data in which N observations (typically species) have covariance due to shared
797 evolutionary histories. Trait covariation at the interspecific level may have interpretations
798 under certain evolutionary models (Felsenstein, 1988; Hansen & Martins, 1996; Revell &
799 Harmon, 2008; Uyeda & Harmon, 2014; Caetano & Harmon, 2019). Under the assumption
800 that trait evolution along phylogeny can be described by (potentially a mixture of) linear
801 invariant Gaussian models, such as the Brownian motion (BM), accelerating–decelerating
802 (ACDC; or early burst), and Ornstein–Uhlenbeck (OU) processes, the joint distribution of the
803 observations is known to be multivariate normal (Hansen & Martins, 1996; Manceau et al.,
804 2017; Mitov et al., 2020). A brief overview is given below for potential applications of the
805 present analytic results to phylogenetically structured data.

806 For BM and its modifications, including BM with a trend, Pagel’s λ , and ACDC
807 models, the covariance matrix of the $N \times p$ dimensional data \mathbf{X} can be factorized into the
808 intertrait and interspecific components in the form of Kronecker product: $\mathbf{\Sigma} \otimes \mathbf{\Psi}$, where $\mathbf{\Psi}$ is
809 the $N \times N$ interspecific covariance matrix specified by the underlying phylogeny and

810 parameter(s) specific to the evolutionary model (see Hansen & Martins, 1996; Freckleton et
 811 al., 2002; Blomberg et al., 2003; Clavel et al., 2015; Mitov et al., 2020). In this case the data
 812 can conveniently be considered as a matrix-variate normal variable (see Gupta & Nagar,
 813 1999): $\mathbf{X} \sim N_{N,p}(\mathbf{M}, \mathbf{\Sigma} \otimes \mathbf{\Psi})$, where \mathbf{M} is a $N \times p$ matrix of means. If $\mathbf{\Psi}$ is known a priori—
 814 that is, we have an accurate phylogenetic hypothesis and parameters—the change of variables
 815 $\mathbf{Y} = \mathbf{\Psi}^{-1/2}\mathbf{X}$ leads to $\mathbf{Y} \sim N_{N,p}(\mathbf{\Psi}^{-1/2}\mathbf{M}, \mathbf{\Sigma} \otimes \mathbf{I}_N)$, thereby essentially avoiding the
 816 complication of dependence between observations. This procedure is widely recognized as
 817 the (phylogenetic) generalized least squares (GLS; e.g., Grafen, 1989; Martins & Hansen,
 818 1997; Rohlf, 2001; Symonds & Blomberg, 2014). If we know the population mean \mathbf{M} in
 819 addition, then the cross-product matrix centered at it,

$$(\mathbf{Y} - \mathbf{\Psi}^{-1/2}\mathbf{M})^T (\mathbf{Y} - \mathbf{\Psi}^{-1/2}\mathbf{M}) = (\mathbf{X} - \mathbf{M})^T \mathbf{\Psi}^{-1} (\mathbf{X} - \mathbf{M}),$$

820 is distributed as $W_p(\mathbf{\Sigma}, N)$. If we don't exactly know \mathbf{M} yet still assume $\mathbf{M} = \mathbf{1}_N \boldsymbol{\mu}^T$ with the
 821 unknown but uniform $p \times 1$ mean vector $\boldsymbol{\mu}$, then the GLS estimate of the mean $\hat{\boldsymbol{\mu}} =$
 822 $(\mathbf{1}_N^T \mathbf{\Psi}^{-1} \mathbf{1}_N)^{-1} \mathbf{1}_N^T \mathbf{\Psi}^{-1} \mathbf{X}$ (e.g., Martins & Hansen, 1997) can be used to obtain a sample-
 823 mean-centered cross-product matrix

$$(\mathbf{Y} - \mathbf{\Psi}^{-1/2} \mathbf{1}_N \hat{\boldsymbol{\mu}}^T)^T (\mathbf{Y} - \mathbf{\Psi}^{-1/2} \mathbf{1}_N \hat{\boldsymbol{\mu}}^T) = (\mathbf{X} - \mathbf{1}_N \hat{\boldsymbol{\mu}}^T)^T \mathbf{\Psi}^{-1} (\mathbf{X} - \mathbf{1}_N \hat{\boldsymbol{\mu}}^T),$$

824 which can be shown to be distributed as $W_p(\mathbf{\Sigma}, N - 1)$. If there are multiple blocks of species
 825 with different means (regimes), then cross-product matrices calculated separately for each of
 826 these can be summed to obtain a Wishart matrix with a modified degree of freedom as
 827 mentioned above, although it would need to be asked first whether those regimes share the
 828 same $\mathbf{\Sigma}$ (Revell & Collar, 2009; Caetano & Harmon, 2019). The present analytic results can
 829 directly be applied to these Wishart matrices. Estimation of $\mathbf{\Sigma}$ based on this transformation
 830 has previously been devised (Revell & Harmon, 2008; see also Huelsenbeck & Rannala,
 831 2003, Revell & Harrison, 2008; Adams & Felice, 2014), and has been shown to have superior

832 accuracy in estimating eigenvalues over estimation ignoring phylogenetic structures under
833 model conditions (Revell, 2009). Variants of this method have already been applied to
834 analyze eccentricity of interspecific covariation (Haber, 2016; Watanabe, 2018). In practice,
835 however, Ψ is virtually never known exactly because phylogeny and parameters of
836 evolutionary models are generally estimated with error, so empirical cross-product matrices
837 may not be strictly Wishart. This source of error is inherent to any phylogenetic comparative
838 analysis. Unlike the GLS estimate of the mean, which remains unbiased even when Ψ is
839 misspecified, the GLS estimate of trait (co)variance is in general biased in this case (see
840 Rohlf, 2006). Although there are certain ways to incorporate phylogenetic uncertainty into
841 statistical inferences (e.g., Huelsenbeck & Rannala, 2003; Garamszegi & Mundry, 2014;
842 Nakagawa & de Villemereuil, 2019), potential consequences of the uncertainty over the
843 distributions of derived statistics require further investigation (see also Revell et al., 2018).
844 Nevertheless, the GLS estimation with slightly inaccurate Ψ is supposed to yield a better
845 estimate of trait (co)variance than the estimation ignoring phylogenetic covariation altogether
846 (Rohlf, 2006). It should be noted that uniform scaling of Ψ translates to the reciprocal scaling
847 of the cross-product matrix; $V(\mathbf{S})$ is sensitive to this scaling, whereas $V_{\text{rel}}(\mathbf{S})$ and $V_{\text{rel}}(\mathbf{R})$ are
848 not. Therefore, specifically under the BM model, the phylogenetic uncertainty would be the
849 only major concern for the latter two indices.

850 Unfortunately, the GLS estimation of trait covariance does not seem feasible for
851 multivariate OU models, where the joint covariance matrix cannot in general be factorized
852 into intertrait and interspecific components (Bartoszek et al., 2012; Mitov et al., 2020). This
853 is notably except when the selection strength matrix is spherical and the tree is ultrametric, in
854 which case a factorization of the form $\Sigma \otimes \Psi$ is possible (the scalar OU model; Bastide et al.,
855 2018) and hence the GLS cross-product matrix can in principle be calculated, assuming that
856 the relevant parameters are known. Otherwise, the random drift/diffusion matrix of the OU

857 model estimated in one or other criteria can potentially be analyzed, although little is known
858 about its sampling properties under various implementations, other than that accurate
859 estimation is notoriously difficult (e.g., Ho & Ané, 2014; Clavel et al., 2015). Further studies
860 are required on technical aspects of quantifying trait covariation in phylogenetically
861 structured data under such complex models, as well as its biological implications (e.g.,
862 Adams & Collyer, 2018, 2019b; Mitov et al., 2019, 2020; Clavel et al., 2019; Clavel &
863 Morlon, 2020).

864

865 **Concluding remarks**

866 Eigenvalue dispersion indices of covariance or correlation matrices are commonly used as
867 measures of trait covariation, but their statistical implications have not been well appreciated
868 by biologists, against which criticism has reasonably been directed (Hansen & Houle, 2008;
869 Blows & McGuigan, 2015; Hansen et al., 2019). As discussed above, $V_{\text{rel}}(\mathbf{S})$ and $V_{\text{rel}}(\mathbf{R})$
870 have clear statistical justifications as test statistics for sphericity and no correlation,
871 respectively. However, sample eigenvalue dispersion indices are biased estimators of the
872 corresponding population values. This paper derived (or restated) exact and approximate
873 expressions for the expectation and variance of $V(\mathbf{S})$, $V_{\text{rel}}(\mathbf{S})$, and $V_{\text{rel}}(\mathbf{R})$ under the
874 respective null and arbitrary conditions, with which empirical values can be compared. All
875 null moments are exact, as well as both moments of $V(\mathbf{S})$ and the expectation of $V_{\text{rel}}(\mathbf{R})$
876 under arbitrary conditions. Moments of $V_{\text{rel}}(\mathbf{S})$ under arbitrary conditions are approximations
877 based on the delta method; the approximate expectation was shown to work reasonably well
878 with a moderate sample size ($N \geq 16-32$), whereas the approximate variance requires a
879 larger sample size to be reliable (e.g., $N \geq 64$, depending on other conditions). Two
880 approximate expressions were given for the variance of $V_{\text{rel}}(\mathbf{R})$ under arbitrary conditions.
881 The one with equations 28 and 36–38 works reasonably well with a moderate to large sample

882 size ($N \geq 16-128$) but requires nontrivial computational time for a large matrix (e.g.,
883 $p = 1024$), whereas the one with equation 39 tends to be more inaccurate in some conditions
884 but can be evaluated almost instantly. Under such conditions where these expressions work,
885 they can be used for (approximate) statistical inferences and hypothesis tests for the
886 magnitude of integration, as well as for determination of appropriate sample sizes in
887 empirical analyses, essentially replacing qualitative thresholds proposed earlier (e.g., Haber,
888 2011; Jung et al., 2020).

889 There are several conceivable ways for statistical inferences and hypothesis testing for
890 eigenvalue dispersion indices. When sample size is so large that distributions of the indices
891 are virtually symmetric ($N \geq 16-128$, depending on other conditions), the moments derived
892 above may potentially be used to construct approximate confidence intervals. If multivariate
893 normality (or any other explicit distribution) can be assumed, then it is straightforward to
894 obtain empirical distributions under appropriate conditions with Monte Carlo simulations.
895 Critical points of the null distributions and empirical power at $\alpha = 0.05$ and 0.01 based on the
896 present simulations are presented in Table S1–S3 as a quick guide for sampling design.
897 Several limiting and approximate distributions have been proposed for related statistics (e.g.,
898 John, 1972; Nagao, 1973; Ledoit & Wolf, 2002; Schott, 2005), which could be used for
899 simple null hypothesis testing with large N . Resampling-based tests are another potential
900 avenue of development. Applicability and performance of these alternative methods would
901 deserve further investigations.

902

903 **Acknowledgements**

904 The author would like to thank Carmelo Fruciano and Christian P. Klingenberg for
905 encouragements and constructive comments in an early stage of the study. This work was
906 partly supported by the Newton International Fellowships by the Royal Society

907 (NIF\R1\180520) and the Overseas Research Fellowships by the Japan Society for the
908 Promotion of Science (202160529). The author declares no conflict of interest.

909

910 **References**

911 **Adams DC. 2016.** Evaluating modularity in morphometric data: challenges with the RV
912 coefficient and a new test measure. *Methods in Ecology and Evolution* **7**: 565–572.

913 <https://doi.org/10.1111/2041-210X.12511>.

914 **Adams DC, Collyer ML. 2018.** Multivariate phylogenetic comparative methods: evaluations,
915 comparisons, and recommendations. *Systematic Biology* **67**: 14–31.

916 <https://doi.org/10.1093/sysbio/syx055>.

917 **Adams DC, Collyer ML. 2019a.** Comparing the strength of modular signal, and evaluating
918 alternative modular hypotheses, using covariance ratio effect sizes with morphometric

919 data. *Evolution* **73**: 2352–2367. <https://doi.org/10.1111/evo.13867>.

920 **Adams DC, Collyer ML. 2019b.** Phylogenetic comparative methods and the evolution of
921 multivariate phenotypes. *Annual Review of Ecology, Evolution, and Systematics* **50**: 405–

922 425. <https://doi.org/10.1146/annurev-ecolsys-110218-024555>.

923 **Adams DC, Felice RN. 2014.** Assessing trait covariation and morphological integration on
924 phylogenies using evolutionary covariance matrices. *PLoS ONE* **9**: e94335.

925 <https://doi.org/10.1371/journal.pone.0094335>.

926 **Agrawal AF, Stinchcombe JR. 2009.** How much do genetic covariances alter the rate of
927 adaptation? *Proceedings of the Royal Society B: Biological Sciences* **276**: 1183–1191.

928 <https://doi.org/10.1098/rspb.2008.1671>.

929 **Anderson TW. 1963.** Asymptotic theory for principal component analysis. *Annals of*

930 *Mathematical Statistics* **34**: 122–148. <https://doi.org/10.1214/aoms/1177704248>.

- 931 **Anderson TW. 2003.** *An Introduction to Multivariate Statistical Analysis*, 3rd edn. Hoboken,
932 New Jersey: John Wiley & Sons.
- 933 **Arlegi M, Veschambre-Couture C, Gómez-Olivencia A. 2020.** Evolutionary selection and
934 morphological integration in the vertebral column of modern humans. *American Journal*
935 *of Physical Anthropology* **171**: 17–36. <https://doi.org/10.1002/ajpa.23950>.
- 936 **Armbruster WS, Hansen TF, Pélabon C, Pérez-Barrales R, Maad J. 2009.** The adaptive
937 accuracy of flowers: measurement and microevolutionary patterns. *Annals of Botany* **103**:
938 1529–1545. <https://doi.org/10.1093/aob/mcp095>.
- 939 **Armbruster WS, Pélabon C, Bolstad GH, Hansen TF. 2014.** Integrated phenotypes:
940 understanding trait covariation in plants and animals. *Philosophical Transactions of the*
941 *Royal Society B: Biological Sciences* **369**: 20130245.
942 <https://doi.org/10.1098/rstb.2013.0245>.
- 943 **Bartoszek K, Pienaar J, Mostad P, Andersson S, Hansen TF. 2012.** A phylogenetic
944 comparative method for studying multivariate adaptation. *Journal of Theoretical Biology*
945 **314**: 204–215. <https://doi.org/10.1016/j.jtbi.2012.08.005>.
- 946 **Bastide P, Ané C, Robin S, Mariadassou M. 2018.** Inference of adaptive shifts for
947 multivariate correlated traits. *Systematic Biology* **67**: 662–680.
948 <https://doi.org/10.1093/sysbio/syy005>.
- 949 **Björklund M. 2019.** Be careful with your principal components. *Evolution* **73**: 2151–2158.
950 <https://doi.org/10.1111/evo.13835>.
- 951 **Blomberg SP, Garland T Jr, Ives AR. 2003.** Testing for phylogenetic signal in comparative
952 data: behavioral traits are more labile. *Evolution* **57**: 717–745.
953 <https://doi.org/10.1111/j.0014-3820.2003.tb00285.x>.

- 954 **Blows MW, McGuigan K. 2015.** The distribution of genetic variance across phenotypic
955 space and the response to selection. *Molecular Ecology* **24**: 2056–2072.
956 <https://doi.org/10.1111/mec.13023>.
- 957 **Bolstad GH, Hansen TF, Pélabon C, Falahati-Anbaran M, Pérez-Baralles R,**
958 **Armbruster WS. 2014.** Genetic constraints predict evolutionary divergence in
959 *Dalechampia* blossoms. *Philosophical Transactions of the Royal Society B: Biological*
960 *Sciences* **369**: 20130255. <https://doi.org/10.1098/rstb.2013.0255>.
- 961 **Brommer JE. 2014.** Using average autonomy to test whether behavioral syndromes
962 constrain evolution. *Behavioral Ecology and Sociobiology* **68**: 691–700.
963 <https://doi.org/10.1007/s00265-014-1699-6>.
- 964 **Burnaby TP. 1966.** Growth-invariant discriminant functions and generalized distances.
965 *Biometrics* **22**: 96–110. <https://doi.org/10.2307/2528217>.
- 966 **Caetano DS, Harmon LJ. 2019.** Estimating correlated rates of trait evolution with
967 uncertainty. *Systematic Biology* **68**: 412–429. <https://doi.org/10.1093/sysbio/syy067>.
- 968 **Cane WP. 1993.** The ontogeny of postcranial integration in the common tern, *Sterna hirundo*.
969 *Evolution* **47**: 1138–1151. <https://doi.org/10.1111/j.1558-5646.1993.tb02141.x>.
- 970 **Chenoweth SF, Rundle HD, Blows MW. 2010.** The contribution of selection and genetic
971 constraints to phenotypic divergence. *American Naturalist* **175**: 186–196.
972 <https://doi.org/10.1086/649594>.
- 973 **Cheverud JM. 1982.** Phenotypic, genetic, and environmental morphological integration in
974 the cranium. *Evolution* **36**: 499–516. <https://doi.org/10.1111/j.1558-5646.1982.tb05070.x>.
- 975 **Cheverud JM. 1988.** A comparison of genetic and phenotypic correlations. *Evolution* **42**:
976 958–968. <https://doi.org/10.1111/j.1558-5646.1988.tb02514.x>.

- 977 **Cheverud JM. 1996.** Quantitative genetic analysis of cranial morphology in the cotton-top
978 (*Saguinus oedipus*) and saddle-back (*S. fuscicollis*) tamarins. *Journal of Evolutionary*
979 *Biology* **9**: 5–42. <https://doi.org/10.1046/j.1420-9101.1996.9010005.x>.
- 980 **Cheverud JM, Rutledge JJ, Atchley WR. 1983.** Quantitative genetics of development:
981 genetic correlations among age-specific trait values and the evolution of ontogeny.
982 *Evolution* **37**: 895–905. <https://doi.org/10.1111/j.1558-5646.1983.tb05619.x>.
- 983 **Cheverud JM, Wagner GP, Dow MM. 1989.** Methods for the comparative analysis of
984 variation patterns. *Systematic Zoology* **38**: 201–213. <https://doi.org/10.2307/2992282>.
- 985 **Clavel J, Aristide L, Morlon H. 2019.** A penalized likelihood framework for high-
986 dimensional phylogenetic comparative methods and an application to New-World
987 monkeys brain evolution. *Systematic Biology* **68**: 93–116.
988 <https://doi.org/10.1093/sysbio/syy045>.
- 989 **Clavel J, Escarguel G, Merceron G. 2015.** mvMORPH: an R package for fitting multivariate
990 evolutionary models to morphometric data. *Methods in Ecology and Evolution* **6**: 1311–
991 1319. <https://doi.org/10.1111/2041-210X.12420>.
- 992 **Clavel J, Morlon H. 2020.** Reliable phylogenetic regressions for multivariate comparative
993 data: illustration with the MANOVA and application to the effect of diet and mandible
994 morphology in phyllostomid bats. *Systematic Biology* **69**: 927–943.
995 <https://doi.org/10.1093/sysbio/syaa010>.
- 996 **Constantine AG. 1963.** Some non-central distribution problems in multivariate analysis.
997 *Annals of Mathematical Statistics* **34**: 1270–1285.
998 <https://doi.org/10.1214/aoms/1177703863>.
- 999 **Cramer JS. 1987.** Mean and variance of R^2 in small and moderate samples. *Journal of*
1000 *Econometrics* **35**: 253–266. [https://doi.org/10.1016/0304-4076\(87\)90027-3](https://doi.org/10.1016/0304-4076(87)90027-3).

- 1001 **Darroch JN, Mosimann JE. 1985.** Canonical and principal components of shape.
1002 *Biometrika* **72**: 241–252. <https://doi.org/10.1093/biomet/72.2.241>.
- 1003 **Davies PI, Higham NJ. 2000.** Numerically stable generation of correlation matrices and
1004 their factors. *BIT Numerical Mathematics* **40**: 640–651.
1005 <https://doi.org/10.1023/A:1022384216930>.
- 1006 **Dochtermann NA. 2011.** Testing Cheverud’s conjecture for behavioral correlations and
1007 behavioral syndromes. *Evolution* **65**: 1814–1820. [https://doi.org/10.1111/j.1558-](https://doi.org/10.1111/j.1558-5646.2011.01264.x)
1008 [5646.2011.01264.x](https://doi.org/10.1111/j.1558-5646.2011.01264.x).
- 1009 **Durand J-L, Le Roux B. 2017.** Linkage index of variables and its relationship with variance
1010 of eigenvalues in PCA and MCA. *Statistica Applicata – Italian Journal of Applied*
1011 *Statistics* **29**: 123–135. <https://doi.org/10.26398/IJAS.0029-006>.
- 1012 **Eddelbuettel D, Balamuta JJ. 2018.** Extending R with C++: a brief introduction to Rcpp.
1013 *American Statistician* **72**: 28–36. <https://doi.org/10.1080/00031305.2017.1375990>.
- 1014 **Felice RN, Randau M, Goswami A. 2018.** A fly in a tube: macroevolutionary expectations
1015 for integrated phenotypes. *Evolution* **72**: 2580–2594. <https://doi.org/10.1111/evo.13608>.
- 1016 **Felsenstein J. 1988.** Phylogenies and quantitative characters. *Annual Review of Ecology and*
1017 *Systematics* **19**: 445–471. <https://doi.org/10.1146/annurev.es.19.110188.002305>.
- 1018 **Fornoni J, Ordano M, Boege K, Domínguez CA. 2009.** Phenotypic integration: between
1019 zero and how much is too much. *New Phytologist* **183**: 248–250.
1020 <https://doi.org/10.1111/j.1469-8137.2009.02911.x>.
- 1021 **Freckleton RP, Harvey PH, Pagel M. 2002.** Phylogenetic analysis of comparative data: a
1022 test and review of evidence. *American Naturalist* **160**: 712–726.
1023 <https://doi.org/10.1086/343873>.
- 1024 **Garamszegi LZ, Mundry R. 2014.** Multimodel-inference in comparative analyses. In:
1025 Garamszegi LZ, ed. *Modern Phylogenetic Comparative Methods and Their Applications*

- 1026 *in Evolutionary Biology: Concepts and Practice*. Berlin: Springer, 305–331.
- 1027 https://doi.org/10.1007/978-3-662-43550-2_12.
- 1028 **Ghosh BK. 1966.** Asymptotic expansions for the moments of the distribution of correlation
1029 coefficient. *Biometrika* **53**: 258–262. <https://doi.org/10.2307/2334076>.
- 1030 **Girshick MA. 1939.** On the sampling theory of roots of determinantal equations. *Annals of*
1031 *Mathematical Statistics* **10**: 203–224. <https://doi.org/10.1214/aoms/1177732180>.
- 1032 **Gleason TC, Staelin R. 1975.** A proposal for handling missing data. *Psychometrika* **40**: 229-
1033 252. <https://doi.org/10.1007/BF02291569>.
- 1034 **Goswami A. 2006.** Morphological integration in the carnivoran skull. *Evolution* **60**: 169–183.
1035 <https://doi.org/10.1111/j.0014-3820.2006.tb01091.x>.
- 1036 **Goswami A, Binder WJ, Mearchen J, O’Keefe FR. 2015.** The fossil record of phenotypic
1037 integration and modularity: a deep-time perspective on developmental and evolutionary
1038 dynamics. *Proceedings of the National Academy of Sciences of the United States of*
1039 *America* **112**: 4891–4896. <https://doi.org/10.1073/pnas.1403667112>.
- 1040 **Goswami A, Finnarelli JA. 2016.** EMLLi: a maximum likelihood approach to the analysis
1041 of modularity. *Evolution* **70**: 1622–1637. <https://doi.org/10.1111/evo.12956>.
- 1042 **Goswami A, Polly PD. 2010.** Methods for studying morphological integration and
1043 modularity. In: Alroy J, Hunt G, eds. *Quantitative Methods in Paleobiology*.
1044 *Paleontological Society Papers* **16**: 213–243.
1045 <https://doi.org/10.1017/S1089332600001881>.
- 1046 **Grabowski M, Porto A. 2017.** How many more? Sample size determination in studies of
1047 morphological integration and evolvability. *Methods in Ecology and Evolution* **8**: 592–
1048 603. <https://doi.org/10.1111/2041-210X.12674>.

- 1049 **Grafen A. 1989.** The phylogenetic regression. *Philosophical Transactions of the Royal*
1050 *Society of London B: Biological Sciences* **326**: 119–157.
1051 <https://doi.org/10.1098/rstb.1989.0106>.
- 1052 **Gupta AK, Nagar DK. 1999.** *Matrix Variate Distributions*. Boca Raton, Florida: Chapman
1053 & Hall/CRC.
- 1054 **Haber A. 2011.** A comparative analysis of integration indices. *Evolutionary Biology* **38**:
1055 476–488. <https://doi.org/10.1007/s11692-011-9137-4>.
- 1056 **Haber A. 2015.** The evolution of morphological integration in the ruminant skull.
1057 *Evolutionary Biology* **42**: 99–114. <https://doi.org/10.1007/s11692-014-9302-7>.
- 1058 **Haber A. 2016.** Phenotypic covariation and morphological diversification in the ruminant
1059 skull. *American Naturalist* **187**: 576–591. <https://doi.org/10.1086/685811>.
- 1060 **Haber A, Dworkin I. 2017.** Disintegrating the fly: a mutational perspective on phenotypic
1061 integration and covariation. *Evolution* **71**: 66–80. <https://doi.org/10.1111/evo.13100>.
- 1062 **Hallgrímsson B, Jamniczky H, Young NM, Rolian C, Parsons TE, Boughner JC,**
1063 **Marcucio RS. 2009.** Deciphering the palimpsest: studying the relationships between
1064 morphological integration and phenotypic covariation. *Evolutionary Biology* **36**: 355–376.
1065 <https://doi.org/10.1007/s11692-009-9076-5>.
- 1066 **Hankin RKS. 2015.** Numerical evaluation of the Gauss hypergeometric function with the
1067 hypergeo package. *The R Journal* **7**: 81–88. <https://doi.org/10.32614/RJ-2015-022>.
- 1068 **Hansen TF, Houle D. 2008.** Measuring and comparing evolvability and constraint in
1069 multivariate characters. *Journal of Evolutionary Biology* **21**: 1201–1219.
1070 <https://doi.org/10.1111/j.1420-9101.2008.01573.x>.
- 1071 **Hansen TF, Martins E. 1996.** Translating between microevolutionary process and
1072 macroevolutionary patterns: the correlation structure of interspecific data. *Evolution* **50**:
1073 1404–1417. <https://doi.org/10.1111/j.1558-5646.1996.tb03914.x>.

- 1074 **Hansen TF, Solvin TM, Pavlicev M. 2019.** Predicting evolutionary potential: a numerical
1075 test of evolvability measures. *Evolution* **73**: 689–703. <https://doi.org/10.1111/evo.13705>.
- 1076 **Harder LD. 2009.** Questions about floral (dis)integration. *New Phytologist* **183**: 247–248.
1077 <https://doi.org/10.1111/j.1469-8137.2009.02881.x>.
- 1078 **Hereford J, Hansen TF, Houle D. 2004.** Comparing strengths of directional selection: how
1079 strong is strong? *Evolution* **58**: 2133–2143. [https://doi.org/10.1111/j.0014-](https://doi.org/10.1111/j.0014-3820.2004.tb01592.x)
1080 [3820.2004.tb01592.x](https://doi.org/10.1111/j.0014-3820.2004.tb01592.x).
- 1081 **Ho LST, Ané C. 2014.** Intrinsic inference difficulties for trait evolution with Ornstein–
1082 Uhlenbeck models. *Methods in Ecology and Evolution* **5**: 1133–1146.
1083 <https://doi.org/10.1111/2041-210X.12285>.
- 1084 **Houle D. 1992.** Comparing evolvability and variability of quantitative traits. *Genetics* **130**:
1085 195–204. <https://doi.org/10.1093/genetics/130.1.195>.
- 1086 **Huelsenbeck JP, Rannala B. 2003.** Detecting correlation between characters in a
1087 comparative analysis with uncertain phylogeny. *Evolution* **57**: 1237–1247.
1088 <https://doi.org/10.1111/j.0014-3820.2003.tb00332.x>.
- 1089 **John S. 1971.** Some optimal multivariate tests. *Biometrika* **58**: 123–127.
1090 <https://doi.org/10.1093/biomet/58.1.123>.
- 1091 **John S. 1972.** The distribution of a statistic used for testing sphericity of normal distributions.
1092 *Biometrika* **59**: 169–173. <https://doi.org/10.1093/biomet/59.1.169>.
- 1093 **Johnstone IM. 2007.** High dimensional statistical inferences and random matrices. In: Sanz-
1094 Solé M, Soria J, Varona JL, Verdera J, eds. *Proceedings of the International Congress of*
1095 *Mathematicians, Madrid, August 22–30, 2006*, Vol. 1. Zürich: European Mathematical
1096 Society, 307–333.
- 1097 **Johnstone IM, Paul D. 2018.** PCA in high dimensions: an orientation. *Proceedings of the*
1098 *IEEE* **106**: 1277–1292. <https://doi.org/10.1109/JPROC.2018.2846730>.

- 1099 **Jolicoeur P. 1963.** The multivariate generalization of the allometry equation. *Biometrics* **19**:
1100 497–499. <https://doi.org/10.2307/2527939>.
- 1101 **Jolliffe IT. 2002.** *Principal Component Analysis*, 2nd edn. New York: Springer.
- 1102 **Jung H, Conaway MA, von Cramon-Taubadel N. 2020.** Examination of sample size
1103 determination in integration studies based on the integration coefficient of variation (ICV).
1104 *Evolutionary Biology* **47**: 293–307. <https://doi.org/10.1007/s11692-020-09514-w>.
- 1105 **Kirkpatrick M. 2009.** Patterns of quantitative genetic variation in multiple dimensions.
1106 *Genetica* **136**: 271–284. <https://doi.org/10.1007/s10709-008-9302-6>.
- 1107 **Klingenberg CP. 1996.** Multivariate allometry. In: Marcus LF, ed. *Advances in*
1108 *Morphometrics*. New York: Plenum Press, 23–49. [https://doi.org/10.1007/978-1-4757-](https://doi.org/10.1007/978-1-4757-9083-2_3)
1109 [9083-2_3](https://doi.org/10.1007/978-1-4757-9083-2_3).
- 1110 **Klingenberg CP. 2014.** Studying morphological integration and modularity at multiple
1111 levels: concepts and analysis. *Philosophical Transactions of the Royal Society B:*
1112 *Biological Sciences* **369**: 20130249. <https://doi.org/10.1098/rstb.2013.0249>.
- 1113 **Klingenberg CP. 2016.** Size, shape, and form: concepts of allometry in geometric
1114 morphometrics. *Development Genes and Evolution* **226**: 113–137.
1115 <https://doi.org/10.1007/s00427-016-0539-2>.
- 1116 **Klingenberg CP. 2020.** Walking on Kendall’s shape space: understanding shape spaces and
1117 their coordinate systems. *Evolutionary Biology* **47**: 334–352.
1118 <https://doi.org/10.1007/s11692-020-09513-x>.
- 1119 **Klingenberg CP. 2021.** How exactly did the nose get that long? A critical rethinking of the
1120 Pinocchio effect and how shape changes relate to landmarks. *Evolutionary Biology* **48**:
1121 115–127. <https://doi.org/10.1007/s11692-020-09520-y>.
- 1122 **Klingenberg CP, Duttke S, Whelan S, Kim M. 2012.** Developmental plasticity,
1123 morphological variation and evolvability: a multilevel analysis of morphometric

- 1124 integration in the shape of compound leaves. *Journal of Evolutionary Biology* **25**: 115–
1125 129. <https://doi.org/10.1111/j.1420-9101.2011.02410.x>.
- 1126 **Konishi S. 1979.** Asymptotic expansions for the distributions of statistics based on the
1127 sample correlation matrix in principal component analysis. *Hiroshima Mathematical*
1128 *Journal* **9**: 647–700. <https://doi.org/10.32917/hmj/1206134750>.
- 1129 **Lande R. 1979.** Quantitative genetic analysis of multivariate evolution, applied to brain:body
1130 size allometry. *Evolution* **33**: 402–416. [https://doi.org/10.1111/j.1558-](https://doi.org/10.1111/j.1558-5646.1979.tb04694.x)
1131 [5646.1979.tb04694.x](https://doi.org/10.1111/j.1558-5646.1979.tb04694.x).
- 1132 **Lande R, Arnold SJ. 1983.** The measurement of selection on correlated characters.
1133 *Evolution* **37**: 1210–1226. <https://doi.org/10.1111/j.1558-5646.1983.tb00236.x>.
- 1134 **Lawley DN. 1956.** Tests of significance for the latent roots of covariance and correlation
1135 matrices. *Biometrika* **43**: 128–136. <https://doi.org/10.2307/2333586>.
- 1136 **Ledoit O, Wolf M. 2002.** Some hypothesis tests for the covariance matrix when the
1137 dimension is large compared to the sample size. *Annals of Statistics* **30**: 1081–1102.
1138 <https://doi.org/10.1214/aos/1031689018>.
- 1139 **Lynch M, Walsh B. 1998.** *Genetics and Analysis of Quantitative Traits*. Sunderland,
1140 Massachusetts: Sinauer Associates.
- 1141 **Machado FA, Hubbe A, Melo D, Porto A, Marroig G. 2019.** Measuring the magnitude of
1142 morphological integration: the effect of differences in morphometric representations and
1143 the inclusion of size. *Evolution* **73**: 2518–2528. <https://doi.org/10.1111/evo.13864>.
- 1144 **Manceau M, Lambert A, Morlon H. 2017.** A unifying comparative phylogenetic
1145 framework including traits coevolving across interacting lineages. *Systematic Biology* **66**:
1146 551–568. <https://doi.org/10.1093/sysbio/syw115>.

- 1147 **Marcus LF, Hingst-Zaher E, Zaher H. 2000.** Application of landmark morphometrics to
1148 skulls representing the orders of living mammals. *Hystrix* **11**: 27–47.
1149 <https://doi.org/10.4404/hystrix-11.1-4135>.
- 1150 **Marroig G, Melo DAR, Garcia G. 2012.** Modularity, noise, and natural selection. *Evolution*
1151 **66**: 1506–1524. <https://doi.org/10.1111/j.1558-5646.2011.01555.x>.
- 1152 **Marroig G, Shirai LT, Porto A, de Oliveira FB, De Conto V. 2009.** The evolution of
1153 modularity in the mammalian skull II: evolutionary consequences. *Evolutionary Biology*
1154 **36**: 136–148. <https://doi.org/10.1007/s11692-009-9051-1>.
- 1155 **Martins E, Hansen TF. 1997.** Phylogenies and the comparative method: a general approach
1156 to incorporating phylogenetic information into the analysis of interspecific data.
1157 *American Naturalist* **149**: 646–667. <https://doi.org/10.1086/286013>.
- 1158 **Meyer K, Kirkpatrick M. 2005.** Restricted maximum likelihood estimation of genetic
1159 principal components and smoothed covariance matrices. *Genetics Selection Evolution*
1160 **37**: 1–30. <https://doi.org/10.1051/gse:2004034>.
- 1161 **Mitov V, Bartoszek K, Asimomitis G, Stadler T. 2020.** Fast likelihood calculation for
1162 multivariate Gaussian phylogenetic models with shifts. *Theoretical Population Biology*
1163 **131**: 66–78. <https://doi.org/10.1016/j.tpb.2019.11.005>.
- 1164 **Mitov V, Bartoszek K, Stadler T. 2019.** Automatic generation of evolutionary hypotheses
1165 using mixed Gaussian phylogenetic models. *Proceedings of the National Academy of*
1166 *Sciences of the United States of America* **116**: 16921–16926.
1167 <https://doi.org/10.1073/pnas.1813823116>.
- 1168 **Mitteroecker P, Gunz P, Neubauer S, Müller G. 2012.** How to explore morphological
1169 integration in human evolution and development? *Evolutionary Biology* **39**: 536–553.
1170 <https://doi.org/10.1007/s11692-012-9178-3>.

- 1171 **Mosimann JE. 1970.** Size allometry: size and shape variables with characterizations of the
1172 lognormal and generalized gamma distributions. *Journal of the American Statistical*
1173 *Association* **65**: 930–945. <https://doi.org/10.1080/01621459.1970.10481136>.
- 1174 **Mosimann JE, James FC. 1979.** New statistical methods for allometry with application to
1175 Florida red-winged blackbirds. *Evolution* **33**: 444–459. <https://doi.org/10.1111/j.1558->
1176 [5646.1979.tb04697.x](https://doi.org/10.1111/j.1558-5646.1979.tb04697.x).
- 1177 **Muirhead RJ. 1982.** *Aspects of Multivariate Statistical Theory*. Hoboken, New Jersey: John
1178 Wiley & Sons.
- 1179 **Nagao H. 1973.** On some test criteria for covariance matrix. *Annals of Statistics* **1**: 700–709.
1180 <https://doi.org/10.1214/aos/1176342464>.
- 1181 **Nakagawa S, de Villemereuil P. 2019.** A general method for simultaneously accounting for
1182 phylogenetic and species sampling uncertainty via Rubin’s rules in comparative analysis.
1183 *Systematic Biology* **68**: 632–641. <https://doi.org/10.1093/sysbio/syy089>.
- 1184 **Olkin I, Siotani M. 1976.** Asymptotic distribution of functions of a correlation matrix. In:
1185 Editorial Committee for Publication of Essays in Probability and Statistics, eds. *Essays in*
1186 *Probability and Statistics in Honor of Professor Junjiro Ogawa*. Tokyo: Shinko Tsusho,
1187 235–251.
- 1188 **Olson EC, Miller RL. 1958.** *Morphological Integration*. [Chicago]: University of Chicago
1189 Press.
- 1190 **Ordano M, Fornoni J, Boege K, Domínguez CA. 2008.** The adaptive value of phenotypic
1191 floral integration. *New Phytologist* **179**: 1183–1192. <https://doi.org/10.1111/j.1469->
1192 [8137.2008.02523.x](https://doi.org/10.1111/j.1469-8137.2008.02523.x).
- 1193 **Pan W, Frank KA. 2004.** An approximation to the distribution of the product of two
1194 dependent correlation coefficients. *Journal of Statistical Computation and Simulation* **74**:
1195 419–443. <https://doi.org/10.1080/00949650310001596822>.

- 1196 **Pavlicev M, Cheverud JM, Wagner GP. 2009.** Measuring morphological integration using
1197 eigenvalue variance. *Evolutionary Biology* **36**: 157–170. [https://doi.org/10.1007/s11692-](https://doi.org/10.1007/s11692-008-9042-7)
1198 008-9042-7.
- 1199 **Pitchers W, Wolf JB, Tregenza T, Hunt J, Dworkin I. 2014.** Evolutionary rates for
1200 multivariate traits: the role of selection and genetic variation. *Philosophical Transactions*
1201 *of the Royal Society B: Biological Sciences* **369**: 20130252.
1202 <https://doi.org/10.1098/rstb.2013.0252>.
- 1203 **Porto A, de Oliveira FB, Shirai LT, De Conto V, Marroig G. 2009.** The evolution of
1204 modularity in the mammalian skull I: morphological integration patterns and magnitudes.
1205 *Evolutionary Biology* **36**: 118–135. <https://doi.org/10.1007/s11692-008-9038-3>.
- 1206 **R Core Team. 2019.** *R: a language and environment for statistical computing, Version 3.5.3.*
1207 Vienna: R Foundation for Statistical Computing. <https://www.R-project.org/>.
- 1208 **Renaud S, Auffray J-C. 2013.** The direction of main phenotypic variance as a channel to
1209 morphological evolution: case studies in murine rodents. *Hystrix* **24**: 85–93.
1210 <https://doi.org/10.4404/hystrix-24.1-6296>.
- 1211 **Revell LJ. 2009.** Size-correction and principal components for interspecific comparative
1212 studies. *Evolution* **63**: 3258–3268. <https://doi.org/10.1111/j.1558-5646.2009.00804.x>.
- 1213 **Revell LJ, Collar DC. 2009.** Phylogenetic analysis of the evolutionary correlation using
1214 likelihood. *Evolution* **63**: 1090–1100. <https://doi.org/10.1111/j.1558-5646.2009.00616.x>.
- 1215 **Revell LJ, González-Valenzuela LE, Alfonso A, Castellanos-García LA, Guarnizo CE,**
1216 **Crawford AJ. 2018.** Comparing evolutionary rates between trees, clades and traits.
1217 *Methods in Ecology and Evolution* **9**: 994–1005. [https://doi.org/10.1111/2041-](https://doi.org/10.1111/2041-210X.12977)
1218 210X.12977.

- 1219 **Revell LJ, Harmon LJ. 2008.** Testing quantitative genetic hypotheses about the
1220 evolutionary rate matrix for continuous characters. *Evolutionary Ecology Research* **10**:
1221 311–331.
- 1222 **Revell LJ, Harrison AS. 2008.** PCCA: a program for phylogenetic canonical correlation
1223 analysis. *Bioinformatics* **24**: 1018–1020. <https://doi.org/10.1093/bioinformatics/btn065>.
- 1224 **Roff DA. 1995.** The estimation of genetic correlations from phenotypic correlations: a test of
1225 Cheverud’s conjecture. *Heredity* **74**: 481–490. <https://doi.org/10.1038/hdy.1995.68>.
- 1226 **Rohlf FJ. 1999.** Shape statistics: Procrustes superimpositions and tangent spaces. *Journal of*
1227 *Classification* **16**: 197–223. <https://doi.org/10.1007/s003579900054>.
- 1228 **Rohlf FJ. 2001.** Comparative methods for the analysis of continuous variables: geometric
1229 interpretations. *Evolution* **55**: 2143–2160. [https://doi.org/10.1111/j.0014-](https://doi.org/10.1111/j.0014-3820.2001.tb00731.x)
1230 [3820.2001.tb00731.x](https://doi.org/10.1111/j.0014-3820.2001.tb00731.x).
- 1231 **Rohlf FJ. 2006.** A comment on phylogenetic correction. *Evolution* **60**: 1509–1515.
1232 <https://doi.org/10.1111/j.0014-3820.2006.tb01229.x>.
- 1233 **Rohlf FJ, Bookstein FL. 2003.** Computing the uniform component of shape variation.
1234 *Systematic Biology* **52**: 66–69. <https://doi.org/10.1080/10635150390132759>.
- 1235 **Rohlf FJ, Slice D. 1990.** Extensions of the Procrustes method for the optimal
1236 superimposition of landmarks. *Systematic Zoology* **39**: 40–59.
1237 <https://doi.org/10.2307/2992207>.
- 1238 **Schluter D. 1996.** Adaptive radiation along genetic lines of least resistance. *Evolution* **50**:
1239 1766–1774. <https://doi.org/10.1111/j.1558-5646.1996.tb03563.x>.
- 1240 **Schott JR. 2005.** Testing for complete independence in high dimensions. *Biometrika* **92**:
1241 951–956. <https://doi.org/10.1093/biomet/92.4.951>.
- 1242 **Shirai LT, Marroig G. 2010.** Skull modularity in Neotropical marsupials and monkeys: size
1243 variation and evolutionary constraint and flexibility. *Journal of Experimental Zoology*,

- 1244 *Part B: Molecular and Developmental Evolution* **314B**: 663–683.
- 1245 <https://doi.org/10.1002/jez.b.21367>.
- 1246 **Slice DE. 2001.** Landmark coordinates aligned by Procrustes analysis do not lie in Kendall’s
- 1247 shape space. *Systematic Biology* **50**: 141–149. <https://doi.org/10.1080/10635150119110>.
- 1248 **Sodini SM, Kemper KE, Wray NR, Trzaskowski M. 2018.** Comparison of genotypic and
- 1249 phenotypic correlations: Cheverud’s conjecture in humans. *Genetics* **209**: 941–948.
- 1250 <https://doi.org/10.1534/genetics.117.300630>.
- 1251 **Soper HE, Young AW, Cave BM, Lee A, Pearson K. 1917.** On the distribution of the
- 1252 correlation coefficient in small samples. Appendix II to the papers of “Student” and R. A.
- 1253 Fisher. *Biometrika* **11**: 328–413. <https://doi.org/10.1093/biomet/11.4.328>.
- 1254 **Srivastava MS, Khatri CG. 1979.** *An Introduction to Multivariate Statistics*. New York:
- 1255 North Holland.
- 1256 **Srivastava MS, Yanagihara H. 2010.** Testing the equality of several covariance matrices
- 1257 with fewer observations than the dimension. *Journal of Multivariate Analysis* **101**: 1319–
- 1258 1329. <https://doi.org/10.1016/j.jmva.2009.12.010>.
- 1259 **Steppan SJ, Phillips PC, Houle D. 2002.** Comparative quantitative genetics: evolution of
- 1260 the **G** matrix. *Trends in Ecology and Evolution* **17**: 320–327.
- 1261 [https://doi.org/10.1016/S0169-5347\(02\)02505-3](https://doi.org/10.1016/S0169-5347(02)02505-3).
- 1262 **Stuart A, Ord JK. 1994.** *Kendall’s Advanced Theory of Statistics*, 6th edn, Vol. 1. London:
- 1263 Hodder Education [Reprinted in 2004 by John Wiley & Sons, Chichester].
- 1264 **Sugiura N. 1972.** Locally best invariant test for sphericity and the limiting distributions.
- 1265 *Annals of Mathematical Statistics* **43**: 1312–1316.
- 1266 <https://doi.org/10.1214/aoms/1177692481>.
- 1267 **Symonds MRE, Blomberg SP. 2014.** A primer on phylogenetic generalized least squares.
- 1268 In: Garamszegi LZ, ed. *Modern Phylogenetic Comparative Methods and Their*

- 1269 *Application in Evolutionary Biology: Concepts and Practice*. Berlin: Springer, 105–130.
- 1270 https://doi.org/10.1007/978-3-662-43550-2_5.
- 1271 **Sztepanacz JL, Blows MW. 2017.** Accounting for sampling error in genetic eigenvalues
- 1272 using random matrix theory. *Genetics* **206**: 1271–1284.
- 1273 <https://doi.org/10.1534/genetics.116.198606>.
- 1274 **Torices R, Méndez M. 2014.** Resource allocation to inflorescence components is highly
- 1275 integrated despite differences between allocation currencies and sites. *International*
- 1276 *Journal of Plant Sciences* **175**: 713–723. <https://doi.org/10.1086/676622>.
- 1277 **Torices R, Muñoz-Pajares AJ. 2015.** PHENIX: an R package to estimate a size-controlled
- 1278 phenotypic integration index. *Applications in Plant Sciences* **3**: 1400104.
- 1279 <https://doi.org/10.3732/apps.1400104>.
- 1280 **Uyeda JC, Harmon LJ. 2014.** A novel Bayesian method for inferring and interpreting the
- 1281 dynamics of adaptive landscapes from phylogenetic comparative data. *Systematic Biology*
- 1282 **63**: 902–918. <https://doi.org/10.1093/sysbio/syu057>.
- 1283 **Van Valen L. 1974.** Multivariate structural statistics in natural history. *Journal of*
- 1284 *Theoretical Biology* **45**: 235–247. [https://doi.org/10.1016/0022-5193\(74\)90053-8](https://doi.org/10.1016/0022-5193(74)90053-8).
- 1285 **Van Valen L. 2005.** The statistics of variation. In: Hallgrímsson B, Hall BK, eds. *Variation*.
- 1286 Amsterdam: Elsevier, 29–47. <https://doi.org/10.1016/B978-012088777-4/50005-3>.
- 1287 **de Waal DJ, Nel DG. 1973.** On some expectations with respect to Wishart matrices. *South*
- 1288 *African Statistical Journal* **7**: 61–67.
- 1289 **Wagner GP. 1984.** On the eigenvalue distribution of genetic and phenotypic dispersion
- 1290 matrices: evidence for a nonrandom organization of quantitative character variation.
- 1291 *Journal of Mathematical Biology* **21**: 77–95. <https://doi.org/10.1007/BF00275224>.

- 1292 **Walker JA. 2000.** Ability of geometric morphometric methods to estimate a known
1293 covariance matrix. *Systematic Biology* **49**: 686–696.
1294 <https://doi.org/10.1080/106351500750049770>.
- 1295 **Waller NG. 2020.** Generating correlation matrices with specified eigenvalues using the
1296 method of alternating projections. *American Statistician* **74**: 21–28.
1297 <https://doi.org/10.1080/00031305.2017.1401960>.
- 1298 **Watanabe J. 2018.** Clade-specific evolutionary diversification along ontogenetic major axes
1299 in avian limb skeleton. *Evolution* **72**: 2632–2652. <https://doi.org/10.1111/evo.13627>.

1300

1301 **Appendix A**

1302 In this part, relationships between eigenvalue dispersion indices and individual eigenvalues
1303 are derived under certain restrictive conditions, in order to facilitate interpretation and to
1304 clarify algorithms used in simulations. For simplicity, it is assumed $\bar{\lambda} = 1$ in the following
1305 discussions; general cases easily follow by scaling.

1306 Let us first consider the simple conditions where the first q ($< p$) population
1307 eigenvalues are equally large and the rest $p - q$ eigenvalues are equally small: $\lambda_1 = \dots =$
1308 $\lambda_q \geq \lambda_{q+1} = \dots = \lambda_p$ (“ q -large λ conditions” in simulations). By noting $\sum \lambda_i = q\lambda_1 +$
1309 $(p - q)\lambda_p = p$, it is seen that

$$1310 \quad V_{\text{rel}}(\mathbf{\Sigma}) = \frac{\sum_{i=1}^p (\lambda_i - 1)^2}{p(p-1)} = \frac{(p-q)}{q(p-1)} (1 - \lambda_p)^2, \quad (\text{A1})$$

1311 and hence

$$\lambda_1 = 1 + \sqrt{\frac{(p-1)(p-q)}{q}} V_{\text{rel}},$$
$$\lambda_p = 1 - \sqrt{\frac{q(p-1)}{p-q}} V_{\text{rel}}.$$

1312 (A2)

1313 By noting the constraint $0 \leq \lambda_p \leq 1$, an upper limit of V_{rel} can be seen from equation A1:

$$1314 \quad V_{\text{rel}}(\boldsymbol{\Sigma}) \leq \frac{(p-q)}{q(p-1)} = \frac{1}{q} - \frac{q-1}{q(p-1)}. \quad (\text{A3})$$

1315 It is then obvious that, under these constraints, a value of V_{rel} greater than 0.5 cannot happen
 1316 when $q > 1$; that is, such a large value implies the dominance of a single component of
 1317 variance. The same arguments equally apply to correlation matrices.

1318 When $q = 1$ for the correlation matrix, $V_{\text{rel}}(\mathbf{P})$ completely specifies the magnitude of
 1319 correlation in every pair of variables. This point can be seen from the definition of
 1320 eigendecomposition:

$$\begin{aligned} \rho_{ij} &= \sum_{k=1}^p \lambda_k v_{ik} v_{jk} \\ &= (\lambda_1 - \lambda_p) v_{i1} v_{j1} + \lambda_p \sum_{k=1}^p v_{ik} v_{jk}, \end{aligned} \quad (\text{A4})$$

1322 where v_{ij} is the (i, j) -th element of the eigenvector matrix. By remembering $\sum_{k=1}^p v_{ik} v_{jk} =$
 1323 δ_{ij} , the Kronecker delta, and noting equation A2 with $q = 1$,

$$1324 \quad 1 = \rho_{ii} = (\lambda_1 - \lambda_p) v_{i1}^2 + \lambda_p = (p v_{i1}^2 - 1) \sqrt{V_{\text{rel}}} + 1, \quad (\text{A5})$$

1325 therefore $v_{i1}^2 = p^{-1/2}$ for any i (that is, the coefficients of the first eigenvector are equal in
 1326 magnitude). Finally, we have

$$1327 \quad \rho_{ij}^2 = (\lambda_1 - \lambda_p)^2 v_{i1}^2 v_{j1}^2 = V_{\text{rel}} \quad (\text{A6})$$

1328 for any combination of i and j ($i \neq j$); the magnitude of correlation is identical across all
 1329 pairs. Taken differently, $\lambda_2 = \dots = \lambda_p = |\rho|$. These relationships have previously been noted
 1330 by Anderson (1963) and Pavlicev et al. (2009).

1331 The population eigenvalues of the linearly and quadratically decreasing λ conditions
 1332 used in simulations are defined as $\lambda_i = (p - i + 1)\lambda_p$ and $\lambda_i = (p - i + 1)^2\lambda_p$ ($i =$

1333 $1, 2, \dots, p)$ for linearly and quadratically decreasing conditions, respectively. Under the
 1334 assumption of a constant average eigenvalue, simple algebra yields the actual values of λ_p
 1335 and $V_{\text{rel}}(\boldsymbol{\Sigma})$ as functions of p . The latter equals $1/3(p + 1)$ and $(8p + 11)/5(p + 1)(2p +$
 1336 $1)$ for the linearly and quadratically decreasing λ conditions, respectively.

1337

1338 **Appendix B**

1339 In this part, the first two moments of $V(\mathbf{S})$ and $V_{\text{rel}}(\mathbf{S})$ under the arbitrary $\boldsymbol{\Sigma}$ are derived,
 1340 assuming multivariate normality. Derivation of the moments of the latter requires evaluation
 1341 of moments of the ratio $\sum l_i^2 / (\sum l_i)^2 = \text{tr}(\mathbf{A}^2) / (\text{tr} \mathbf{A})^2$, which are not guaranteed to coincide
 1342 with the ratios of moments except under the null hypothesis. Here we utilize the
 1343 approximation based on the delta method (eq. 32). In turn, we need $E[\text{tr}(\mathbf{A}^2)]$, $E[(\text{tr} \mathbf{A})^2]$,
 1344 $\text{Var}[\text{tr}(\mathbf{A}^2)]$, $\text{Var}[(\text{tr} \mathbf{A})^2]$, and $\text{Cov}[\text{tr}(\mathbf{A}^2), (\text{tr} \mathbf{A})^2]$.

1345 We will follow Srivastava & Yanagihara's (2010) approach to obtain these moments.

1346 As in the text, let the $n \times p$ matrix \mathbf{Z} be $(\mathbf{z}_1, \mathbf{z}_2, \dots, \mathbf{z}_n)^T$, where $\mathbf{z}_i \sim N_p(\mathbf{0}_p, \boldsymbol{\Sigma})$ for $i =$
 1347 $1, 2, \dots, n$. Consider the cross-product matrix

$$1348 \quad \mathbf{A} = \mathbf{Z}^T \mathbf{Z}, \quad (\text{B1})$$

1349 such that $\mathbf{A} \sim W_p(\boldsymbol{\Sigma}, n)$. Let the spectral decomposition of $\boldsymbol{\Sigma}$:

$$1350 \quad \boldsymbol{\Sigma} = \mathbf{Y} \boldsymbol{\Lambda} \mathbf{Y}^T, \quad (\text{B2})$$

1351 with the orthogonal matrix of eigenvectors \mathbf{Y} and the diagonal matrix of eigenvalues $\boldsymbol{\Lambda}$. Let

1352 the $n \times p$ matrix \mathbf{J} be $(\mathbf{j}_1, \mathbf{j}_2, \dots, \mathbf{j}_n)^T$, where \mathbf{j}_i are i.i.d. $N_p(\mathbf{0}, \mathbf{I}_p)$, such that $\mathbf{Z} = \mathbf{J} \boldsymbol{\Sigma}^{1/2}$ with

1353 $\boldsymbol{\Sigma}^{1/2} = \mathbf{Y} \boldsymbol{\Lambda}^{1/2} \mathbf{Y}^T$. Then, it is possible to write

$$1354 \quad \mathbf{A} = \boldsymbol{\Sigma}^{1/2} \mathbf{J}^T \mathbf{J} \boldsymbol{\Sigma}^{1/2} = \mathbf{Y} \boldsymbol{\Lambda}^{1/2} \mathbf{Y}^T \mathbf{J}^T \mathbf{J} \mathbf{Y} \boldsymbol{\Lambda}^{1/2} \mathbf{Y}^T = \mathbf{Y} \boldsymbol{\Lambda}^{1/2} \mathbf{V}^T \mathbf{V} \boldsymbol{\Lambda}^{1/2} \mathbf{Y}^T, \quad (\text{B3})$$

1355 where $\mathbf{V} = \mathbf{J} \mathbf{Y} = (\mathbf{v}_1, \mathbf{v}_2, \dots, \mathbf{v}_p)$ with \mathbf{v}_i being i.i.d. $N_n(\mathbf{0}, \mathbf{I}_n)$. Furthermore, let $w_{ij} = \mathbf{v}_i^T \mathbf{v}_j$,

1356 such that w_{ii} are i.i.d. chi-square variables with n degrees of freedom χ_n^2 . Obviously $w_{ij} =$

1357 w_{ji} . Note that

$$1358 \quad \text{tr } \mathbf{A} = \text{tr}(\mathbf{Y}\mathbf{\Lambda}^{1/2}\mathbf{V}^T\mathbf{V}\mathbf{\Lambda}^{1/2}\mathbf{Y}^T) = \text{tr}(\mathbf{\Lambda}\mathbf{V}^T\mathbf{V}) = \sum_{i=1}^n \lambda_i w_{ii}. \quad (\text{B4})$$

1359 From well-known results on normal and chi-square moments, we have the following:

$$\begin{aligned} E(w_{ii}^r) &= n(n+2) \dots (n+2r-2), \quad r = 1, 2, \dots, \\ E(w_{ii}^r w_{ij}^r) &= E[\text{tr}(w_{ii}^r \mathbf{v}_i \mathbf{v}_i^T \mathbf{v}_j \mathbf{v}_j^T)] \\ &= \text{tr}[E(w_{ii}^r \mathbf{v}_i \mathbf{v}_i^T) E(\mathbf{v}_j \mathbf{v}_j^T)] \\ &= \text{tr}[E(w_{ii}^r \mathbf{v}_i \mathbf{v}_i^T) \mathbf{I}_n] \\ &= n(n+2) \dots (n+2r), \quad i \neq j, \quad r = 0, 1, \dots, \\ E(w_{ii} w_{jj} w_{ij}^2) &= E[\text{tr}(w_{ii} \mathbf{v}_i \mathbf{v}_i^T w_{jj} \mathbf{v}_j \mathbf{v}_j^T)] \\ &= \sum_{\alpha, \beta, \gamma, \delta}^n E(v_{i\alpha}^2 v_{i\gamma} v_{i\delta}) E(v_{j\beta}^2 v_{j\delta} v_{j\gamma}) \\ &= 9n + 6n(n-1) + n(n-1)^2 \\ &= n(n+2)^2, \quad i \neq j, \\ E(w_{ij}^2 w_{ik}^2) &= \sum_{\alpha, \beta}^n E(v_{i\alpha}^2 v_{i\beta}^2) E(v_{j\alpha}^2) E(v_{k\beta}^2) \\ &= 3n + n(n-1) \\ &= n(n+2), \quad i \neq j \neq k, \\ E(w_{ij}^4) &= \sum_{\alpha, \beta, \gamma, \delta}^n E(v_{i\alpha} v_{i\beta} v_{i\gamma} v_{i\delta}) E(v_{j\alpha} v_{j\beta} v_{j\delta} v_{j\gamma}) \\ &= 9n + 3n(n-1) \\ &= 3n(n+2), \quad i \neq j, \end{aligned}$$

1360 (B5)

1361 where intervening equations can be confirmed by direct enumeration of the nonzero moments.

1362 From the above expectations, one can evaluate the desired moments as follows:

$$E[\text{tr}(\mathbf{A}^2)] = E[\text{tr}(\mathbf{\Lambda}\mathbf{V}^T\mathbf{V}\mathbf{\Lambda}\mathbf{V}^T\mathbf{V})]$$

$$\begin{aligned}
 &= \mathbb{E} \left(\sum_{i,j}^n \lambda_i \lambda_j w_{ij}^2 \right) \\
 &= \sum_i^n \lambda_i^2 \mathbb{E}(w_{ii}^2) + \sum_{i \neq j}^n \lambda_i \lambda_j \mathbb{E}(w_{ij}^2) \\
 &= n(n+2) \sum_i^n \lambda_i^2 + n \sum_{i \neq j}^n \lambda_i \lambda_j,
 \end{aligned}$$

$$\mathbb{E}[(\text{tr } \mathbf{A})^2] = \mathbb{E}[(\text{tr}(\mathbf{\Lambda} \mathbf{V}^T \mathbf{V}))^2]$$

$$\begin{aligned}
 &= \mathbb{E} \left(\sum_{i,j}^n \lambda_i \lambda_j w_{ii} w_{jj} \right) \\
 &= \sum_i^n \lambda_i^2 \mathbb{E}(w_{ii}^2) + \sum_{i \neq j}^n \lambda_i \lambda_j \mathbb{E}(w_{ii}) \mathbb{E}(w_{jj}) \\
 &= n(n+2) \sum_i^n \lambda_i^2 + n^2 \sum_{i \neq j}^n \lambda_i \lambda_j,
 \end{aligned}$$

$$\mathbb{E}[(\text{tr}(\mathbf{A}^2))^2] = \mathbb{E}[(\text{tr}(\mathbf{\Lambda} \mathbf{V}^T \mathbf{V} \mathbf{\Lambda} \mathbf{V}^T \mathbf{V}))^2]$$

$$\begin{aligned}
 &= \mathbb{E} \left(\sum_{i,j,k,l}^n \lambda_i \lambda_j \lambda_k \lambda_l w_{ij}^2 w_{kl}^2 \right) \\
 &= \sum_i^n \lambda_i^4 \mathbb{E}(w_{ii}^4) + 4 \sum_{i \neq j}^n \lambda_i^3 \lambda_j \mathbb{E}(w_{ii}^2 w_{ij}^2) \\
 &\quad + \sum_{i \neq j}^n \lambda_i^2 \lambda_j^2 [\mathbb{E}(w_{ii}^2) \mathbb{E}(w_{jj}^2) + 2 \mathbb{E}(w_{ij}^4)] \\
 &\quad + \sum_{i \neq j \neq k}^n \lambda_i^2 \lambda_j \lambda_k [2 \mathbb{E}(w_{ii}^2) \mathbb{E}(w_{jk}^2) + 4 \mathbb{E}(w_{ij}^2 w_{ik}^2)] \\
 &\quad + \sum_{i \neq j \neq k \neq l}^n \lambda_i \lambda_j \lambda_k \lambda_l \mathbb{E}(w_{ij}^2) \mathbb{E}(w_{kl}^2)
 \end{aligned}$$

$$\begin{aligned}
&= n(n+2)(n+4)(n+6) \sum_i^n \lambda_i^4 + 4n(n+2)(n+4) \sum_{i \neq j}^n \lambda_i^3 \lambda_j \\
&+ n(n+2)(n^2+2n+6) \sum_{i \neq j}^n \lambda_i^2 \lambda_j^2 + 2n(n+2) \sum_{i \neq j \neq k}^n \lambda_i^2 \lambda_j \lambda_k \\
&+ n^2 \sum_{i \neq j \neq k \neq l}^n \lambda_i \lambda_j \lambda_k \lambda_l,
\end{aligned}$$

$$E[(\text{tr } \mathbf{A})^4] = E[(\text{tr}(\mathbf{A}\mathbf{V}^T\mathbf{V}))^4]$$

$$\begin{aligned}
&= E\left(\sum_{i,j,k,l}^n \lambda_i \lambda_j \lambda_k \lambda_l w_{ii} w_{jj} w_{kk} w_{ll}\right) \\
&= \sum_i^n \lambda_i^4 E(w_{ii}^4) + 4 \sum_{i \neq j}^n \lambda_i^3 \lambda_j E(w_{ii}^3) E(w_{jj}) + 3 \sum_{i \neq j}^n \lambda_i^2 \lambda_j^2 E(w_{ii}^2) E(w_{jj}^2) \\
&+ 6 \sum_{i \neq j \neq k}^n \lambda_i^2 \lambda_j \lambda_k E(w_{ii}^2) E(w_{jj}) E(w_{kk}) \\
&+ \sum_{i \neq j \neq k \neq l}^n \lambda_i \lambda_j \lambda_k \lambda_l E(w_{ii}) E(w_{jj}) E(w_{kk}) E(w_{ll}) \\
&= n(n+2)(n+4)(n+6) \sum_i^n \lambda_i^4 + 4n^2(n+2)(n+4) \sum_{i \neq j}^n \lambda_i^3 \lambda_j \\
&+ 3n^2(n+2)^2 \sum_{i \neq j}^n \lambda_i^2 \lambda_j^2 + 6n^3(n+2) \sum_{i \neq j \neq k}^n \lambda_i^2 \lambda_j \lambda_k \\
&+ n^4 \sum_{i \neq j \neq k \neq l}^n \lambda_i \lambda_j \lambda_k \lambda_l,
\end{aligned}$$

$$E[\text{tr}(\mathbf{A}^2) \cdot (\text{tr } \mathbf{A})^2] = E[\text{tr}(\mathbf{A}\mathbf{V}^T\mathbf{V}\mathbf{A}\mathbf{V}^T\mathbf{V}) \cdot [\text{tr}(\mathbf{A}\mathbf{V}^T\mathbf{V})]^2]$$

$$= E\left(\sum_{i,j,k,l}^n \lambda_i \lambda_j \lambda_k \lambda_l w_{ij}^2 w_{kk} w_{ll}\right)$$

$$\begin{aligned}
&= \sum_i^n \lambda_i^4 E(w_{ii}^4) + \sum_{i \neq j}^n \lambda_i^3 \lambda_j [2 E(w_{ii}^3) E(w_{jj}) + 2 E(w_{ii}^2 w_{ij}^2)] \\
&+ \sum_{i \neq j}^n \lambda_i^2 \lambda_j^2 [E(w_{ii}^2) E(w_{jj}^2) + 2 E(w_{ii} w_{jj} w_{ij}^2)] \\
&+ \sum_{i \neq j \neq k}^n \lambda_i^2 \lambda_j \lambda_k [E(w_{ii}^2) E(w_{jj}) E(w_{kk}) + 4 E(w_{ii} w_{ij}^2) E(w_{kk}) \\
&+ E(w_{ii}^2) E(w_{jk}^2)] + \sum_{i \neq j \neq k \neq l}^n \lambda_i \lambda_j \lambda_k \lambda_l E(w_{ij}^2) E(w_{kk}) E(w_{ll}) \\
&= n(n+2)(n+4)(n+6) \sum_i^n \lambda_i^4 + 2n(n+1)(n+2)(n+4) \sum_{i \neq j}^n \lambda_i^3 \lambda_j \\
&+ n(n+2)^3 \sum_{i \neq j}^n \lambda_i^2 \lambda_j^2 + n^2(n+2)(n+5) \sum_{i \neq j \neq k}^n \lambda_i^2 \lambda_j \lambda_k \\
&+ n^3 \sum_{i \neq j \neq k \neq l}^n \lambda_i \lambda_j \lambda_k \lambda_l,
\end{aligned}$$

1363 (B6)

1364 where notations of the form $i \neq j \neq k \neq l$ represent inequality of every pairwise combination
1365 of the subscripts concerned.

1366 Although equations B6 can be evaluated for any Σ , calculating the product of all
1367 possible combinations of eigenvalues is rather cumbersome when p is large. For this reason,
1368 it would be preferable to simplify these expressions by noting

$$\begin{aligned}
\sum_i^n \lambda_i^r &= \text{tr}(\mathbf{\Lambda}^r), \quad r = 1, 2, \dots, \\
\sum_{i \neq j}^n \lambda_i \lambda_j &= \left(\sum_{i=1}^n \lambda_i \right)^2 - \sum_{i=1}^n \lambda_i^2 = (\text{tr } \mathbf{\Lambda})^2 - \text{tr}(\mathbf{\Lambda}^2),
\end{aligned}$$

$$\begin{aligned}\sum_{i \neq j}^n \lambda_i^3 \lambda_j &= \text{tr } \mathbf{\Lambda} \text{tr}(\mathbf{\Lambda}^3) - \text{tr}(\mathbf{\Lambda}^4), \\ \sum_{i \neq j}^n \lambda_i^2 \lambda_j^2 &= 3[\text{tr}(\mathbf{\Lambda}^2)]^2 - \text{tr}(\mathbf{\Lambda}^4), \\ \sum_{i \neq j \neq k}^n \lambda_i^2 \lambda_j \lambda_k &= (\text{tr } \mathbf{\Lambda})^2 \text{tr}(\mathbf{\Lambda}^2) - 2 \text{tr } \mathbf{\Lambda} \text{tr}(\mathbf{\Lambda}^3) - [\text{tr}(\mathbf{\Lambda}^2)]^2 + 2 \text{tr}(\mathbf{\Lambda}^4),\end{aligned}$$

1369 (B7)

1370 Then, equations B6 can be written as follows:

$$\begin{aligned}E[\text{tr}(\mathbf{A}^2)] &= n(\text{tr } \mathbf{\Lambda})^2 + n(n+1) \text{tr}(\mathbf{\Lambda}^2), \\ E[(\text{tr } \mathbf{A})^2] &= n^2(\text{tr } \mathbf{\Lambda})^2 + 2n \text{tr}(\mathbf{\Lambda}^2), \\ E[[\text{tr}(\mathbf{A}^2)]^2] &= n^2(\text{tr } \mathbf{\Lambda})^4 + 2n(n^2 + n + 4)(\text{tr } \mathbf{\Lambda})^2 \text{tr}(\mathbf{\Lambda}^2) + 16n(n+1) \text{tr } \mathbf{\Lambda} \text{tr}(\mathbf{\Lambda}^3) \\ &\quad + n(n^3 + 2n^2 + 5n + 4)[\text{tr}(\mathbf{\Lambda}^2)]^2 + 4n(2n^2 + 5n + 5) \text{tr}(\mathbf{\Lambda}^4), \\ E[(\text{tr } \mathbf{A})^4] &= n^4(\text{tr } \mathbf{\Lambda})^4 + 12n^3(\text{tr } \mathbf{\Lambda})^2 \text{tr}(\mathbf{\Lambda}^2) + 12n^2 \text{tr } \mathbf{\Lambda} \text{tr}(\mathbf{\Lambda}^3) \\ &\quad + 32n^2[\text{tr}(\mathbf{\Lambda}^2)]^2 + 48n \text{tr}(\mathbf{\Lambda}^4), \\ E[\text{tr}(\mathbf{A}^2) \cdot (\text{tr } \mathbf{A})^2] &= n^3(\text{tr } \mathbf{\Lambda})^4 + n^2(n^2 + n + 10)(\text{tr } \mathbf{\Lambda})^2 \text{tr}(\mathbf{\Lambda}^2) \\ &\quad + 8n(n^2 + n + 2) \text{tr } \mathbf{\Lambda} \text{tr}(\mathbf{\Lambda}^3) + 2n(n^2 + n + 4)[\text{tr}(\mathbf{\Lambda}^2)]^2 \\ &\quad + 24n(n+1) \text{tr}(\mathbf{\Lambda}^4).\end{aligned}$$

1371 (B8)

1372 Finally,

$$\begin{aligned}\text{Var}[\text{tr}(\mathbf{A}^2)] &= E[[\text{tr}(\mathbf{A}^2)]^2] - E[\text{tr}(\mathbf{A}^2)]^2 \\ &= 8n(\text{tr } \mathbf{\Lambda})^2 \text{tr}(\mathbf{\Lambda}^2) + 16n(n+1) \text{tr } \mathbf{\Lambda} \text{tr}(\mathbf{\Lambda}^3) \\ &\quad + 4n(n+1)[\text{tr}(\mathbf{\Lambda}^2)]^2 + 4n(2n^2 + 5n + 5) \text{tr}(\mathbf{\Lambda}^4), \\ &= 8n^3(\text{tr } \mathbf{\Lambda})^2 \text{tr}(\mathbf{\Lambda}^2) + 32n^2 \text{tr } \mathbf{\Lambda} \text{tr}(\mathbf{\Lambda}^3) + 8n^2[\text{tr}(\mathbf{\Lambda}^2)]^2 \\ &\quad + 48n \text{tr}(\mathbf{\Lambda}^4),\end{aligned}$$

$$= 8n^2(\text{tr } \mathbf{\Lambda})^2 \text{tr}(\mathbf{\Lambda}^2) + 8n(n^2 + n + 2) \text{tr } \mathbf{\Lambda} \text{tr}(\mathbf{\Lambda}^3) + 8n[\text{tr}(\mathbf{\Lambda}^2)]^2 + 24n(n + 1) \text{tr}(\mathbf{\Lambda}^4).$$

1373 (B9)

1374 Inserting equations B8 and B9 into equations 12, 19, and 32 yields the desired results.

1375 Identical results can be derived from del Waal & Nel's (1973) results on the
 1376 expectations of elementary symmetric functions of eigenvalues and their products for a
 1377 Wishart matrix. However, these results appear to have been proved only under the condition
 1378 $n > p - 1$ (see also Constantine, 1963; Muirhead, 1982: chapter 7). The above derivation is
 1379 valid for any combination of p and n .

1380

1381 **Appendix C**

1382 This part demonstrates that $\text{Cov}(r_{ij}^2, r_{kl}^2) = 0$ for $(i, j) \neq (k, l)$ under the condition $\mathbf{P} = \mathbf{I}_p$, as
 1383 cursorily mentioned by Schott (2005). Under this condition, a sample covariance can be
 1384 written as $s_{ij} = n_*^{-1}(\sigma_{ii}\sigma_{jj})^{1/2} \mathbf{v}_i^T \mathbf{v}_j$, with \mathbf{v}_i and \mathbf{v}_j being i.i.d. $N_n(\mathbf{0}, \mathbf{I}_n)$. Therefore, a sample
 1385 correlation coefficient can be written as $r_{ij} = s_{ij}(s_{ii}s_{jj})^{-1/2} = \mathbf{u}_i^T \mathbf{u}_j$, where $\mathbf{u}_i =$
 1386 $(\mathbf{v}_i^T \mathbf{v}_i)^{-1/2} \mathbf{v}_i$ are uniformly distributed on the surface of the unit hypersphere in the n -
 1387 dimensional space. By noting $\mathbf{u}_i^T \mathbf{u}_i = 1$, it is possible to see $E(\mathbf{u}_i \mathbf{u}_i^T) = n^{-1} \mathbf{I}_n$ for any i ,
 1388 because the elements of \mathbf{u}_i are symmetric and uncorrelated with one another (a formal
 1389 demonstration probably requires introduction of the density function; see Anderson, 2003: p.
 1390 49). With these preliminaries, it is easily seen, for $i \neq j \neq k$,

$$\begin{aligned} E(r_{ij}^2 r_{ik}^2) &= E(\mathbf{u}_i^T \mathbf{u}_j \mathbf{u}_j^T \mathbf{u}_i \mathbf{u}_i^T \mathbf{u}_k \mathbf{u}_k^T \mathbf{u}_i) \\ &= E[\mathbf{u}_i^T E(\mathbf{u}_j \mathbf{u}_j^T) \mathbf{u}_i \mathbf{u}_i^T E(\mathbf{u}_k \mathbf{u}_k^T) \mathbf{u}_i] \\ &= n^{-2} E[\mathbf{u}_i^T \mathbf{u}_i \mathbf{u}_i^T \mathbf{u}_i] \\ &= n^{-2} = E(r_{ij}^2) E(r_{ik}^2). \end{aligned}$$

1391 (C1)

1392 The second equation is valid because \mathbf{u}_i , \mathbf{u}_j , and \mathbf{u}_k are stochastically independent from one
1393 another. Therefore, $\text{Cov}(r_{ij}^2, r_{ik}^2) = 0$ for partly overlapping subscripts. Similarly,
1394 $\text{Cov}(r_{ij}^2, r_{kl}^2) = 0$ for non-overlapping subscripts, although this could also be seen as a direct
1395 consequence of the independence between r_{ij} and r_{kl} in this case.

1396

1397 **Appendix D**

1398 This part outlines assumptions under the heuristic approximation of $\text{Cov}(r_{ij}^2, r_{kl}^2)$ (eq. 37).
1399 Pan & Frank (2004) derived approximate moments for the product of two correlation
1400 coefficients with overlapping subscripts (i.e., r_{ij} and r_{ik}). Equivalent results for general
1401 combinations of subscripts can be obtained by following the derivation up to their equation
1402 3.8. The relevant result is:

$$\text{E}(r_{ij}^2 r_{kl}^2) \approx \text{E}(r_{ij}^2) \text{E}(r_{kl}^2) + 4 \text{E}(r_{ij}) \text{E}(r_{kl}) \text{Cov}(r_{ij}, r_{kl}) + 2[\text{Cov}(r_{ij}, r_{kl})]^2$$

1403 (D1)

1404 Derivation of this result only requires the assumption that the third and fourth moments of
1405 correlation coefficients approximately behaves like normal moments; namely, $\text{E}([r_\alpha -$
1406 $\text{E}(r_\alpha)][r_\beta - \text{E}(r_\beta)][r_\gamma - \text{E}(r_\gamma)]) \approx 0$ and $\text{E}([r_\alpha - \text{E}(r_\alpha)][r_\beta - \text{E}(r_\beta)][r_\gamma - \text{E}(r_\gamma)][r_\delta -$
1407 $\text{E}(r_\delta)]) \approx \text{Cov}(r_\alpha, r_\beta) \text{Cov}(r_\gamma, r_\delta) + \text{Cov}(r_\alpha, r_\gamma) \text{Cov}(r_\beta, r_\delta) + \text{Cov}(r_\alpha, r_\delta) \text{Cov}(r_\beta, r_\gamma)$, where
1408 α , β , γ , and δ are arbitrary pairs of subscripts. Of course these do not strictly hold, except
1409 asymptotically under $n \rightarrow \infty$ (e.g., Olkin & Siotani, 1976; Konishi, 1979). Equation 37 is
1410 immediate from equation D1.

1411

1412 **Appendix E**

1413 In this part, an asymptotic expression for the variance of $V_{\text{rel}}(\mathbf{R})$ is derived for arbitrary non-
 1414 null conditions with $p > 2$. Konishi (1979) gave an asymptotic theory for the distribution of
 1415 an arbitrary function of eigenvalues of a sample correlation matrix $f(l_1, \dots, l_p)$ under
 1416 multivariate normality. In particular, when $n \rightarrow \infty$, $\sqrt{n}[f(l_1, \dots, l_p) - f(\lambda_1, \dots, \lambda_p)]$ was
 1417 shown to be normally distributed with mean 0 and variance

$$\tau^2 = 2 \sum_{\alpha, \beta=1}^p \lambda_\alpha \lambda_\beta \left[\delta_{\alpha\beta} - (\lambda_\alpha + \lambda_\beta) \sum_{i=1}^p v_{i\alpha}^2 v_{i\beta}^2 + \sum_{i,j=1}^p \rho_{ij}^2 v_{i\alpha}^2 v_{j\beta}^2 \right] f_\alpha f_\beta,$$

1418 (E1)

1419 where the summations are over all combinations of subscripts, $\delta_{\alpha\beta}$ is the Kronecker delta, $v_{i\alpha}$
 1420 is the (i, α) -th element of the population eigenvector matrix \mathbf{Y} , and
 1421 $f_\alpha = \partial f / \partial l_\alpha |_{(l_1, \dots, l_p) = (\lambda_1, \dots, \lambda_p)}$, the partial derivative of f with respect to l_α evaluated at
 1422 $(l_1, \dots, l_p) = (\lambda_1, \dots, \lambda_p)$. Note that Konishi's (1979; corollary 2.2) original notation also
 1423 concerned potential multiplicity of population eigenvalues, which is ignored here for
 1424 simplicity; the population eigenvectors corresponding to multiplied eigenvalues can in
 1425 practice be chosen arbitrarily as a suite of orthogonal vectors in the appropriate subspace, as
 1426 is done in numerical determination of eigenvectors. The derivative of $V_{\text{rel}}(\mathbf{R})$ is simply

$$f_\alpha = \frac{\partial}{\partial l_\alpha} V_{\text{rel}}(\mathbf{R}) \Big|_{(l_1, \dots, l_p) = (\lambda_1, \dots, \lambda_p)} = \frac{2}{p(p-1)} \lambda_\alpha.$$

1427 (E2)

1428 Inserting equation E2 into equation E1, we obtain τ^2/n as an asymptotic expression of the
 1429 variance of $V_{\text{rel}}(\mathbf{R})$ (eq. 39). It should be noted that this expression will be inaccurate around
 1430 $\mathbf{P} = \mathbf{\Lambda} = \mathbf{I}_p$. This is because, under this condition, we can arbitrarily put $\mathbf{Y} = \mathbf{I}_p$ to obtain
 1431 $\tau^2 = 0$ from equation E1, which is clearly untrue for finite n .

1432 An empirically equivalent result can be obtained from the alternative expression of
1433 $V_{\text{rel}}(\mathbf{R})$ as average squared correlation coefficients (eq. 11), from a similar theory for
1434 functions of a sample correlation matrix by Konishi (1979: theorem 6.2). However, that
1435 alternative expression does not seem to bear much practical advantage, for it typically takes
1436 substantially more computational time to evaluate as p grows.
1437

1438 **Table 1.** Summary of selected simulation results for eigenvalue variance of covariance
 1439 matrix $V(\mathbf{S})$. Theoretical expectation ($E[V(\mathbf{S})]$) and standard deviation ($SD[V(\mathbf{S})]$), as well as
 1440 empirical median, mean, standard deviation (ESD), and bias of mean in standard error unit
 1441 ($T = \sqrt{5000}\{\text{Mean} - E[V_{\text{rel}}(\mathbf{S})]\}/\text{ESD}$, which should roughly follow t distribution with
 1442 4999 degrees of freedom if the expectation is exact) from 5000 simulation runs are shown for
 1443 selected conditions. See Table S1 for full results.

	$E[V(\mathbf{S})]$	$SD[V(\mathbf{S})]$	Median	Mean	ESD	T
$p = 2, V(\mathbf{\Sigma}) = 0$						
$N = 8$	0.2857	0.3582	0.1731	0.2876	0.3464	0.3845
$N = 16$	0.1333	0.1501	0.0876	0.1330	0.1466	-0.1703
$N = 32$	0.0645	0.0686	0.0438	0.0646	0.0689	0.0489
$N = 64$	0.0317	0.0327	0.0221	0.0315	0.0315	-0.6336
$p = 4, V(\mathbf{\Sigma}) = 0$						
$N = 8$	0.2143	0.1551	0.1734	0.2131	0.1534	-0.5437
$N = 16$	0.1000	0.0602	0.0861	0.0996	0.0603	-0.4826
$N = 32$	0.0484	0.0261	0.0429	0.0481	0.0261	-0.8676
$N = 64$	0.0238	0.0120	0.0216	0.0239	0.0119	0.5321
$p = 16, V(\mathbf{\Sigma}) = 0$						
$N = 8$	0.1518	0.0304	0.1482	0.1510	0.0307	-1.8948
$N = 16$	0.0708	0.0102	0.0702	0.0708	0.0102	-0.0003
$N = 32$	0.0343	0.0038	0.0341	0.0342	0.0037	-0.4806
$N = 64$	0.0169	0.0015	0.0168	0.0169	0.0015	-0.6023
$p = 64, V(\mathbf{\Sigma}) = 0$						
$N = 8$	0.1473	0.0203	0.1464	0.1477	0.0204	1.2947
$N = 16$	0.0688	0.0067	0.0688	0.0689	0.0066	1.7306
$N = 32$	0.0333	0.0024	0.0332	0.0333	0.0024	0.6721

Table 1 (continued)

	$E[V(\mathbf{S})]$	$SD[V(\mathbf{S})]$	Median	Mean	ESD	T
$N = 64$	0.0164	0.0009	0.0163	0.0164	0.0009	-0.4407
$p = 256, V(\Sigma) = 0$						
$N = 8$	0.1440	0.0097	0.1436	0.1440	0.0099	0.1215
$N = 16$	0.0672	0.0031	0.0672	0.0672	0.0031	0.9739
$N = 32$	0.0325	0.0011	0.0325	0.0325	0.0011	-0.8132
$N = 64$	0.0160	0.0004	0.0160	0.0160	0.0004	0.0842
$p = 1024, V(\Sigma) = 0$						
$N = 8$	0.1431	0.0048	0.1430	0.1431	0.0048	-0.6874
$N = 16$	0.0668	0.0015	0.0668	0.0668	0.0015	1.7324
$N = 32$	0.0323	0.0005	0.0323	0.0323	0.0005	0.3227
$N = 64$	0.0159	0.0002	0.0159	0.0159	0.0002	0.3522
$p = 2, q = 1, V(\Sigma) = 0.4$						
$N = 8$	0.6857	0.8717	0.3967	0.6901	0.8663	0.3572
$N = 16$	0.5333	0.4852	0.3972	0.5426	0.4981	1.3183
$N = 32$	0.4645	0.3023	0.3936	0.4616	0.3011	-0.6854
$N = 64$	0.4317	0.2002	0.4044	0.4337	0.2019	0.6886
$p = 4, q = 1, V(\Sigma) = 0.4$						
$N = 8$	0.6429	0.7343	0.3949	0.6372	0.7364	-0.5426
$N = 16$	0.5133	0.4137	0.3968	0.5132	0.4183	-0.0225
$N = 32$	0.4548	0.2598	0.3937	0.4544	0.2661	-0.1087
$N = 64$	0.4270	0.1728	0.4025	0.4292	0.1756	0.8791
$p = 16, q = 1, V(\Sigma) = 0.4$						
$N = 8$	0.6107	0.6427	0.4130	0.6165	0.6509	0.6282
$N = 16$	0.4983	0.3668	0.4060	0.5036	0.3748	0.9922
$N = 32$	0.4476	0.2322	0.4057	0.4492	0.2314	0.5001
$N = 64$	0.4234	0.1552	0.4005	0.4227	0.1546	-0.3205

Table 1 (continued)

	$E[V(\mathbf{S})]$	$SD[V(\mathbf{S})]$	Median	Mean	ESD	T
$p = 64, q = 1, V(\mathbf{\Sigma}) = 0.4$						
$N = 8$	0.6027	0.6206	0.4227	0.6052	0.5988	0.2997
$N = 16$	0.4946	0.3554	0.4061	0.5021	0.3631	1.4613
$N = 32$	0.4458	0.2255	0.4003	0.4445	0.2244	-0.4124
$N = 64$	0.4225	0.1509	0.3986	0.4237	0.1546	0.5322
$p = 256, q = 1, V(\mathbf{\Sigma}) = 0.4$						
$N = 8$	0.6007	0.6151	0.4140	0.6076	0.6137	0.7995
$N = 16$	0.4936	0.3526	0.4000	0.4873	0.3492	-1.2751
$N = 32$	0.4453	0.2239	0.4068	0.4465	0.2213	0.3813
$N = 64$	0.4223	0.1499	0.4003	0.4234	0.1505	0.5054
$p = 1024, q = 1, V(\mathbf{\Sigma}) = 0.4$						
$N = 8$	0.6002	0.6138	0.3961	0.5940	0.6361	-0.6814
$N = 16$	0.4934	0.3519	0.4015	0.4977	0.3638	0.8432
$N = 32$	0.4452	0.2235	0.4037	0.4489	0.2304	1.1498
$N = 64$	0.4222	0.1496	0.4020	0.4240	0.1526	0.8140
$p = 2, q = 1, V(\mathbf{\Sigma}) = 0.8$						
$N = 8$	1.0857	1.2651	0.6587	1.0792	1.3030	-0.3520
$N = 16$	0.9333	0.7343	0.7440	0.9364	0.7250	0.3003
$N = 32$	0.8645	0.4698	0.7732	0.8675	0.4675	0.4571
$N = 64$	0.8317	0.3157	0.7840	0.8333	0.3172	0.3574
$p = 4, q = 1, V(\mathbf{\Sigma}) = 0.8$						
$N = 8$	1.0714	1.2182	0.6903	1.0730	1.2081	0.0917
$N = 16$	0.9267	0.7096	0.7454	0.9328	0.7139	0.6117
$N = 32$	0.8613	0.4549	0.7682	0.8585	0.4565	-0.4368
$N = 64$	0.8302	0.3061	0.7903	0.8350	0.3069	1.1137
$p = 16, q = 1, V(\mathbf{\Sigma}) = 0.8$						

Table 1 (continued)

	$E[V(\mathbf{S})]$	$SD[V(\mathbf{S})]$	Median	Mean	ESD	T
$N = 8$	1.0607	1.1840	0.6778	1.0687	1.1804	0.4765
$N = 16$	0.9217	0.6917	0.7517	0.9147	0.6842	-0.7221
$N = 32$	0.8589	0.4442	0.7847	0.8683	0.4387	1.5248
$N = 64$	0.8290	0.2992	0.7925	0.8358	0.3067	1.5855
<hr/>						
$p = 64, q = 1, V(\Sigma) = 0.8$						
$N = 8$	1.0580	1.1756	0.6979	1.0755	1.2081	1.0231
$N = 16$	0.9204	0.6873	0.7463	0.9304	0.7024	1.0083
$N = 32$	0.8583	0.4415	0.7643	0.8495	0.4352	-1.4315
$N = 64$	0.8287	0.2975	0.7873	0.8292	0.2977	0.1296
<hr/>						
$p = 256, q = 1, V(\Sigma) = 0.8$						
$N = 8$	1.0574	1.1735	0.6982	1.0818	1.1935	1.4492
$N = 16$	0.9201	0.6862	0.7373	0.9122	0.6746	-0.8321
$N = 32$	0.8581	0.4409	0.7749	0.8663	0.4540	1.2689
$N = 64$	0.8286	0.2971	0.7824	0.8219	0.2873	-1.6582
<hr/>						
$p = 1024, q = 1, V(\Sigma) = 0.8$						
$N = 8$	1.0572	1.1729	0.6881	1.0573	1.1723	0.0072
$N = 16$	0.9200	0.6859	0.7655	0.9344	0.6943	1.4624
$N = 32$	0.8581	0.4407	0.7709	0.8531	0.4414	-0.7945
$N = 64$	0.8286	0.2969	0.7840	0.8292	0.2987	0.1364

1444

1445 **Table 2.** Summary of selected simulation results for relative eigenvalue variance of
 1446 covariance matrix $V_{\text{rel}}(\mathbf{S})$. (Approximate) theoretical expectation ($E[V_{\text{rel}}(\mathbf{S})]$) and standard
 1447 deviation ($SD[V_{\text{rel}}(\mathbf{S})]$), as well as empirical median, mean, standard deviation (ESD), and
 1448 bias of mean in standard error unit (T) from 5000 simulation runs are shown for selected
 1449 conditions. See Table 1 for further information and Table S2 for full results.

	$\approx E[V_{\text{rel}}(\mathbf{S})]$	$\approx SD[V_{\text{rel}}(\mathbf{S})]$	Median	Mean	ESD	T
$p = 2, V_{\text{rel}}(\mathbf{\Sigma}) = 0$						
$N = 8$	0.2500	0.1936	0.2079	0.2514	0.1924	0.4961
$N = 16$	0.1250	0.1102	0.0953	0.1259	0.1098	0.6000
$N = 32$	0.0625	0.0587	0.0448	0.0628	0.0597	0.3234
$N = 64$	0.0313	0.0303	0.0224	0.0309	0.0289	-0.8301
$p = 4, V_{\text{rel}}(\mathbf{\Sigma}) = 0$						
$N = 8$	0.2000	0.0840	0.1856	0.2002	0.0858	0.1644
$N = 16$	0.0968	0.0433	0.0907	0.0968	0.0434	0.0620
$N = 32$	0.0476	0.0219	0.0438	0.0474	0.0221	-0.6146
$N = 64$	0.0236	0.0110	0.0218	0.0237	0.0110	0.6544
$p = 16, V_{\text{rel}}(\mathbf{\Sigma}) = 0$						
$N = 8$	0.1579	0.0193	0.1562	0.1580	0.0197	0.3764
$N = 16$	0.0744	0.0091	0.0738	0.0746	0.0094	1.4158
$N = 32$	0.0361	0.0044	0.0357	0.0361	0.0044	-1.2604
$N = 64$	0.0178	0.0022	0.0177	0.0178	0.0022	0.4338
$p = 64, V_{\text{rel}}(\mathbf{\Sigma}) = 0$						
$N = 8$	0.1467	0.0047	0.1462	0.1466	0.0046	-0.6909
$N = 16$	0.0686	0.0022	0.0685	0.0686	0.0022	0.5618
$N = 32$	0.0332	0.0010	0.0332	0.0332	0.0011	0.0446
$N = 64$	0.0164	0.0005	0.0163	0.0164	0.0005	-0.5869

Table 2 (continued)

	$\approx E[V_{\text{rel}}(\mathbf{S})]$	$\approx \text{SD}[V_{\text{rel}}(\mathbf{S})]$	Median	Mean	ESD	T
$p = 256, V_{\text{rel}}(\boldsymbol{\Sigma}) = 0$						
$N = 8$	0.1438	0.0012	0.1437	0.1438	0.0012	-0.0173
$N = 16$	0.0672	0.0005	0.0671	0.0672	0.0005	1.4545
$N = 32$	0.0325	0.0003	0.0325	0.0325	0.0003	-0.7481
$N = 64$	0.0160	0.0001	0.0160	0.0160	0.0001	0.3608
$p = 1024, V_{\text{rel}}(\boldsymbol{\Sigma}) = 0$						
$N = 8$	0.1431	0.0003	0.1431	0.1431	0.0003	-0.5105
$N = 16$	0.0668	0.0001	0.0668	0.0668	0.0001	0.0231
$N = 32$	0.0323	0.0001	0.0323	0.0323	0.0001	-1.3055
$N = 64$	0.0159	0.0000	0.0159	0.0159	0.0000	-0.0022
$p = 2, q = 1, V_{\text{rel}}(\boldsymbol{\Sigma}) = 0.4$						
$N = 8$	0.4377	0.2825	0.4939	0.4804	0.2334	12.9356
$N = 16$	0.4232	0.1982	0.4457	0.4384	0.1764	6.0670
$N = 32$	0.4132	0.1378	0.4169	0.4152	0.1297	1.1224
$N = 64$	0.4070	0.0963	0.4108	0.4083	0.0945	0.9214
$p = 4, q = 1, V_{\text{rel}}(\boldsymbol{\Sigma}) = 0.4$						
$N = 8$	0.4319	0.2065	0.4730	0.4675	0.1658	15.1734
$N = 16$	0.4200	0.1444	0.4316	0.4288	0.1272	4.8902
$N = 32$	0.4113	0.1001	0.4147	0.4125	0.0944	0.9058
$N = 64$	0.4060	0.0699	0.4073	0.4067	0.0682	0.7503
$p = 16, q = 1, V_{\text{rel}}(\boldsymbol{\Sigma}) = 0.4$						
$N = 8$	0.4275	0.1691	0.4657	0.4626	0.1346	18.4219
$N = 16$	0.4174	0.1175	0.4302	0.4270	0.1049	6.4710
$N = 32$	0.4098	0.0813	0.4161	0.4129	0.0762	2.8682
$N = 64$	0.4052	0.0566	0.4070	0.4058	0.0548	0.7118
$p = 64, q = 1, V_{\text{rel}}(\boldsymbol{\Sigma}) = 0.4$						

Table 2 (continued)

	$\approx E[V_{\text{rel}}(\mathbf{S})]$	$\approx \text{SD}[V_{\text{rel}}(\mathbf{S})]$	Median	Mean	ESD	T
$N = 8$	0.4264	0.1613	0.4670	0.4599	0.1273	18.6017
$N = 16$	0.4168	0.1119	0.4286	0.4266	0.0996	6.9651
$N = 32$	0.4095	0.0773	0.4125	0.4109	0.0726	1.3497
$N = 64$	0.4050	0.0538	0.4063	0.4056	0.0532	0.7287
<hr/>						
$p = 256, q = 1, V_{\text{rel}}(\mathbf{\Sigma}) = 0.4$						
$N = 8$	0.4261	0.1594	0.4637	0.4606	0.1249	19.5222
$N = 16$	0.4166	0.1105	0.4262	0.4228	0.0977	4.4222
$N = 32$	0.4094	0.0763	0.4148	0.4120	0.0718	2.5791
$N = 64$	0.4050	0.0531	0.4066	0.4058	0.0520	1.1405
<hr/>						
$p = 1024, q = 1, V_{\text{rel}}(\mathbf{\Sigma}) = 0.4$						
$N = 8$	0.4261	0.1590	0.4566	0.4548	0.1261	16.1041
$N = 16$	0.4166	0.1102	0.4272	0.4246	0.0990	5.7314
$N = 32$	0.4094	0.0761	0.4140	0.4123	0.0718	2.8690
$N = 64$	0.4050	0.0530	0.4068	0.4058	0.0521	1.1494
<hr/>						
$p = 2, q = 1, V_{\text{rel}}(\mathbf{\Sigma}) = 0.8$						
$N = 8$	0.7847	0.1153	0.8314	0.7947	0.1473	4.8016
$N = 16$	0.7929	0.0866	0.8164	0.7963	0.1004	2.4327
$N = 32$	0.7969	0.0625	0.8090	0.7990	0.0672	2.2207
$N = 64$	0.7986	0.0445	0.8030	0.7983	0.0470	-0.3966
<hr/>						
$p = 4, q = 1, V_{\text{rel}}(\mathbf{\Sigma}) = 0.8$						
$N = 8$	0.7841	0.0920	0.8207	0.7927	0.1170	5.1526
$N = 16$	0.7927	0.0692	0.8086	0.7945	0.0793	1.6175
$N = 32$	0.7968	0.0498	0.8039	0.7967	0.0537	-0.1966
$N = 64$	0.7985	0.0354	0.8026	0.7993	0.0368	1.5352
<hr/>						
$p = 16, q = 1, V_{\text{rel}}(\mathbf{\Sigma}) = 0.8$						
$N = 8$	0.7838	0.0810	0.8153	0.7913	0.1049	5.0688

Table 2 (continued)

	$\approx E[V_{\text{rel}}(\mathbf{S})]$	$\approx \text{SD}[V_{\text{rel}}(\mathbf{S})]$	Median	Mean	ESD	T
$N = 16$	0.7926	0.0609	0.8067	0.7943	0.0696	1.7415
$N = 32$	0.7968	0.0437	0.8044	0.7989	0.0452	3.3474
$N = 64$	0.7985	0.0310	0.8019	0.7990	0.0323	1.0675
<hr/>						
$p = 64, q = 1, V_{\text{rel}}(\mathbf{\Sigma}) = 0.8$						
$N = 8$	0.7837	0.0787	0.8157	0.7915	0.1022	5.4258
$N = 16$	0.7926	0.0592	0.8072	0.7956	0.0669	3.2349
$N = 32$	0.7967	0.0425	0.8021	0.7967	0.0447	-0.0106
$N = 64$	0.7985	0.0301	0.8018	0.7989	0.0308	0.8231
<hr/>						
$p = 256, q = 1, V_{\text{rel}}(\mathbf{\Sigma}) = 0.8$						
$N = 8$	0.7836	0.0781	0.8150	0.7930	0.0994	6.6508
$N = 16$	0.7926	0.0588	0.8058	0.7944	0.0663	1.9392
$N = 32$	0.7967	0.0422	0.8033	0.7976	0.0455	1.3138
$N = 64$	0.7985	0.0299	0.8010	0.7983	0.0303	-0.5863
<hr/>						
$p = 1024, q = 1, V_{\text{rel}}(\mathbf{\Sigma}) = 0.8$						
$N = 8$	0.7836	0.0780	0.8140	0.7904	0.1011	4.7652
$N = 16$	0.7926	0.0587	0.8081	0.7959	0.0665	3.5530
$N = 32$	0.7967	0.0421	0.8026	0.7967	0.0448	-0.0218
$N = 64$	0.7985	0.0299	0.8012	0.7987	0.0307	0.4338

1450

1451 **Table 3.** Summary of selected simulation results for relative eigenvalue variance of
 1452 correlation matrix $V_{\text{rel}}(\mathbf{R})$. Theoretical expectation ($E[V_{\text{rel}}(\mathbf{R})]$) and (approximate) standard
 1453 deviation ($SD[V_{\text{rel}}(\mathbf{R})]$), as well as empirical median, mean, standard deviation (ESD), and
 1454 bias of mean in standard error unit (T) from 5000 simulation runs are shown for selected
 1455 conditions. The theoretical standard deviations shown in this table are from heuristic
 1456 approximation (eqs. 28, 36–38) except under the null conditions. See Table 1 for further
 1457 information and Table S3 for full results.

	$E[V_{\text{rel}}(\mathbf{R})]$	$\approx SD[V_{\text{rel}}(\mathbf{R})]$	Median	Mean	ESD	T
$p = 2, V_{\text{rel}}(\mathbf{P}) = 0$						
$N = 8$	0.1429	0.1650	0.0792	0.1429	0.1635	0.0363
$N = 16$	0.0667	0.0856	0.0336	0.0679	0.0862	1.0235
$N = 32$	0.0323	0.0435	0.0163	0.0326	0.0427	0.6113
$N = 64$	0.0159	0.0219	0.0075	0.0156	0.0205	-1.0380
$p = 4, V_{\text{rel}}(\mathbf{P}) = 0$						
$N = 8$	0.1429	0.0673	0.1332	0.1432	0.0673	0.3148
$N = 16$	0.0667	0.0349	0.0608	0.0661	0.0344	-1.0696
$N = 32$	0.0323	0.0178	0.0292	0.0321	0.0175	-0.6906
$N = 64$	0.0159	0.0090	0.0142	0.0157	0.0087	-1.0749
$p = 16, V_{\text{rel}}(\mathbf{P}) = 0$						
$N = 8$	0.1429	0.0151	0.1411	0.1428	0.0151	-0.0917
$N = 16$	0.0667	0.0078	0.0663	0.0669	0.0080	1.7743
$N = 32$	0.0323	0.0040	0.0319	0.0322	0.0039	-1.7517
$N = 64$	0.0159	0.0020	0.0158	0.0159	0.0020	0.7127
$p = 64, V_{\text{rel}}(\mathbf{P}) = 0$						
$N = 8$	0.1429	0.0037	0.1425	0.1428	0.0036	-0.4617
$N = 16$	0.0667	0.0019	0.0666	0.0667	0.0019	0.4407

	$E[V_{\text{rel}}(\mathbf{R})]$	$\approx \text{SD}[V_{\text{rel}}(\mathbf{R})]$	Median	Mean	ESD	T
$N = 32$	0.0323	0.0010	0.0322	0.0323	0.0010	-0.0725
$N = 64$	0.0159	0.0005	0.0159	0.0159	0.0005	-0.6525
<hr/>						
$p = 256, V_{\text{rel}}(\mathbf{P}) = 0$						
$N = 8$	0.1429	0.0009	0.1428	0.1429	0.0009	0.0105
$N = 16$	0.0667	0.0005	0.0667	0.0667	0.0005	1.8676
$N = 32$	0.0323	0.0002	0.0323	0.0323	0.0002	-0.9701
$N = 64$	0.0159	0.0001	0.0159	0.0159	0.0001	0.3244
<hr/>						
$p = 1024, V_{\text{rel}}(\mathbf{P}) = 0$						
$N = 8$	0.1429	0.0002	0.1428	0.1429	0.0002	-0.9639
$N = 16$	0.0667	0.0001	0.0667	0.0667	0.0001	0.5220
$N = 32$	0.0323	0.0001	0.0323	0.0323	0.0001	-1.8393
$N = 64$	0.0159	0.0000	0.0159	0.0159	0.0000	-0.0357
<hr/>						
$p = 2, q = 1, V_{\text{rel}}(\mathbf{P}) = 0.4$						
$N = 8$	0.4318	0.2495	0.4362	0.4294	0.2516	-0.6571
$N = 16$	0.4111	0.1844	0.4230	0.4147	0.1832	1.3640
$N = 32$	0.4046	0.1326	0.4056	0.4041	0.1322	-0.2806
$N = 64$	0.4021	0.0944	0.4058	0.4025	0.0954	0.3294
<hr/>						
$p = 4, q = 1, V_{\text{rel}}(\mathbf{P}) = 0.4$						
$N = 8$	0.4318	0.1950	0.4314	0.4287	0.1750	-1.2271
$N = 16$	0.4111	0.1380	0.4141	0.4093	0.1317	-0.9769
$N = 32$	0.4046	0.0975	0.4054	0.4034	0.0960	-0.8743
$N = 64$	0.4021	0.0688	0.4033	0.4022	0.0687	0.1270
<hr/>						
$p = 16, q = 1, V_{\text{rel}}(\mathbf{P}) = 0.4$						
$N = 8$	0.4318	0.1621	0.4321	0.4329	0.1391	0.5780
$N = 16$	0.4111	0.1130	0.4149	0.4120	0.1073	0.5980
$N = 32$	0.4046	0.0793	0.4084	0.4055	0.0773	0.7996

	$E[V_{\text{rel}}(\mathbf{R})]$	$\approx \text{SD}[V_{\text{rel}}(\mathbf{R})]$	Median	Mean	ESD	T
$N = 64$	0.4021	0.0559	0.4030	0.4021	0.0552	-0.0283
$p = 64, q = 1, V_{\text{rel}}(\mathbf{P}) = 0.4$						
$N = 8$	0.4318	0.1542	0.4366	0.4332	0.1304	0.7802
$N = 16$	0.4111	0.1074	0.4144	0.4129	0.1015	1.2079
$N = 32$	0.4046	0.0754	0.4052	0.4039	0.0733	-0.6457
$N = 64$	0.4021	0.0531	0.4029	0.4021	0.0535	0.0493
$p = 256, q = 1, V_{\text{rel}}(\mathbf{P}) = 0.4$						
$N = 8$	0.4318	0.1522	0.4348	0.4343	0.1278	1.3865
$N = 16$	0.4111	0.1061	0.4118	0.4091	0.0995	-1.4526
$N = 32$	0.4046	0.0744	0.4078	0.4052	0.0726	0.5664
$N = 64$	0.4021	0.0524	0.4033	0.4024	0.0522	0.4500
$p = 1024, q = 1, V_{\text{rel}}(\mathbf{P}) = 0.4$						
$N = 8$	0.4318		0.4266	0.4286	0.1287	-1.7550
$N = 16$	0.4111		0.4127	0.4111	0.1008	-0.0454
$N = 32$	0.4046		0.4072	0.4055	0.0726	0.8769
$N = 64$	0.4021		0.4035	0.4024	0.0524	0.4578
$p = 2, q = 1, V_{\text{rel}}(\mathbf{P}) = 0.8$						
$N = 8$	0.7831	0.1596	0.8250	0.7853	0.1571	0.9790
$N = 16$	0.7918	0.1015	0.8141	0.7928	0.1033	0.6253
$N = 32$	0.7961	0.0674	0.8076	0.7976	0.0680	1.5536
$N = 64$	0.7981	0.0462	0.8024	0.7976	0.0473	-0.6617
$p = 4, q = 1, V_{\text{rel}}(\mathbf{P}) = 0.8$						
$N = 8$	0.7831	0.1115	0.8149	0.7840	0.1249	0.4605
$N = 16$	0.7918	0.0749	0.8059	0.7913	0.0815	-0.4682
$N = 32$	0.7961	0.0516	0.8027	0.7953	0.0543	-1.0173
$N = 64$	0.7981	0.0360	0.8019	0.7987	0.0370	1.2077

	$E[V_{\text{rel}}(\mathbf{R})]$	$\approx \text{SD}[V_{\text{rel}}(\mathbf{R})]$	Median	Mean	ESD	T
$p = 16, q = 1, V_{\text{rel}}(\mathbf{P}) = 0.8$						
$N = 8$	0.7831	0.0927	0.8102	0.7835	0.1116	0.2370
$N = 16$	0.7918	0.0638	0.8045	0.7913	0.0716	-0.5326
$N = 32$	0.7961	0.0445	0.8035	0.7976	0.0457	2.4043
$N = 64$	0.7981	0.0313	0.8013	0.7984	0.0325	0.7108
$p = 64, q = 1, V_{\text{rel}}(\mathbf{P}) = 0.8$						
$N = 8$	0.7831	0.0896	0.8098	0.7841	0.1083	0.6205
$N = 16$	0.7918	0.0619	0.8046	0.7928	0.0687	0.9579
$N = 32$	0.7961	0.0432	0.8009	0.7955	0.0452	-0.9741
$N = 64$	0.7981	0.0303	0.8012	0.7983	0.0309	0.4419
$p = 256, q = 1, V_{\text{rel}}(\mathbf{P}) = 0.8$						
$N = 8$	0.7831	0.0890	0.8098	0.7857	0.1056	1.7052
$N = 16$	0.7918	0.0614	0.8031	0.7915	0.0681	-0.3408
$N = 32$	0.7961	0.0429	0.8022	0.7963	0.0460	0.3738
$N = 64$	0.7981	0.0301	0.8004	0.7977	0.0305	-0.9565
$p = 1024, q = 1, V_{\text{rel}}(\mathbf{P}) = 0.8$						
$N = 8$	0.7831	0.0888	0.8088	0.7830	0.1074	-0.0831
$N = 16$	0.7918	0.0613	0.8057	0.7930	0.0683	1.2443
$N = 32$	0.7961	0.0428	0.8014	0.7954	0.0454	-0.9758
$N = 64$	0.7981	0.0301	0.8006	0.7981	0.0308	0.0710

1458

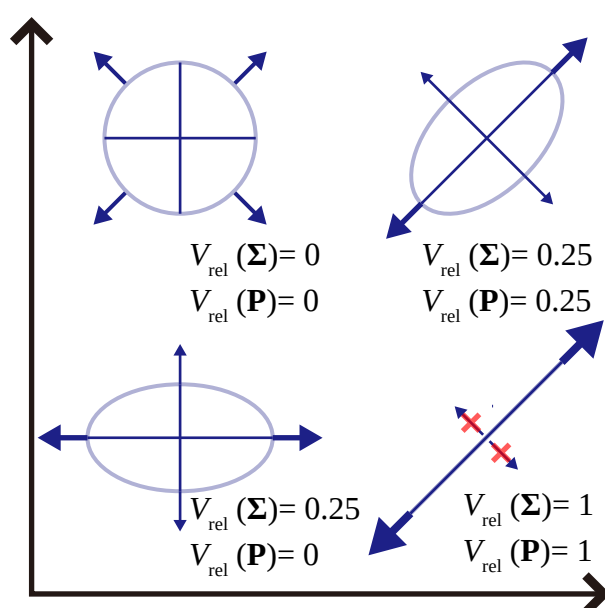


Figure 1. Schematic illustration of eigenvalue dispersion indices in bivariate cases. Ellipses representing equiprobability contours are shown on a Cartesian space of two hypothetical variables for four conditions, as well as the relative eigenvalue variance of the corresponding covariance and correlation matrices ($V_{rel}(\Sigma)$ and $V_{rel}(\mathbf{P})$, respectively). The scale is arbitrary but identical for the two axes. The axes of each ellipse are proportional to square roots of the two eigenvalues of the respective covariance matrix. $V_{rel}(\Sigma)$ represents eccentricity of variation and is sensitive to differing scale changes between axes but not to rotation (change of eigenvectors), whereas $V_{rel}(\mathbf{P})$ represents magnitude of correlation and is insensitive to scale changes. Arrows schematically represent variation along major axes (whose directions are arbitrary when $V_{rel}(\Sigma) = 0$).

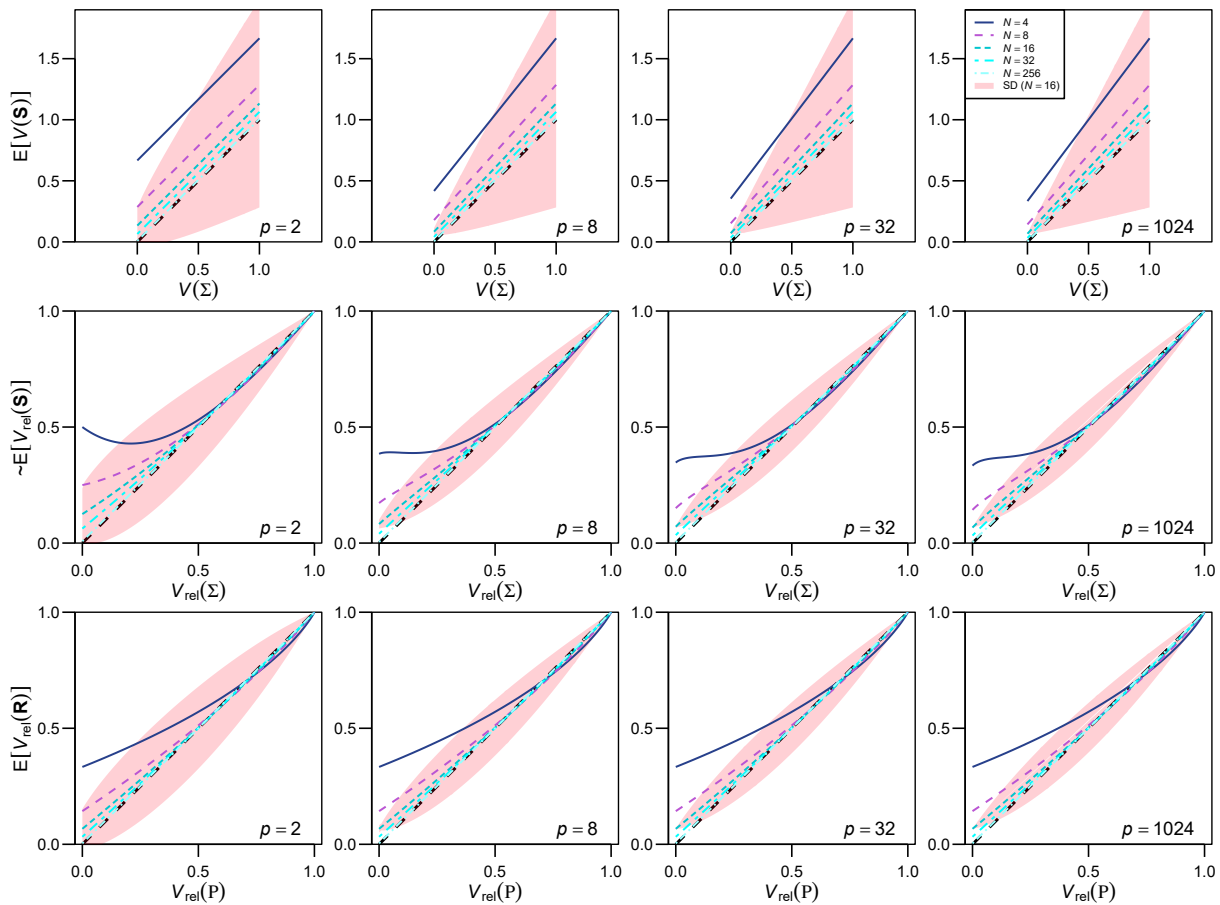


Figure 2. Profiles of the expectations of eigenvalue dispersion measures in selected conditions. The expectations of $V(\mathbf{S})$ (top row), $V_{\text{rel}}(\mathbf{S})$ (approximate; middle row), and $V_{\text{rel}}(\mathbf{R})$ (bottom row) are drawn with solid lines, for $p = 2, 8, 32,$ and 1024 (from left to right) and for $N = 4, 8, 16, 32,$ and 256 (from top to bottom on the left end of each box). In all cases, $n = N - 1$. The breadth of one standard deviation at $N = 16$ is also shown around the mean profiles with pink fills; these are approximations for $V_{\text{rel}}(\mathbf{S})$ and for $V_{\text{rel}}(\mathbf{R})$ with $p > 2$ (the latter is from eq. 39; eqs. 36–38 yielded similar values under these conditions). Note that actual distributions might be skewed unlike these fills. There are generally many suites of eigenvalues corresponding to a single value of V_{rel} , and $E[V_{\text{rel}}(\mathbf{R})]$ can also depend on eigenvector configurations; the profiles shown here are from such eigenvalue configurations that there is one large eigenvalue, with the rest being equally small, in which case $E[V_{\text{rel}}(\mathbf{R})]$ does not depend on eigenvector configurations. The population covariance matrix Σ is scaled so that $\text{tr} \Sigma = p(p - 1)^{-1/2}$. The initial decrease of the $E[V_{\text{rel}}(\mathbf{S})]$ profiles in some cases seems to be an artifact of approximation. See text for further technical details.

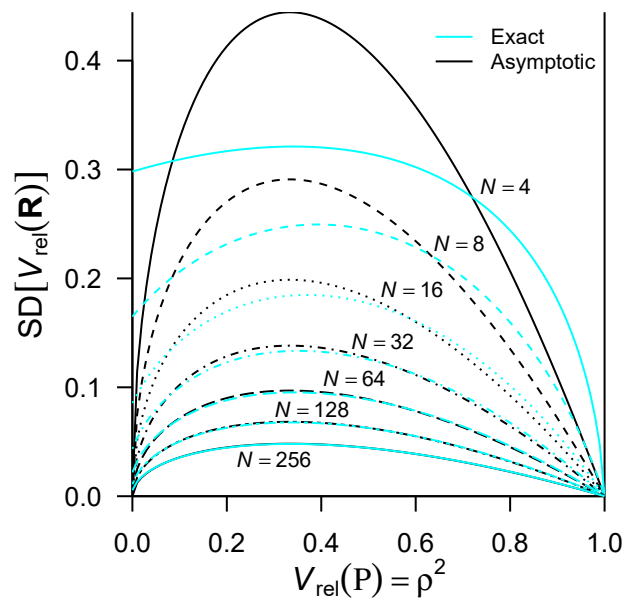


Figure 3. Comparison of exact and asymptotic standard deviations of $V_{rel}(\mathbf{R})$. Profiles of the exact (cyan lines; eq. 36) and asymptotic (black lines; eq. 39) standard deviations for $p = 2$ are shown across the entire range of the population value $V_{rel}(\mathbf{P})$, for $N = 4, 8, 16, 32, 64, 128$, and 256 (from top to bottom as labeled; shown with different line styles). Note that the asymptotic profiles converge to 0 when $V_{rel}(\mathbf{P}) = 0$.

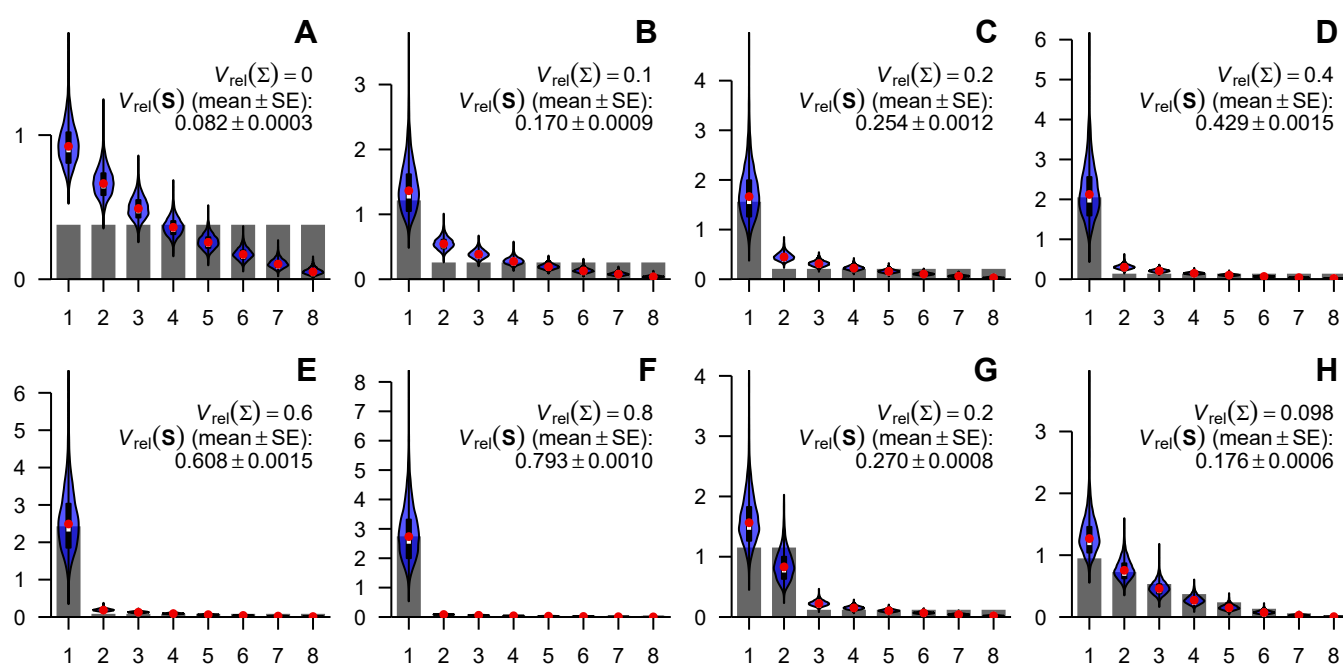


Figure 4. Selected population eigenvalue structures used in simulations and distributions of sample eigenvalues, examples for $p = 8$. The eigenvalues of population covariance matrix are shown as scree plots, and distributions of sample eigenvalues with $N = 16$ are shown as violin plots. **A**, null condition; **B–G**, q -large λ conditions, $q = 1$ (**B–F**) or 2 (**G**), with $V_{\text{rel}}(\Sigma) = 0.1, 0.2, 0.4, 0.6, 0.8$, and 0.2, respectively; **H**, quadratically decreasing λ condition. Red dots denote empirical means of sample eigenvalues, whereas white bars (mostly overlapping with red dots) denote medians. Thick black bars within violins denote interquartile ranges. Note different scales of vertical axes.

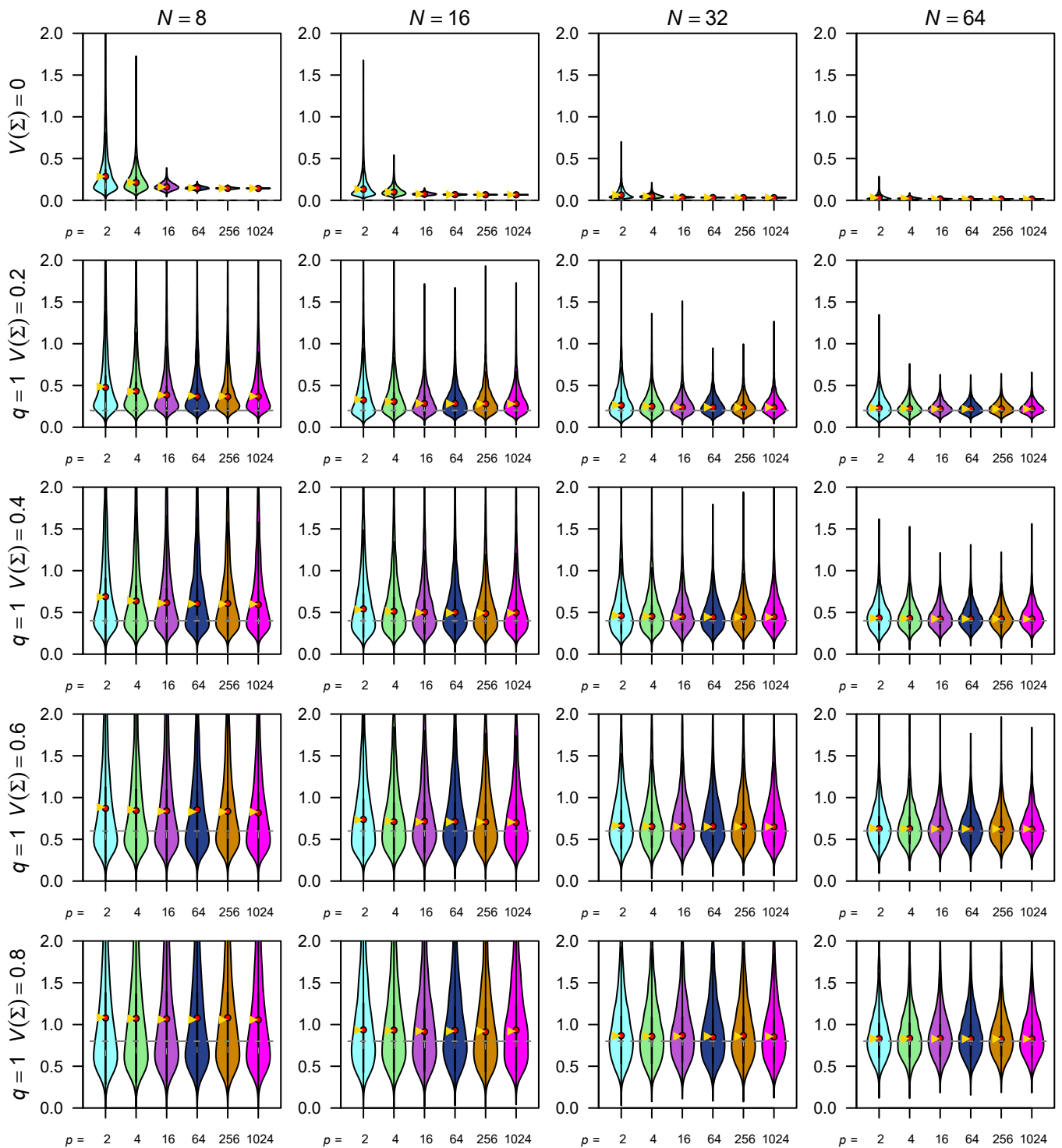


Figure 5. Selected simulation results for the eigenvalue variance of covariance matrix $V(S)$. Empirical distributions of simulated $V(S)$ values are shown as violin plots, whose tails extend to the extreme values. Red dots denote empirical means, whereas yellow triangles denote expectations (which are exact). Thick black bars within violins denote interquartile ranges, with white bars near the center (in some cases overlapping with red dots) denote medians. Rows of panels correspond to varying population values of $V(\Sigma)$ (under 1-large λ conditions), whereas columns correspond to varying sample size N . Columns within each panel correspond to varying number of variables p . Note that extreme values in some panels are cropped for visual clarity. See Figure S4–S6 for full results.

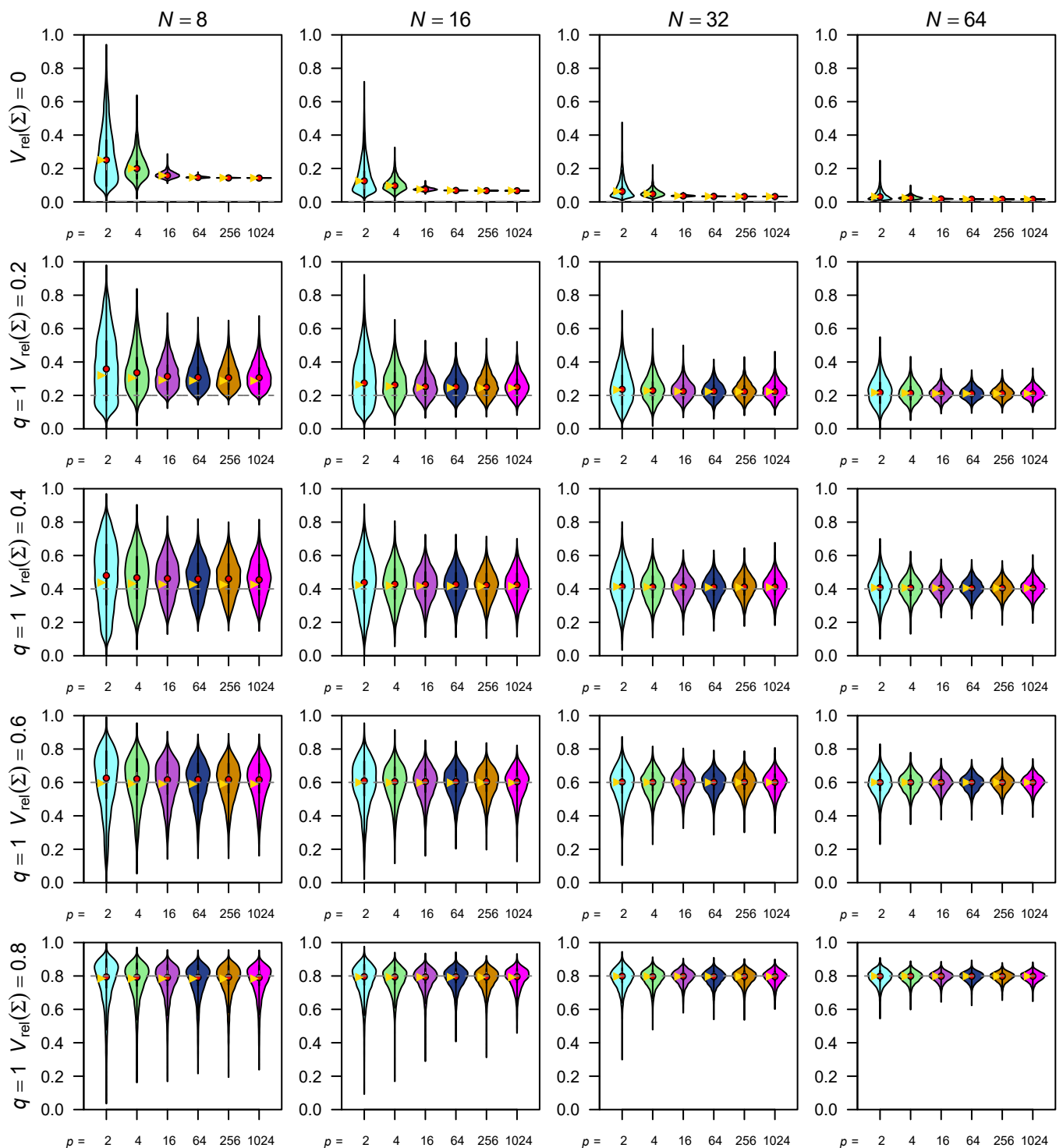


Figure 6. Selected simulation results for the relative eigenvalue variance of covariance matrix $V_{\text{rel}}(\mathbf{S})$. Empirical distributions of simulated $V_{\text{rel}}(\mathbf{S})$ values are shown as violin plots. Yellow triangles denote expectations (which are approximate except under the null condition). Rows of panels correspond to varying population values of $V_{\text{rel}}(\Sigma)$ (under 1-large λ conditions). Other legends are as in Fig. 5. See Figure S6–S8 for full results.

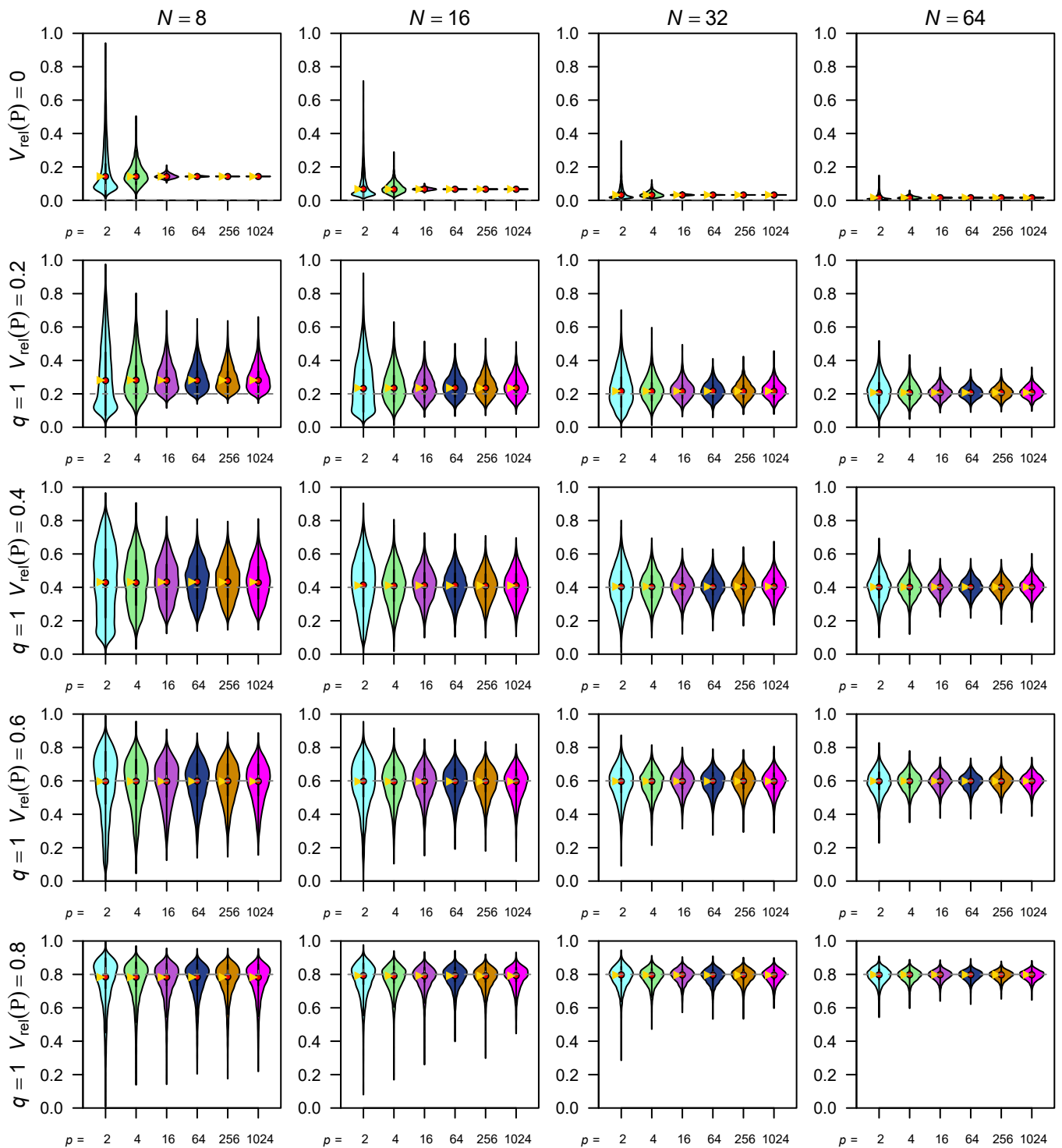


Figure 7. Selected simulation results for the relative eigenvalue variance of correlation matrix $V_{\text{rel}}(\mathbf{R})$. Empirical distributions of simulated $V_{\text{rel}}(\mathbf{R})$ values are shown as violin plots. Yellow triangles denote expectations (which are exact). Rows of panels correspond to varying population values of $V_{\text{rel}}(\mathbf{P})$ (under 1-large λ conditions). Other legends are as in Fig. 5. See Figure S6, S9, and S10 for full results.